

**UNIVERSITY POLITEHNICA OF BUCHAREST
FACULTY OF APPLIED CHEMISTRY AND
MATERIAL SCIENCE**

**MODELING AND SIMULATION OF
CONTINUOUS CATALYTIC DISTILLATION
PROCESSES.**

**CASE STUDY: TERT-AMYL-METHYL-
ETHER (TAME) SYNTHESIS**

PhD student: ing. Alexandra Elena PLEȘU

Supervisor: Prof.dr.ing. Grigore BOZGA

February 2008

TABLE OF CONTENTS

Chapter 1. Preliminaries and Tools – Literature Survey	5
1.1. An Introduction to Distillation	5
1.1.1. Motivation	5
1.1.2. Zeotropic Distillation.....	5
1.1.3. Azeotropic and Reactive Distillation.....	6
1.2. Multiple Steady States.....	8
1.2.1. Definition of Multiplicities in Distillation.....	8
1.2.2. Multiplicities and the Column Configuration.....	8
1.3. Tools for Distillation Design and Analysis	9
1.3.1. Simple Distillation Residue Curves.....	9
1.3.2. Distillation Lines	10
1.3.3. Topological Classification of Residue Curve Maps	10
1.3.4. Column Profiles at Infinite and Total Reflux	13
1.3.5. ∞/∞ Analysis	14
1.3.5.1. Existence of Multiple Steady States (Bekiaris et al. (1993)).	16
1.3.5.2. Analysis	20
1.3.5.3. Geometry of the Distillation Boundaries.....	22
1.3.5.4. Appropriate Feed Composition	23
Chapter 2. Multiple Steady States: A Review	25
2.1 MSS in Azeotropic Distillation	25
2.1.1 Early Contributions: Analysis and Simulation	25
2.1.2 Heterogeneous Simulation Studies Reporting MSS.....	26
2.1.3. From Homogeneous to Heterogeneous System Analysis.....	27
2.1.4. Experimental Verification of Multiple Steady States.....	28
2.1.5. Various Studies on Multiple Steady States.....	29
2.2 MSS in Reactive Distillation	30
Chapter 3. Multiple Steady States in Reactive Distillation - Non-Hybrid ∞/∞ Analysis	33
3.1 Introduction to Reactive Distillation	33
3.1.1 Motivation	33
3.1.2 Assumptions, Definitions and Literature.....	33

3.1.3 Multiple Steady States in Reactive Distillation	34
3.2 Non-Hybrid Column Profiles	35
3.2.1 Reactive Composition Transformation.....	35
3.2.2 Feasible Non-Hybrid ∞/∞ Profiles	36
3.3 Non-Hybrid Reactive ∞/∞ Analysis	38
3.3.1 Non-Hybrid ∞/∞ Bifurcation Analysis.....	38
3.3.2 Non-Hybrid MSS Feed Region Condition	39
3.3.3. ∞/∞ Singularity Analysis.....	40
3.3.3.1 A United Approach to the Prediction of MSS	40
3.3.3.2 The Product Singularity Functions	40
3.3.3.3 Calculating Singularities in Practice.....	42
3.3.4. Reactive ∞/∞ Singularity Analysis.....	43
3.3.5. Non-Hybrid ∞/∞ Predictions: Inputs and Results	44
3.3.5 Implications for Finite Reactive Columns.....	45
3.4. Reactive ∞/∞ Procedures.....	45
3.4.1 Reactive Geometrical Multiplicity Condition	45
3.4.2 Non-Hybrid MSS Feed Region Construction.....	46
3.4.3 Back-transformation of the ∞/∞ Predictions	47
 Chapter 4 - Hybrid ∞/∞ Analysis	 48
4.1 Hybrid ∞/∞ Profiles	48
4.1.1 Preliminaries.....	48
4.1.2 ∞/∞ Assumptions for Hybrid Columns	49
4.1.3 Infinite Internal Flows and Infinite Column Length.....	49
4.1.4 Material Balances for Hybrid Columns.....	50
4.1.5 Feasible Hybrid ∞/∞ Profiles	52
4.1.6 Graphical Interpretation.....	52
4.2 Hybrid ∞/∞ Methods	54
4.2.1 The Exact Method	54
4.2.2 The Approximate Method	55
4.2.3 Discussion of the Reactive Methods	57
4.2.4 Possible Physical Causes	58
4.3. A Fictitious Example System	59
4.3.1 Thermodynamic Description	59
4.3.2 Hybrid ∞/∞ Bifurcation Analysis.....	60
4.3.3 Hybrid MSS Feed Region	64
4.3.4 Discussion of the Physical Cause	65

Chapter 5 – Previous studies regarding TAME synthesis system	66
5.1 Analysis of the TAME Process (Güttinger (PhD thesis, 1998))...	66
5.1.1. Thermodynamics and Process Description.....	66
5.1.2 Non-Hybrid ∞/∞ Bifurcation Analysis.....	68
5.1.3 ∞/∞ Favorable TAME Feed Locations.....	69
5.2. Residue curve maps for heterogeneously catalysed reactive distillation of fuel ether TAME	70
Chapter 6 – Application of the infinite/infinite analysis to the TAME synthesis	78
6.1. Analysis of the chemical non-equilibrium system – non-hybrid case	78
6.2. Analysis of the chemical non-equilibrium system in a hybrid distillation column	98
Conclusions	108
References	109

Chapter 1. Preliminaries and Tools – Literature Survey

1.1. An Introduction to Distillation

1.1.1. Motivation

Most of the chemical industrial processes consist of two basic tasks: chemical reaction and product separation. In contrast to the frequent opinion that separation is the less substantial task of both, Humphrey (1995) adequately stresses the economical and ecological importance of the separation task:

“Separation processes are the main cog in the manufacturing wheel of the chemical process industries. They are used for such essential chores as removal of contaminants from raw materials, recovery and purification of primary products, and elimination of contaminants from effluent water and air streams.” Distillation is the most used separation process and it represents a point of reference in the comparison with the other alternatives that can be approached; although it has a very good performance, it requires the consumption of high amounts of energy.

The key of any separation process is its primary mass-separating agent, which can be an additional chemical species (as for absorption, extraction, and stripping processes), a membrane (membrane separations) or energy in form of heat (as for distillation or crystallization). By definition, distillation processes separate chemical components of a fluid mixture based on their different boiling points by adding and removing heat for evaporation and condensation.

Distillation is the most common unit operation in the chemical process industries. It has an extensive product history and is still reported as “the method of choice for many separations and the method against which other options must be compared” (Kunesh et al., 1995; Kister, 1997). Humphrey’s (1995) estimates for the United States consist of 40’000 distillation columns in operation, which handle more than 90% of all separations for product recovery and purification. The capital investment for these distillation systems is reported to be at least $8 \cdot 10^9$ US\$. Since distillation is by far the dominant separation process, the reader is referred to the literature mentioned for a detailed treatment of its advances.

The motivation for research in distillation originates from its serious drawbacks: Distillation columns tend to use huge amounts of energy because of the evaporation steps involved. Typically, more than half of the process heat distributed to plant operations ends up in the reboilers of distillation columns (Kunesh et al., 1995). By this, high-level energy is fed at the base of the column and about the same amount of energy is released at the top, unfortunately at a much lower temperature level. The difference between the two Gibbs energies can be seen as the necessary energy investment to reverse the mixing entropy and to separate the components of a given feed by a distillation process (Kaibel and Blass, 1989). Often, the energy feed cannot be used for heat integration but is discharged to the atmosphere.

1.1.2. Zeotropic Distillation

The driving force for any separation by distillation is the difference between the compositions of a component in the liquid phase, x_i , and the vapour phase in equilibrium, y_i . In vapour-liquid equilibrium (VLE, bubble—point formulation), the vapour composition y and the bubble-point temperature T are implicit functions of the liquid composition x and the system pressure p :

$$[y, T] = VLE(x, p) \quad (1.1)$$

If $y_i > x_i$ for any component in the mixture, this component is enriched in the vapour phase. As long as the inequality holds, the component can be further purified in the vapour by repeatedly evaporating a part of the liquid followed by condensation of the resulting vapour until,

theoretically, the pure component is obtained. If the driving force, $x - y(x)$, is zero for some composition x , a singular point of the vapour-liquid equilibrium relationship is obtained. Obviously, pure components, where only one species is present, belong to the set of singular points of a mixture. If this set only consists of all pure components of the entire physical meaningful composition space, the mixture is called to behave zeotropic. Theoretically, any given feed composition of such a mixture could be separated into its pure components by means of distillation (although an infinite amount of energy or capital investment may be needed), since it is always possible to enrich one component in the vapour and reduce its fraction in the liquid. A c -component mixture is called ideal if both the liquid and vapour phase are ideal mixtures of ideal components. Thus, the partial pressure of component i , p_i , in the vapour phase is proportional to its mole fraction in the vapour phase (Dalton's Law), and proportional to its mole fraction in the liquid phase (Raoult's Law). A McCabe—Thiele diagram of a binary ideal mixture is shown in Figure 1.1a. Zeotropic mixtures not following Raoult's Law are denoted non-ideal mixtures (Figure 1.1b). The separation of ideal multicomponent systems has been topic of intensive research and most of the results can be found in standard chemical engineering textbooks.

1.1.3. Azeotropic and Reactive Distillation

Azeotropes are singular points in the VLE relationship (1.1) beside of the pure components. They are denoted binary, ternary or quaternary (etc) according to the number of components involved. Since the driving force is zero at azeotropic points, azeotropes cannot be separated by conventional distillation. An azeotrope is called minimum-boiling if its boiling point temperature is lower than those of all pure components involved (Figures 1.1c and d). Maximum and intermediate boiling azeotropes are defined in a straightforward manner.

The problem of separating binary azeotropic mixtures has lead to enhanced distillation techniques (Stichlmair et al., 1989). If pressure-swing distillation cannot be used to shift the composition of the azeotrope (Fien and Liu, 1994), there are four basic methods remaining to separate a binary azeotrope through distillation (Laroche et al., 1991). Depending on the action of the additional component, the entrainer, which is introduced as an extra mass separating agent (despite of heat), the following process types can be distinguished:

Salted Distillation: The entrainer dissociates into ions and changes the chemical potential and thus the azeotropic composition in the solution. This process type allows an azeotropic mixture to be separated in a column sequence.

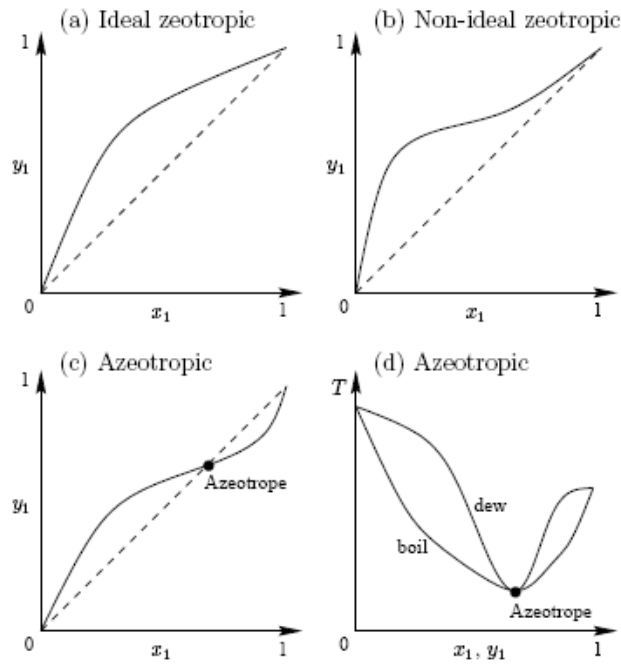


Figure 1.1: Illustrations of the VLE of binary mixtures. McCabe--Thiele diagrams of (a) an ideal zeotropic mixture, (b) a non--ideal zeotropic mixture, and (c) a minimum boiling azeotropic mixture. (d) shows the T - x,y diagram of the azeotropic mixture.

Heterogeneous Azeotropic Distillation: The entrainer induces a phase-split and introduces a heterogeneous azeotrope with one of the original components. This azeotrope must be lower boiling than the azeotrope to separate in order to make the separation in a decanter feasible.

Homogeneous Azeotropic Distillation: The entrainer does not induce a phase-split and the mixture remains homogeneous, i.e., there is a single liquid phase throughout the composition space. If the entrainer does not introduce additional azeotropes, the following three general separation schemes exist, depending on the boiling point of the entrainer (Laroche et al., 1991; 1992a; 1992b):

Heavy Entrainer: The entrainer is the heaviest boiling component in the system. This process is also known as *extractive distillation* and is widely spread in industry.

Intermediate Entrainer: The entrainer is intermediate boiling compared to the two components forming the azeotrope.

Light entrainer: The entrainer is the lightest boiling component in the system and introduces a curved boundary. These separation schemes can be generalized if the entrainer introduces additional azeotropes.

Reactive (Catalytic) Distillation: The entrainer undergoes reversible chemical reactions with one or more of the other components present (or acts as a catalyst for a reaction), thereby overcoming the azeotrope.

Azeotropic distillation is one of the most widely used and important separation processes in the chemical and specialty chemical industries. Moreover, reactive distillation has gained increasing importance during the last decade. Among the surprising features of both azeotropic and reactive distillation, multiple steady states have been discovered.

1.2. Multiple Steady States

1.2.1. Definition of Multiplicities in Distillation

Definition 1 (Multiple Steady States in Single Columns:) By multiple steady states (MSS) in a distillation column we refer to output multiplicities, i.e., that a column of a given design exhibits different column profiles (and therefore different product compositions) at steady state for the same set of inputs and the same values of the operating parameters.

For a given column design (number of stages, feed locations, column pressure, type of condenser and reboiler), a given feed flowrate F , composition x^F and quality (e.g. temperature T^F), there are two degrees of freedom for a homogeneous two-product distillation column (Figure 1.2 and Appendix B). If the distillate flowrate D and the reboiler heat duty Q_r are selected as the operating parameters, more than one steady state may exist in terms of the product compositions x^D and x^B (the outputs) for given values of D and Q_r (the inputs). This phenomena is denoted an output multiplicity and will be referred to as multiple steady states (MSS) hereafter.

Note that MSS belong to the general mathematical notion of multiplicities, where a system of equations with as many parameters specified as there are degrees of freedom exhibits different solutions at steady state. Additionally, two different types of multiplicities can be found in the distillation literature (Jacobsen and Skogestad, 1991; Bekiaris et al., 1993):

Input multiplicities: If a column of a given design with given feed (F , x^F , T^F) exhibits input multiplicities, the same product compositions x^D and x^B can be achieved for different values of the operating parameters (e.g. D and Q_r , Figure 1.2). This type is quite frequent in azeotropic and reactive distillation and has mainly economical importance (Laroche et al., 1992b).

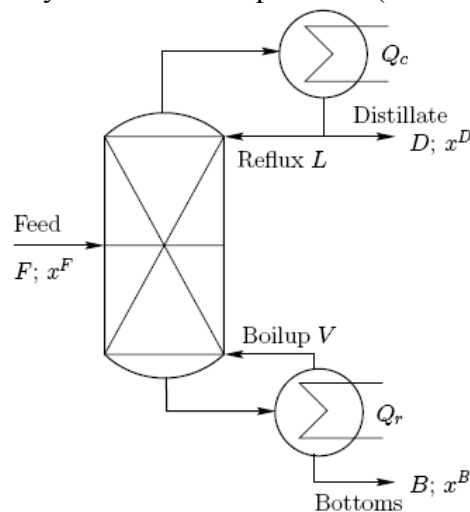


Figure 1.2: A homogeneous, two-product distillation column.

(Internal) state multiplicities: State multiplicities are a special case of output multiplicities where more than one solution with identical product compositions x^D and x^B exist for the same inputs and operating parameters. These solutions do only differ by the column profiles (excluding the products).

In general, MSS can exist in a single apparatus, e.g. a distillation column, or they can occur in interlinked columns or column sequences (Vadapalli and Seader, 1997). Note that MSS are also known in chemical reactors for specific exothermic reactions (Schmitz, 1975), e.g. in the industrial production of ammonia (Morud, 1996).

1.2.2. Multiplicities and the Column Configuration

Definition 1 (MSS) is formulated from a mathematical, steady-state point of view. In terms of control, any homogeneous distillation column can be viewed as a 5-by-5 multiple-input-

multiple-output system (Figure 1.2). Five manipulated variables (e.g. L , D , B , Q_r and Q_c) can be used to control the column pressure, the levels of the reflux drum and the reboiler as well as all the product compositions (Jacobsen et al., 1991). The feed flowrate, composition and quality are assumed to be given. They act as the major source of disturbances.

The set of the two operating parameters selected to control the product purity is denoted by the configuration of a distillation column – the remaining three operating parameters are needed to stabilize the levels of the reflux drum and the reboiler, and to control the pressure (or the operation of the condenser). Assume that the pressure at the top of the column is given and that perfect pressure control is achieved. Configurations are indicated by squared brackets, e.g. $[D^M, Q_r]$ is the configuration where the distillate flowrate (on a mass basis) and the reboiler heat duty are used for operating the distillation column.

Again, perfect control is assumed for the two remaining loops manipulating L and B to stabilize the levels. As a consequence, the existence of MSS as defined above fundamentally depends on the column configuration.

1.3. Tools for Distillation Design and Analysis

1.3.1. Simple Distillation Residue Curves

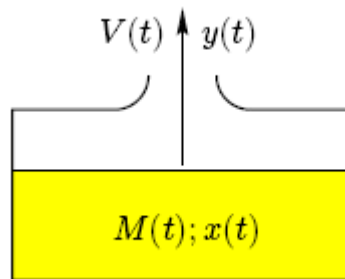


Figure 1.3: Batch still for an open—evaporation process (simple distillation).

The first reports about simple distillation residue curves have been published early in this century (Ostwald, 1900; Schreinemakers, 1901). Since then, residue curves have become the standard tool for design and analysis of azeotropic distillation columns. Recent reviews have been published by Fien and Liu (1994) and Widagdo and Seider (1996).

Consider the batch still shown in Figure 1.3 where an open evaporation process (simple distillation) takes place. The still is loaded with an initial amount $M(t=0)$ of moles of liquid with composition $x(t=0)$. It is assumed to be perfectly mixed. By gradual heating, the vapour y in equilibrium with x is continuously removed. A residue curve is defined as the locus of the liquid composition $x(t)$ remaining at any given time t in the still (the “residue”). A material balance provides (Doherty and Perkins, 1978a; Westerberg and Wahnschafft, 1996):

$$\begin{aligned} \frac{d}{dt}(x_i M) &= x_i \frac{dM}{dt} + M \frac{dx_i}{dt} = -y_i V \quad i = 1..(c-1) \\ \frac{dM}{dt} &= -V \end{aligned} \quad (1.2)$$

Combining these two equations one gets:

$$M(t) \frac{dx_i}{dt} = V(t)(x_i - y_i(x)) \quad i = 1..(c-1) \quad (1.3)$$

Since the vapour flow $V(t)$ is an arbitrary (but strictly positive) function of time (the heating policy), the differential equation is non-autonomous. In order to obtain an autonomous formulation, the dimensionless “warped” time ξ is introduced (Doherty and Perkins, 1978a):

$$\xi(t) = \ln\left(\frac{M(0)}{M(t)}\right) = \frac{V(t)}{M(t)}t \quad (1.4)$$

resulting in the final formulation:

$$\frac{dx_i}{d\xi} = x_i - y_i(x) \quad i = 1..(c-1) \quad (1.5)$$

Since $V(t) > 0$, $M(t)$ decreases in time (equation 1.2). By equation (1.4), $\xi(t)$ is monotonically increasing as a function of time. By convention, increasing time is used as the direction of the residue curves. Although residue curves of homogeneous mixtures have been established to point in direction of increasing temperature, this result is questionable for heterogeneous mixtures (Doherty and Perkins, 1978a; Pham and Doherty, 1990). The other results presented here can be applied to heterogeneous mixtures by replacing the two-phase VLE with a three-phase VLLE calculation.

From a mathematical point of view, equations (1.5) represent a system of nonlinear, autonomous ordinary differential equations (ODE’s), which can be integrated over the dimensionless time ξ . The resulting solution trajectory of the system is a single residue curve.

1.3.2. Distillation Lines

Unfortunately, distillation lines, which have first been reported in the Russian literature (Zharov, 1968; Zharov and Serafimov, 1975), are not uniquely defined. However, the concept originates from the description of tray columns operated at total reflux. Zharov and Serafimov (1975) define a distillation line as the set of points x whose vapour composition in equilibrium, $y(x)$, also lies on the same line. Exact distillation lines are hard to obtain, but a sequence of points lying on the same line can be calculated applying the following recursion formula forward and backward (Stichlmair et al., 1989; Stichlmair and Herguijuela, 1992):

$$x^{t+1} = y^t(x^t) = VLE(x^t) \quad (1.6)$$

Distillation lines are not coinciding with residue curves but have very similar properties – detailed comparisons have been given by Bekiaris et al. (1996) and Widagdo and Seider (1996). Distillation lines and residue curves exhibit identical singular points and behave similarly in the vicinity of those points (Zharov and Serafimov, 1975).

1.3.3. Topological Classification of Residue Curve Maps

A residue curve (RC) map is a plot of several residue curves in the phase diagram and illustrates the basic properties of the vapour-liquid equilibrium (VLE). For ternary mixtures, the phase diagram is the unit triangle (a two-dimensional simplex); for quaternary mixtures the unit tetrahedron (three-dimensional simplex).

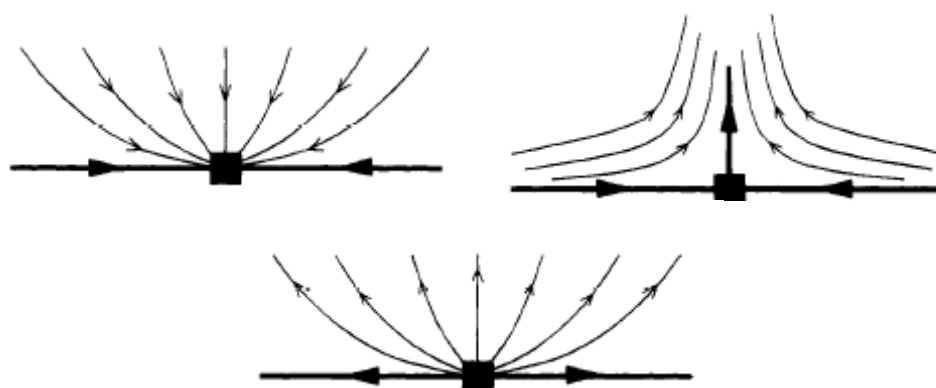
Apart from experimentally using the simple batch still, we can also generate RCs mathematically, by integrating the mass and energy balances and thermodynamic equilibrium relationships that describe this simple still. *Vertices* are the so-called “singular solutions of these mathematical expressions and the collective topological name for azeotropes and pure components.

In the case of ternary azeotropic systems, the presence of azeotropes divides the triangular diagram into separate *distillation regions* by introducing “distillation boundaries”. The binary azeotropes are located on the edges of the triangular diagram, while ternary azeotropes are located inside the triangle. *Minimum-boiling azeotropes* have a lower boiling point than that of any of the components involved, while *maximum-boiling azeotropes* have a higher boiling point. Much theoretical research has been conducted to investigate azeotropy in multicomponent mixtures, notably in a series of papers by Doherty and Perkins (1978a,b, 1979a, 1982) and by Van Dongen and Doherty (1984). Others (Gani, 1993; Matsuyama and Nishimura, 1977) have applied the field of mathematical topology and index theory to find relationships in RCMs, leading to the theory of “nodes and saddles”. This theory suggests some heuristic guidelines for the construction of fairly accurate RCMs from *minimal* data. These data include the boiling temperatures of all components in the mixture, as well as the boiling temperatures and compositions of all occurring azeotropes. Applying the heuristic guidelines, in most cases, enables us to construct RCMs, *without* requiring the explicit numerical integration of component mass/energy balances and thermodynamic equilibrium equations.

It has been established that RCs point toward increasing temperature. This implies that they “diverge” from low-boiling vertices (pure components or azeotropes) and converge toward high-boiling vertices.

At the same time, intermediate-boiling vertices exist, at which no RC ever starts or ends. From now on, we shall call the starting and end points of RCs “*nodes*”, and all other vertices “*saddles*”. Nodes are either “stable” or “unstable” (Figure 6). A stable node is like a valley, in which a rolling ball will settle down in a stable position; all RCs in a distillation region point toward (arrive at) a stable node. In any distillation region, the highest-boiling vertex is a stable node. An unstable node is analogous to a mountain top, from which a ball will roll down toward a more stable position. In any distillation region, the lowest-boiling vertex is an unstable node, from which all RCs in that region will start. A saddle point, as shown in Figure 7, has no RCs coming in or going out. Moving in one direction along the triangle edge is like going downhill (toward a stable node), while going in another direction resembles going uphill (toward an unstable node).

In order to determine the nature of pure-component vertices, arrows are drawn on every segment of the ternary diagram's outer border, between pure components and binary azeotropes, and let these point toward the segment end with the highest boiling temperature. Stable nodes will only have arrows pointing inward, unstable nodes will have all arrows pointing outward, and saddles will have some arrows pointing inward and some pointing outward.



If a ternary azeotrope exists, it is important to determine its nature as a node or a saddle. Foucher et al. (1991) stated that a *ternary saddle azeotrope* must always have four connections to other vertices: two higher-boiling and two lower-boiling vertices. If these connections are not available, the ternary azeotrope must be a node. Thus, a ternary azeotrope is a node (**I**) if it is one of the two highest-boiling or the two lowest-boiling species (excluding pure-component

saddles) in the system or **(2)** when the sum of the number of pure-component nodes and the number of binary azeotropes is smaller than 4. Otherwise, the ternary azeotrope is a saddle.

Not all combinations of azeotropes can freely exist, due to thermodynamic and topological constraints. Matsuyama and Nishimura (1977) reduce the total number of possible configurations to 113, by making the assumption that there can be at most one ternary azeotrope per system and one binary azeotrope per triangle edge.

Matsuyama and Nishimura (1977) find that ternary systems can be classified according to their number and type of azeotropes. Of the three digits, the first one corresponds to the A-B binary pair, the second one to the B-C pair, and the third one to the A-C pair, where A, B, and C represent the lowest-, intermediate-, and highest-boiling components, respectively. The meaning of the digits is:

- 0: no azeotrope
- 1: binary minimum-boiling azeotrope - *unstable node*
- 2: binary minimum-boiling azeotrope - *saddle*
- 3: binary maximum-boiling azeotrope - *stable node*
- 4: binary maximum-boiling azeotrope - *saddle*

If a ternary azeotrope is present, the three-digit code is followed by one of three letters:

- m: minimum-boiling azeotrope
- M: maximum-boiling azeotrope
- S: intermediate-boiling azeotrope

The 87 RCM configurations that contain at least one minimum-boiling binary azeotrope are given in Doherty and Caldarola (1985). The cases most commonly encountered in industry are among those 87.

One illustrative example of a residue curve diagram is shown in Figure 1.4. The common fixed points of the equations (1.5) and (1.6) are the singular points of the corresponding residue curve (distillation line) map. They can either be pure components or azeotropes (Gurikov, 1958). The singular point of a residue curve map are the equilibria of equation 1.5, i.e, the solution of $0 = y(x) - x$. Thus, the singular points are the pure components and the azeotropes in the composition space. For the isobaric case, there are only isolated singular points. The singular points have real nonzero eigenvalues. They can be categorized as *stable nodes*, *unstable nodes*, and *saddles* (both positive and negative eigenvalues). The topology at these singular points is determined by the eigenvalues of (1.5), which are all distinct and real (Doherty and Perkins, 1978a). A stable node results if all eigenvalues are smaller than zero, an unstable node if all eigenvalues are larger than zero and a saddle singular point for mixed signs. A zero eigenvalue (not observed for the VLE) would result at a non-elementary singular point. Residue curves originate from unstable nodes and end at stable nodes. At saddles, residue curves end and start. By definition, residue curves do not intersect. Therefore, there are no closed cycles.

The following definitions apply (Serafimov et al., 1971; Bekiaris et al., 1996): A *distillation region* is a subset of the composition simplex in which all residue curves originate from the same, locally lowest-boiling singular point and end at the same, locally highest-boiling singular point. If there exists more than one node of the same kind (stable or unstable), there will be at least as many simple distillation regions as there are nodes of that same kind. The curves which separate different distillation regions are called *residue curve boundaries*. In this work, the term boundary is used for both residue curve boundaries and the edges of the composition simplex (Figure 1.5). At least one of the ends of a residue curve boundary must be a saddle. The residue curve map shown in Figure 1.4 has two simple distillation regions. The pure component L is the

only unstable node where all residue curves originate. The residue curves either end in pure I or pure H, which are the two stable nodes of this mixture. Thus, there are two simple distillation regions that are separated by the residue curve boundary, which originates from pure L and ends in the I-H azeotrope, the saddle of the system.

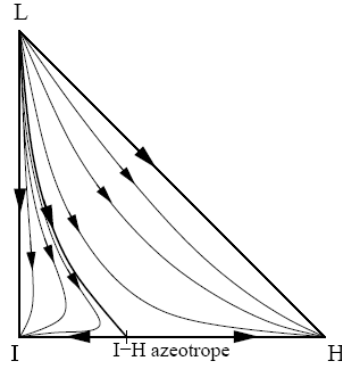


Figure 1.4: Residue curve map of the L, I, and H forming a 020 mixture (Matsuyama and Nishimura, 1977).

For a constant pressure, the temperature always increases along a residue curve, as one would expect to happen according to the original definition of residue curves. The liquid phase depletes in the more volatile components which increases the boiling temperature of the residue. If the boiling point temperatures are plotted over the composition space giving a temperature surface, the unstable nodes represent the local minima of this surface while the stable nodes represent the local maxima of this surface. The globally lowest (highest) boiling point is always at an unstable (stable) node.

The topological classification of binary mixtures is trivial: A mixture can exhibit a minimum boiling, a maximum boiling or no azeotrope. Note that the rare cases with multiple binary azeotropes or intermediate boiling azeotropes are excluded. Under the assumption of at most one ternary azeotrope present, the following topological equation relates the types and numbers of singular points for ternary mixtures (Gurikov, 1958; Doherty and Perkins, 1979):

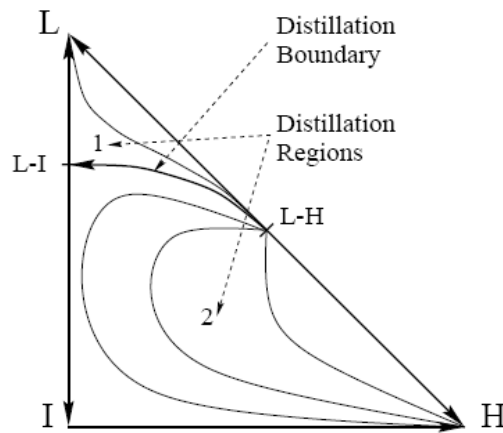


Figure 1.5: Illustration of a residue curve map for a mixture belonging to the 201 class. Types and numbers of singular points for ternary mixtures (Gurikov, 1958; Doherty and Perkins, 1979):

$$4(N^{(3)} - S^{(3)}) + 2(N^{(2)} - S^{(2)}) + (N^{(1)} - S^{(1)}) = 1 \quad (1.7)$$

where N refers to a node, S to a saddle and the superscripts indicate the number of components present at these singular points. For the example in Figure 1.4, $N^{(2)} = S^{(2)} = 1$, $N^{(1)} = 2$ and $S^{(1)} = 1$ and therefore, $4 \cdot 0 - 2 \cdot 0 + 2 - 1 = 1$.

1.3.4. Column Profiles at Infinite and Total Reflux

In this section, the conditions for feasible column profiles at *total* and at *infinite* reflux are reviewed. In general, feasibility of column profiles can be assigned to a real distillation plant (if the profile is measured) or to a distillation column model (steady-state solution profiles). The model of primary interest here is a distillation column at infinite reflux. In the following, it is important to point at the fundamental difference between total reflux and infinite reflux. Unfortunately, literature does often not differentiate between these two cases (Widagdo and Seider, 1996; Westerberg and Wahnschafft, 1996).

Total reflux is the limiting case of a distillation column with no feed and no product flows: $F = 0$, $D = 0$ and $B = 0$ (compare to Figure 1.2). Thus, the overall mass balance is fulfilled by definition and an external graphical lever rule does not exist. As a result, the molar reflux and boilup flows have identical finite flowrates at each column intersection. In total reflux, the profiles of packed distillation columns coincide with the residue curves (1.5) under the assumption that the liquid phase is perfectly mixed and thus, all the mass-transfer resistance is in the vapour phase (Serafimov et al., 1973; Pollmann and Blass, 1994).

Similar statements can be made for other assumptions on the mass-transfer resistances. By definition, the profile of a tray column at total reflux coincides with a distillation line. Unlike total reflux, *a column at infinite reflux exhibits infinite internal flows while the feed and product flowrates are not zero:* There are feeds entering the column and products withdrawn at the top and the bottom. Therefore, the overall and the component material balances have to be fulfilled for a feasible column design:

$$\begin{aligned} F &= D + B \\ Fx^F &= Dx^D + Bx^B \end{aligned} \tag{1.8}$$

As a result, the distillation lever rule can be applied to any operating point of such a column. However, the reflux and boil-up flowrates are infinitely large at any location along the column and thus, this case is also referred to as the limiting case of infinite internal flows.

Laroche et al. (1992a) have shown that the *differential equations describing the profile of a packed column at infinite reflux become identical to the residue curve equations* (1.5). Similarly and by definition, *the profiles of tray columns coincide with the distillation lines*. Moreover, the locations of the feeds entering a column at infinite reflux have no impact on the column profile (Petlyuk and Avetyan, 1971).

Feasibility of profiles at infinite reflux in a single column or a column sequence has been extensively studied in the literature, e.g. Laroche et al. (1992a; 1992b) and Westerberg and Wahnschafft (1996). Due to the similar properties of distillation lines and residue curves, *residue curves are considered to be a very good approximation to the profiles of homogeneous tray columns at infinite reflux* (Laroche et al., 1992a; Widagdo and Seider, 1996), which is not true for heterogeneous mixtures (Bekiaris et al., 1996). Since residue curves exactly describe profiles of packed columns and approximate tray columns, they will be used for both column types hereafter as long as the mixture is homogeneous (with no phase-split).

1.3.5. ∞/∞ Analysis

The ∞/∞ analysis is a framework that predicts possible *product paths* of a distillation column based on residue curve map information only. A product path is obtained by the continuation of solutions found by varying, for example, the distillate flow rate D from 0 to its maximum, the feed flow rate F . In general, this product path can be generated by either a series of case studies using a distillation column model implemented in a commercial simulator such as AspenPlus, or by a “continuation” of solutions using a simplified model (Güttinger, 1998) or a rigorous model as implemented in AspenPlus (Vadapalli and Seader, 1997). To predict the product path based

on residue curve map information only, two main simplifying assumptions¹ are necessary: Infinite reflux (internal flow rates) and infinite length of the column / number of trays.

Infinite Reflux. If a column is operated at infinite reflux, the composition profile of a packed column will follow a part of a residue curve (Van Dongen and Doherty, 1985; Laroche et al., 1992a). Hence, a feed F of composition x^F can be split into two products D and B with compositions x^D and x^B if x^D and x^B lie on one residue curve and are collinear with x^F according to the mass balance of the column (equation 1.8). This implies that the distillate and the bottom product have to lie in the same distillation region. Note that the feed composition x^F does not necessarily have to lie in the same distillation region. This represents one of the key features of the boundary separation scheme. For a column with trays, the composition profile follows a distillation line which has qualitatively the same properties as a residue curve (Bekiaris et al., 1996).

Infinite Length. For an infinitely long column, the profile must contain a *pinch*. In this context, the column profile contains a pinch if it exhibits a zone where the composition is constant. The most well known pinch in distillation is the pinch at minimum reflux. At this point, the number of stages goes to infinity.

Infinite Reflux / Infinite Length. The combination of these two asymptotic cases is the basis of the ∞/∞ analysis. If a column of infinite length is operated at infinite reflux, then the pinch must be a singular point in the residue curve map. This combination was studied first by Petlyuk and Avetyan (1971). About 20 years later, Bekiaris et al. (1993) developed this combination into a tool that can be used to predict the product path of distillation columns based on residue curve map information only. Using this framework, the existence of multiple steady states was predicted and explained for homogeneous azeotropic distillation columns (Bekiaris et al., 1993) and heterogeneous azeotropic distillation columns (Bekiaris et al., 1996).

There are three possible profiles for an ∞/∞ column (Bekiaris et al., 1993) which are shown in Figure 1.6:

Type I. The column profile is a type I profile if the distillate composition x^D is at the unstable node (L in this case). The column profile starts at L and follows the indicated residue curve until it is at x^B that is collinear with x^F and x^D . For a different split D/F , the profile would follow a different residue curve.

Type II. The column profile is a type II profile if the bottom composition x^B is at the stable node (H in this case). The column profile starts at an arbitrary point x^D that is collinear with x^F and x^B and follows the indicated residue curve until it is at the stable node (H in this case).

Type III. The column profile is a type III profile if the profile contains at least one saddle (the I-H azeotrope in this case). The column profile starts either at the edge of the triangle or on a residue curve boundary, as in this case. It follows the residue curve boundary, passes the I-H azeotrope, and ends somewhere at the binary I-H edge.

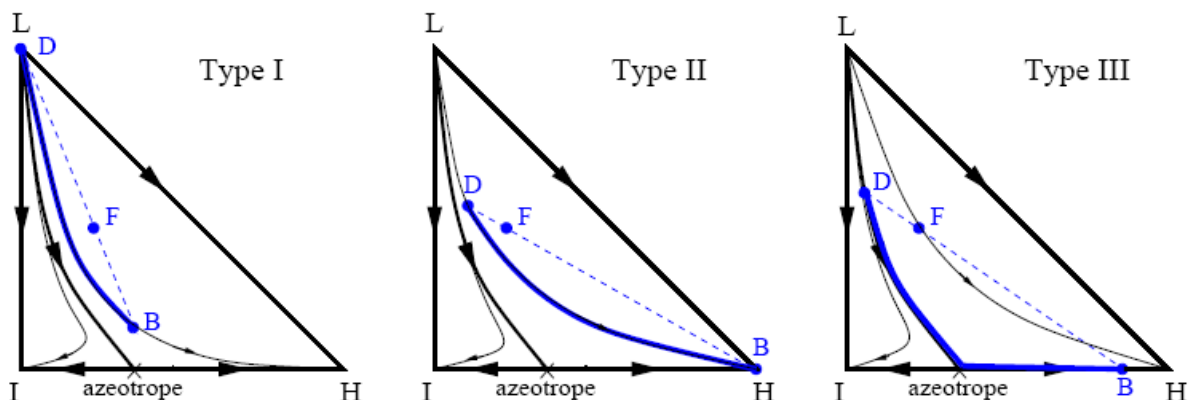


Figure 1.6: Three possible ∞/∞ column profiles illustrated for a 020 mixture.

For a given feed composition x^F and flow rate F , the distillate flow D , which is the only unspecified parameter, can be varied from 0 to F to track all possible product compositions x^D and x^B . This gives the product paths for the distillate and the bottom (Figure 1.7a). Figure 1.7b shows the distillate and bottom compositions x^D and x^B for a continuation of the parameter D/F . There are no multiple steady states.

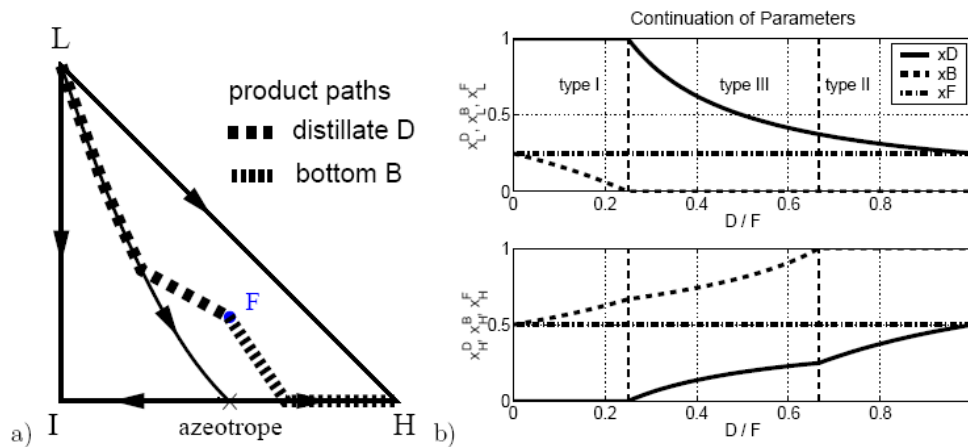


Figure 1.7: a) ∞/∞ product paths of the distillate and bottom composition for a 020 mixture, b) distillate and bottom compositions for a continuation of D/F .

Bekiaris et al. (1993) elaborated also a framework for homogenous distillation columns.

1.3.5.1. Existence of Multiple Steady States (Bekiaris et al. (1993))

This section presents a detailed study of the ∞/∞ case. For the analysis of this situation, a 001 class ternary mixture is used. Figure 1.8 shows the residue curve map of this type of ternary mixture. In this diagram, there is only one minimum boiling binary azeotrope between the light (**L**) and the heavy (**H**) component. The azeotrope is an unstable node, the light and the intermediate pure component corners are saddles, and the heavy component corner is a stable node. All residue curves start from the azeotrope and end at the heavy component corner; there are no interior distillation boundaries in this diagram and hence the whole triangle forms a single distillation region. At infinite reflux, column profiles coincide with residue curves. In the special case of columns with an infinite number of trays there is one additional requirement: The column profile should include a pinch point. There are four candidate pinch points in the residue curve map shown in Figure 1.8, namely the three pure component corners and the azeotrope. Therefore, in the ∞/∞ case, the only acceptable columns belong to one of the following types:

I. Columns whose distillate composition is that of the azeotrope (unstable node). In this case, the column profile **starts** from the azeotrope (top of the column), follows a residue curve, and ends at an arbitrary point on the same residue curve (bottom product).

II. Columns whose bottom product composition is pure heavy component (stable node). In this case, the column profile **starts** from an arbitrary point in the composition triangle, follows the residue curve that passes through this starting point, and ends at the heavy component corner (bottom product).

III. Columns whose composition profiles run along the edges of the triangle and contain at least one of the saddle corners (light and intermediate component corners). In this case, the top and bottom products lie on the edges of the triangle.

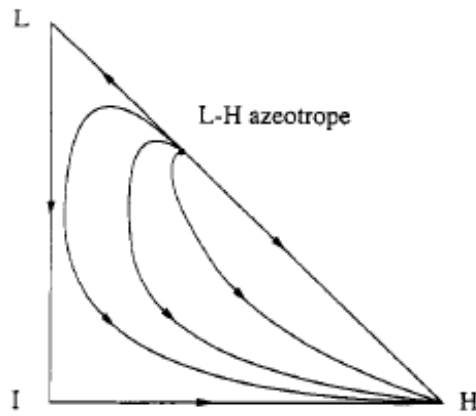
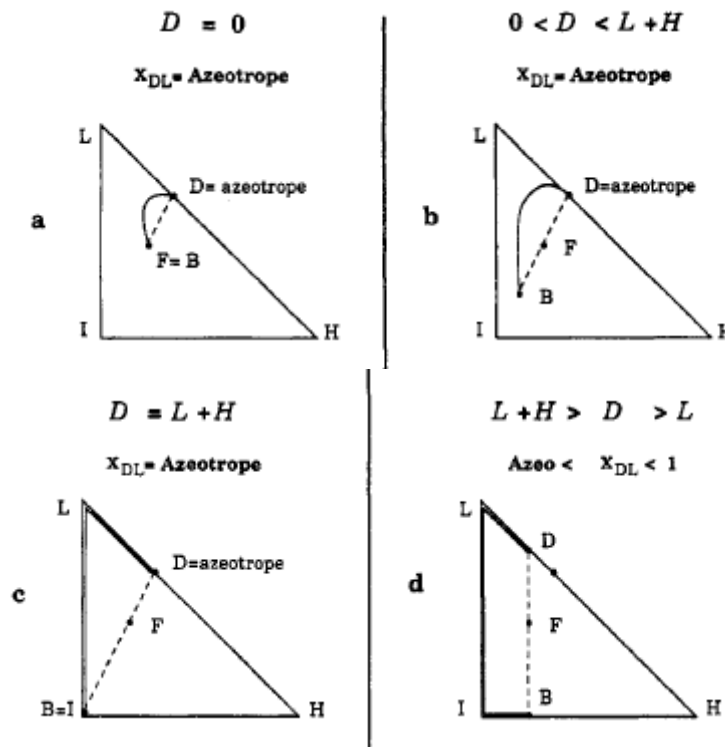


Figure 1.8. Residue curve diagram of a 001 class ternary mixture

In the ∞/∞ case, given a feed composition and a feed flow rate F , the only unspecified parameter is the distillate flow rate D (the bottom flow rate is $B = F - D$ from the overall material balance). In order to find whether multiple steady states can occur (i.e., whether different column profiles correspond to the same value of D), all the possible composition profiles are found by tracking the distillate and bottoms in the composition triangle, starting from the column profile with $D = 0$ and ending with the column profile with $D = F$, performing in this way a bifurcation study (continuation of solutions), using the distillate flow as the bifurcation parameter. This task can be achieved because in the ∞/∞ case a continuation of solutions can be carried out based on physical arguments only. The light component mole fraction in the distillate x_{DL} is recorded along this “continuation path.”



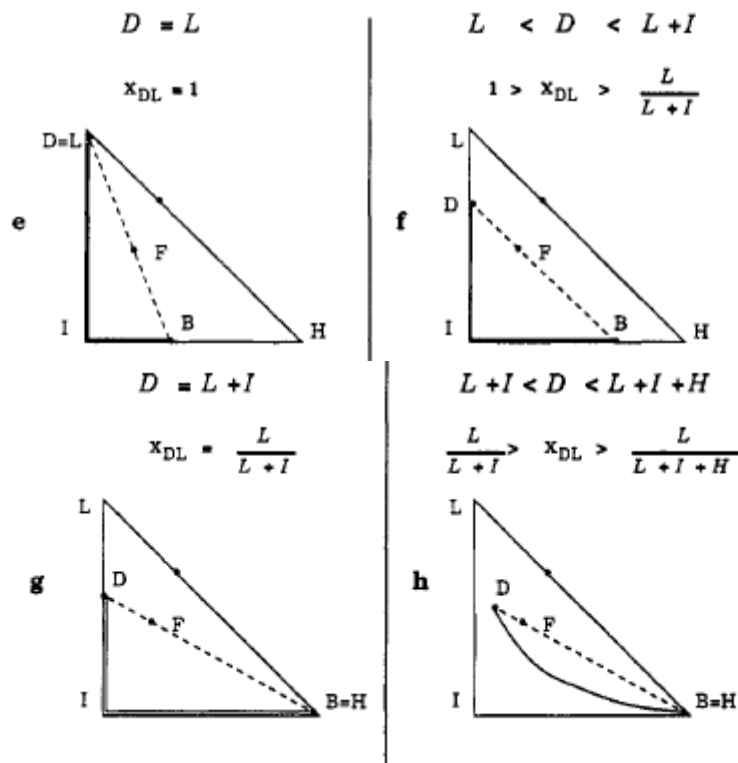


Figure 1.9. (a-h) Column profiles with infinite number of trays at infinite reflux.

The following analysis can be applied to any feed composition, but just for simplicity, it is assumed a feed that lies on the line connecting the azeotrope and the corner I. Therefore, $F = L + I + H$ and $L/(L + H)$ equals the azeotropic composition of the light component.

If $D = 0$, then $B = F = L + I + H$ and therefore the composition of the bottom product coincides with that of the feed F . Hence the bottom product composition is an interior point of the composition triangle (i.e., it does not lie on an edge). The only acceptable column profile (as defined above) that ends (bottom product) at an interior point of the triangle is the one that starts (top of the column) from the azeotrope and follows the residue curve that the bottoms composition lies on. This is a type I column profile. Figure 1.9a shows the column profile for $D = 0$. Therefore, in this case, $x_{DL} = L/(L + H)$ the azeotropic composition.

Using this as a starting profile, all possible type I column profiles are found for the given feed. Since, for this type of profile, the top of the column coincides with the azeotrope, the material balance line is a segment of the line connecting the azeotrope, the feed, and the intermediate component corner (for this particular choice of feed composition). Therefore the bottom composition (B) can be any point on the line segment between the feed F and the intermediate component corner (I).

Figure 1.9b illustrates a type I column profile with the characteristics mentioned before. As B moves along the FI line segment from F to I , the line BF continuously lengthens. Therefore, according to the lever material balance rule, the bottoms flow decreases monotonically from the initial F to I while the distillate flow will increase monotonically from initially 0 to $L + H$. The composition of L in the distillate (x_{DL}) for all type I column profiles is kept constant and equal to the azeotropic composition ($L/(L + H)$). Therefore, a column profile of type I (similar to that of Figure 1.9b) exists for $0 < D < H + L$.

Figure 1.9c shows the profile with the bottoms composition B located at the intermediate component corner (I) and the distillate composition located at the azeotrope. In this case, $D = H + L$ and $B = I$. Both B and D lie on an edge of the composition triangle, and therefore in this case the column profile belongs to type III. Using this as a starting profile, all possible type

III column profiles are found for the given feed. In this type of profiles, both D and B must lie on the edges of the triangle. There are two alternative routes: B should move along either the IL edge or the IH edge. In the first case, the material balance implies that D has to move on the line segment between the azeotrope and the heavy component corner (HI). This is not allowable though because there is no residue curve connecting D and B. In the second case, D has to move along the line segment between the azeotrope and the light component corner while B lies on the IH edge. In this case, there is a residue curve connecting B and D.

Figure 1.9d illustrates such a column profile. Since D lies on the LH edge, the composition of the intermediate component I in the distillate is zero and therefore the whole amount of I fed into the column is recovered in the bottom product. Because B lies on the IH edge, there are some amounts of heavy component in the bottom product while the whole amount of L fed is recovered entirely in the distillate. Therefore $B > I$ and consequently $D < H + L$. As D moves along the LH side from the azeotrope to the light component corner, the amount of the heavy component in the distillate decreases and consequently the distillate flow decreases monotonically from $L + H$ to L (when D is located at the light component corner). Therefore, a column profile of type III similar to that shown in Figure 1.9d exists for $L + H > D > L$. Since all the light component fed is recovered in the distillate, $x_{DL} = L/D$. Therefore, along this part of the continuation path, the light component concentration in the distillate increases monotonically from $L/(L + H)$ to 1.

Figure 1.9e shows the profile with the distillate composition D located at the light component corner (L). In this case $D = L$ and $B = I + H$. As B moves further along the IH side toward the H corner, D moves along the LI edge toward the I corner. Figure 1.9f illustrates such a type III column profile. In this case, D contains no heavy component, some amount of the intermediate component, and all the light component fed. Consequently, B contains no light component, some amount of the intermediate component, and all the heavy component fed into the column. As B moves along the IH edge toward the heavy component corner, the bottom product flow decreases monotonically from the initial $I + H$ to H (when B is located at the H corner). Consequently along this part of the continuation path the distillate flow increases monotonically from L to $L + I$. Therefore a column profile of type III similar to that shown in Figure 1.9f exists for $H < D < I + H$. Along this part of the continuation path, $x_{DL} = L/D$ and hence x_{DL} decreases monotonically from 1 to $L/(L + I)$.

Figure 1.9g shows the column profile with the bottoms composition B located at the heavy component corner (H). In this case $B = H$, $D = L + I$, and $x_{DL} = L/(L + I)$. B is not allowed to move along the HL edge because a residue curve connecting B and D does not exist. Therefore all type III profiles have been found.

The last case to be examined is the type II profiles. In this case the bottoms product composition is 100 % heavy component (H corner). Therefore, the material balance line lies on the line connecting the feed F and the heavy component corner H. Hence, the distillate composition D can be any point on this line between the feed F and the LI edge. Figure 1.9g shows a type II column profile with the characteristics mentioned before. As D moves toward F, the length of DF decreases. Therefore, according to the lever material balance rule, the distillate flow increases monotonically from the initial $I + L$ to $I + L + H (=F)$ while the bottoms flow decreases from H to zero. Therefore a column profile of type II similar to that shown in Figure 1.9h exists for $I + L < D < I + L + H = F$. Along this part of the continuation path, the composition of L in the distillate decreases from $L/(L + I)$ to $L/(L + I + H)$ according to the rule $x_{DL} = L/D$. Finally, the endpoint of this exhaustive search for all possible column profiles is the column profile with $D = F$, $B = 0$ and $x_{DL} = x_{FL}$.

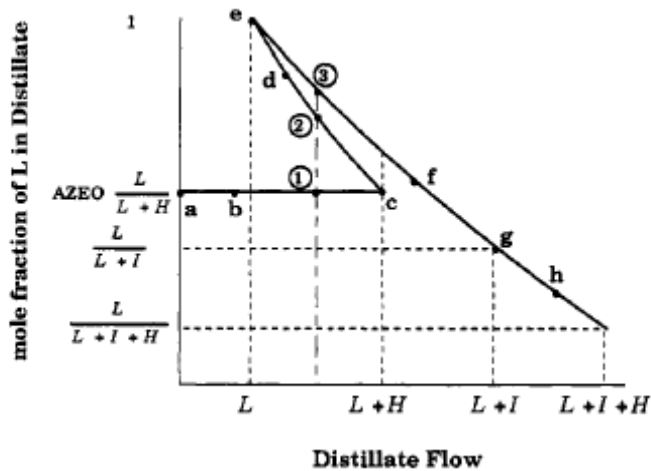


Figure 1.10. Composition of L in the distillate along the continuation path.

Gathering all the results obtained, the diagram presented in figure 1.10 is obtained, plotting x_{DL} vs D . In the beginning as D increases from zero to $L + H$, x_{DL} remains constant at $L/(L + H)$ (the azeotropic composition). Then D decreases from $L + H$ to L while $x_{DL} = L/D$ and therefore increases from $L/(L + H)$ to 1. Then D increases again from L to $L + I$ and finally to F while $x_{DL} = L/D$ and hence decreases from 1 to $L/(L + I)$ and finally to L/F (the feed composition). In Figure 1.10, the points a-h correspond to the column profiles shown in Figures 1.9a- 1.9h. Figure 1.10 shows that for D between L and $L + H$ there are three steady states (points 1-3):

- Point 1 always corresponds to a column profile of type I like the one depicted in Figure 1.9b.
- Point 2 always corresponds to a type III column profile where the distillate composition lies on the line segment between the azeotrope and L (similar to Figure 1.9d).
- For point 3 there are two cases:
 - (i) If $I < H$ and $D > L + I$, then point 3 corresponds to a type II column profile (similar to that of Figure 1.9h).
 - (ii) In the case that $I > H$ (Figure 1.10) as well as in the case that $I < H$ but $D < L + I$, point 3 corresponds to a type III column profile where the distillate composition lies on the LI edge (similar to that in Figure 1.9f).

In this analysis, a special choice of feed composition has been used. It is very simple to apply the same procedure to any feed composition and prove that for any feed composition inside the composition triangle three steady states exist. Therefore, for this class of residue curve diagrams, namely the 001 class, three steady states exist for any feed composition. Moreover, in this case the existence of multiplicities is independent of the thermodynamic model used to describe the vapour-liquid equilibrium.

Given any ternary mixture, its residue curve diagram, and a feed composition, it is very simple to conclude whether multiple steady states can occur in the ∞/∞ case by applying the procedure described above.

1.3.5.2. Analysis

In the previous section, a “path” generating all possible column profiles has been generated, starting from the column profile with $D = 0$ (type I) and ending at the column profile with $D = F$ (type 11). In the beginning D increases, then decreases, and then increases again. The key feature that brought about the multiple steady states is that in a segment along this “path” D decreased. Any distillation region containing n ($n \geq 3$) singular points is an n -polygon. In every distillation region there is one unstable node (the origin of all residue curves in the region), one stable node

(the endpoint of all residue curves in the region), and $n - 2$ saddles. Finally, it is assumed that F is an interior point of a distillation region. It is easy to show that, for feeds on a straight distillation region boundary, D cannot decrease along the continuation path. This is the case for any feed located on the edges of the triangle (binary feeds) in Figure 1.8.

Using the arguments which were discussed in the previous section, the following can be proven:

Fact 1. Along the continuation path, D increases monotonically as we track all type I and type II column profiles.

Therefore, a decrease in D can only occur as we track the type III column profiles, i.e., columns whose composition profiles run along the edges of the distillation region where F is located and contain at least one of the saddle singular points. In this case, the top and bottom products lie on the edges of the distillation region.

Fact 2. Along the continuation path, D increases monotonically for all type III column profiles that contain only one saddle singular point.

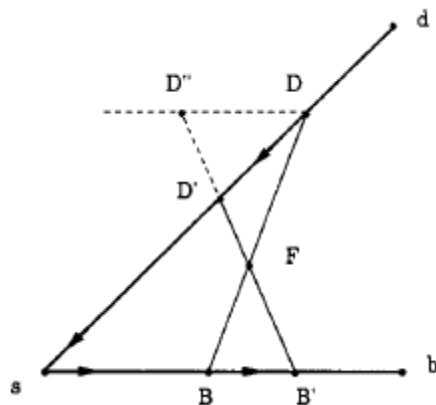


Figure 1.11. Monotonic increase of D for column profiles that contain only one saddle singular point.

Figure 1.11 shows a column profile (DsB) that contains only one saddle point. The lines ds and sb are distillation region boundaries. The arrows on ds and sb show the direction of the residue curves; this direction coincides with the direction of the continuation path. $D'sB'$ is another, “later,” column profile along this path. Drawing the line that is parallel to BB' and passes through D , D'' is obtained, which is the point where this line intersects the $D'B'$ line. By construction, $FB/DF = FB'/D''F$. Since $D''F > D'F$, then $FB/DF < FB'/D'F$. Therefore, by the lever material balance rule, it is concluded that D increases along the continuation path. This result is independent of the angle dsb , and therefore D increases monotonically for all type III column profiles that contain only one saddle singular point.

Fact 2 is equivalent to the following:

Fact 3. A decrease in D can only occur as we track type III column profiles that contain at least two saddles.

Two consequences of fact 3 are the following:

1. If multiplicities exist, one of the multiple steady state profiles will contain at least two saddles.
2. A necessary condition for the existence of this type of multiplicities is that the residue curve diagram contains at least two neighboring saddles.

The situation of at least two neighbouring saddles arises in 77 out of the 113 possible residue curve diagrams (as classified by Matsuyama and Nishimura (1977)). Among the residue curve diagrams that do not contain two neighbouring saddles are the ideal case (000 class) and the case of a heavy entrainer that does not introduce any additional azeotropes (100 class), which are depicted in Figure 1.12.

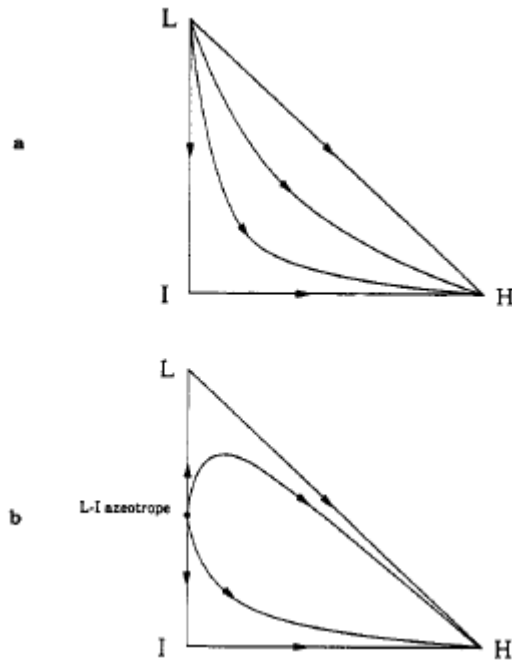


Figure 1.12. Residue curve diagrams of (a) a 000 class and (b) a 100 class ternary mixture.

No more than three steady states can exist in the case of two neighbouring saddles while for certain feed compositions it is possible that more than three steady states exist in the case of more than two neighbouring saddles.

However, the condition of at least two neighbouring saddles is not sufficient for the existence of multiple steady states. There are two additional requirements.

1.3.5.3. Geometry of the Distillation Boundaries

The existence of multiplicities depends on the geometry of the distillation boundaries that form the two saddles. Figure 1.13 illustrates two cases of two neighbouring saddles.

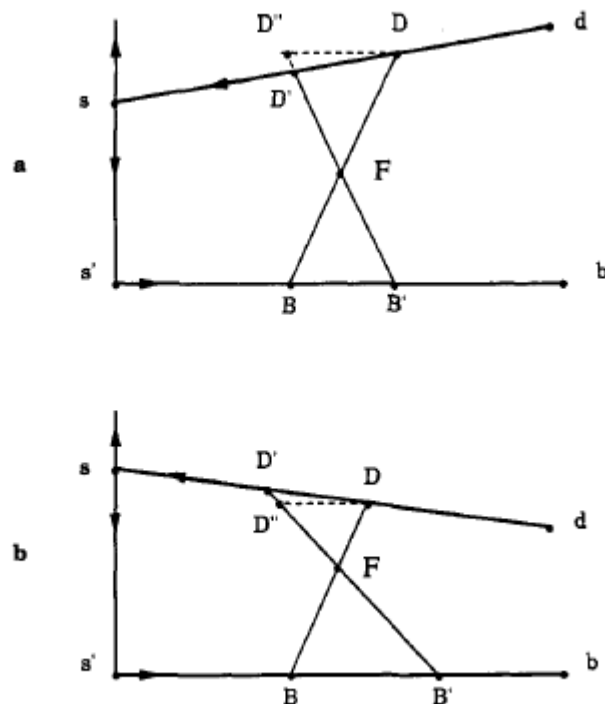


Figure 1.13. Geometry of the distillation region boundaries. (a) D increases; (b) D decreases along the continuation path.

The only difference between the two is the orientation of the ds distillation boundary. In order to check if D increases or decreases along the continuation path, the procedure used for the proof of fact 2 is applied.

In Figure 1.13b, the line from D that is parallel to BB' crosses the $D'B'$ line segment while it does not cross it in Figure 1.13a. Hence in Figure 1.13a, $D''F > D'F$, while $D''F < D'F$ in Figure 1.13b. As a result, D increases in Figure 1.13a whereas D decreases in Figure 1.13b. Therefore multiple steady states exist only for the situation depicted in Figure 1.13b. The existence of multiple steady states depends on the relative position of the boundaries ds and $s'b$ while the location of the ss' boundary does not play any role. If the boundaries ds and $s'b$ are parallel, then D remains constant along this part of the continuation path. Therefore, in this case there is an infinite number of profiles with different product compositions for a constant distillate flow D .

In summary, for the existence of multiplicities the following is required (**geometrical condition**): While moving along the continuation path from D to D' and accordingly from B to B' , the line that passes from D and is parallel to BB' crosses the $D'B'$ line segment.

1.3.5.4. Appropriate Feed Composition

Even if a residue curve diagram contains two neighbouring saddles with the appropriate geometry (as described above) for the existence of multiplicities, there might be some feed compositions for which multiple steady states do not exist.

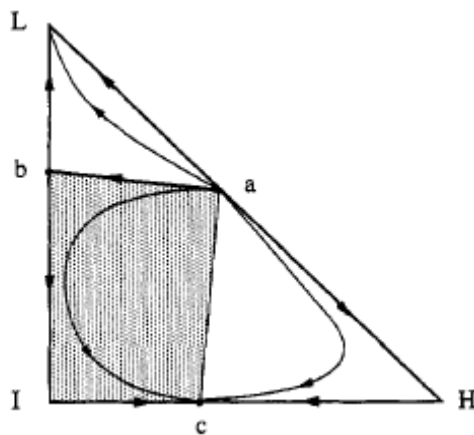


Figure 1.14. Residue curve diagram of a 231 class ternary mixture and the appropriate feed region.

Figure 1.14 shows a residue curve diagram that belongs in the 231 class. In this diagram there are two distillation regions. In the lower region there are three saddles (two of them neighbouring) while in the upper region there is only one saddle. Therefore if the feed composition lies in the upper region, a unique steady state exists for each value of D . However, placing the feed in the lower region is not sufficient for the existence of multiple steady states.

As can be seen from Figure 1.14, ab and Ic form the only pair of boundaries that enables the existence of multiple steady states. Hence, the only feed compositions that will exhibit multiple steady states are those that can be separated in a distillate lying on ab and a bottom product lying on Ic for some value of D . Therefore, multiple steady states exist for any feed located in the convex hull formed by ab and IC (shaded region in Figure 1.14).

In summary, multiple steady states exist only for the feed compositions that lie in the convex hull formed by a pair of distillation region boundaries that satisfy the geometrical condition described above.

In this section the ∞/∞ case for a ternary mixture was studied, under the assumption of straight line boundaries. A necessary condition for the existence of multiplicities (at least two neighbouring saddles) was found. Furthermore, the conditions developed above for the geometry of the boundaries and the appropriate feed compositions constitute a necessary and sufficient condition for the existence of multiple steady states in the ∞/∞ case.

Chapter 2. Multiple Steady States: A Review

This chapter contains a review of the literature on multiple steady states in distillation. Note that uniqueness of the steady state in distillation was widely believed over a long time (Doherty and Perkins, 1982): “In spite of significant nonlinearities even in the simplest model, the distillation literature generally takes it for granted that distillation models possess a globally asymptotically stable singular point.”

Fortunately, this believe was not justified by anything. To date, 70 major contributions to MSS in distillation are known, which can be divided into contributions for non-reactive (52 papers) and reactive distillation (18 papers). For the review, the contributions have been classified according to the general type of results: simulations, analytical work or experiments.

2.1 MSS in Azeotropic Distillation

2.1.1 Early Contributions: Analysis and Simulation

Rosenbrock (1962) [homogeneous analysis]: In a pioneering work, Rosenbrock applied Lyapunov's second method and rigorously proved that the steady state of a distillation column separating a binary mixture is unique. He assumed constant molar flows (CMO, see Appendix B) and a unique $y(x)$ relationship, i.e., that to every vapour composition y there corresponds a unique liquid composition value x in equilibrium with y . Obviously, the second condition excludes all heterogeneous systems, but not the cases of non-ideal zeotropic or azeotropic behavior.

Balashov et al. (1970), Petlyuk and Avetyan (1971) [homogeneous analysis]: Petlyuk and Avet'yan provided a bifurcation diagram showing the existence of MSS in the distillation of a ternary homogeneous system. Their analysis bases on the assumption of CMO, and the Wilson activity coefficient model was used to describe the non-ideal VLE. Moreover, the authors first presented the conceptual idea of the ∞/∞ case of columns which was reinvented by Bekiaris and coworkers later on. However, the condition developed by Petlyuk and Avet'yan for the existence of MSS (two neighboring saddles) is neither necessary nor sufficient (Bekiaris et al., 1993). Their results show the possibility of MSS for one specific class of systems, but no real mixture exhibiting multiple steady states is reported. Similar results have been published in the Russian book of Balashov et al. (1970), which is only available in the central libraries of Russia.

Shewchuk (1974) [heterogeneous simulations]: In his PhD thesis, Shewchuk first reported simulation evidence for the existence of multiplicities in the heterogeneous ternary mixture ethanol, benzene and water, which belongs to the 222-m class according to Matsuyama and Nishimura (1977).

Shewchuk's statement: “It was also found that the dehydration tower converged to two different steady states depending on the starting guesses. Both of these solutions [. . .] satisfied the highly nonlinear equations.” At that time, the phenomenon looked quite awkward and its existence was opposing the widely-spread believe quoted earlier. Therefore, Shewchuk considered bad thermodynamic data to be responsible for his observation and did not report the results in great detail. Consequently, it is hard to justify his results, although the column profiles shown closely resemble those of Magnussen et al. (1979).

Magnussen et al. (1979) [heterogeneous simulations]: Magnussen and coworkers presented simulation results that show the existence of three steady states (two of them stable and one unstable) for the heterogeneous EWB mixture at atmospheric pressure. In their calculations, CMO, constant pressure and ideal vapour phase were assumed. The phase splitter (decanter) of the column is removed and instead, a second feed enters at the top of the column. This second feed would consist of the entrainer recycle (from the decanter) and the entrainer make-up stream | its composition and flowrate are identical for all three steady states and for the same VLE model. Therefore, the three steady states represent an output multiplicity. Importantly, the liquid

composition profiles of all three steady states are reported to lie entirely in the single liquid phase region (homogeneous profiles), only the overhead vapour exhibits two liquid phases after condensation.

It is noteworthy that the multiplicities were observed with the UNIQUAC and NRTL activity coefficient models (and the corresponding parameters), but a unique steady state was found using the Wilson model and data, which was reported to poorly represent the VLE of this mixture (despite of the fact that the Wilson model cannot predict a liquid – liquid phase split). The parameter sets used for the VLE calculations are questionable and have not been clearly reported. Finally, the authors observed a similar multiplicity for the mixture of ethanol, water and pentane.

2.1.2 Heterogeneous Simulation Studies Reporting MSS

Magnussen and co-workers results triggered great interest in distillation multiplicities. The belief that heterogeneity of the mixture was a possible cause for such multiplicities directed the attention towards heterogeneous azeotropic distillation. Consequently, several simulation studies were published for the ethanol-water-benzene system and for a few other heterogeneous mixtures.

Prokopakis et al. (1981) [heterogeneous simulations]: Using a column without decanter (with a second feed of fixed composition and flowrate entering at the column top) and the NRTL activity coefficient model, Prokopakis and coworkers verified the three operating regimes of Magnussen et al. (1979) for the EWB mixture, but not steady-state multiplicity. In their model, they included energy balances and pressure drops along the column. Unfortunately, the critical simulation results on multiplicities are not reported in necessary detail. Next, the authors studied a mixture of isopropanol, water and cyclohexane and reported several steady states for the same “specifications”. In these steady states, however, the entrainer flowrate in the boilup stream and the reflux flowrate and compositions are held constant, while the product flowrates differ. Since in practice, compositions of an internal column stream can only be specified by means of control, this case does not correspond to an “open-loop” output multiplicity.

The main advance compared with earlier studies on the heterogeneous system lies in the fact, that the entire column sequence, consisting of the azeotropic column with decanter and including the idealized mass balance of the recovery column, was simulated.

Kovach III and Seider (1987a; 1987b) [heterogeneous simulations]: Kovach III and Seider presented homotopy continuations and experimental results for the mixture sec-butanol, water and di-secondary-butyl ether (mixed with butylenes and methyl-ethyl- ketone impurities). They modeled a sub-cooled decanter and used the reboiler heat duty as well as the organic and aqueous reflux ratios as the specification. Such a configuration closely corresponds to [LN,Qr] for homogeneous mixtures. Although no multiplicities were found in the study, they located two steady states (one with a single liquid phase on all trays and the other one with two liquid phases on 70% of the trays) over a narrow range of the reflux ratio (high parametric sensitivity). Finally, they conclude that the observations in the simulation are consistent with the experimentally observed erratic behavior of the distillation tower.

Venkataraman and Lucia (1988), Kingsley and Lucia (1988) [heterogeneous simulations]: Venkataraman and Lucia performed a continuation study for the EWB column of Prokopakis and Seider (1983b) with the molar bottoms flowrate as the bifurcation parameter, but without a decanter (second feed at the column top). They found three steady states over a narrow range of bottoms flowrates in the bifurcation analysis (output multiplicities). Kingsley and Lucia (1988) showed for the same column that there is a minimum tray efficiency where these three steady states disappear. For columns with a tray efficiency less than this minimum, a unique steady state exists in the whole range of bottoms flowrates. Above this minimum, three steady states exist in some bottoms flowrate interval. However, these steady states were calculated without taking into account the presence or absence of two liquid phases on a tray (thus ignoring the liquid split).

Hence, they do not correspond to realistic column profiles but can be used as starting points of a heterogeneous distillation calculation, see also Pham and Doherty (1990). By this, all three profiles “ultimately lead to the same heterogeneous solution” and thus, no heterogeneous multiplicities have been produced.

Widagdo et al. (1989) [heterogeneous simulations]: Widagdo and co-workers performed parameterization with respect to the aqueous reflux ratio for the mixture sec-butanol, water and di-secondary-butyl ether, which was also studied by Kovach III and Seider. They found three steady states on a narrow range of the aqueous reflux ratio | a multiplicity where the top tray exhibits a second liquid phase. A bifurcation analysis for a single-stage column showed a unique solution and the authors suggested that other effects, “beyond those characterizing a single stage”, may be responsible. This result compares to that of Doherty and Perkins (1982).

Cairns and Furzer (1990) [heterogeneous simulations]: The authors study the multiplicities reported by Magnussen et al. (1979), but using the UNIFAC model to describe the liquid phase behaviour of the EWB mixture. The existence of three steady states (output multiplicities) was verified, but two of them were only obtained by ignoring the liquid-phase split on the column trays. Hence, it was concluded that these two profiles are fictitious. Moreover, two steady states (one again obtained by ignoring the liquid split) are reported for the mixture ethanol, water and iso-octane. Clearly, the authors were able to demonstrate that erroneous solutions can occur when ignoring the liquid-phase split, but do not compute MSS with their corrected algorithms.

Rovaglio and Doherty (1990) [heterogeneous simulations]: Rovaglio and Doherty studied the EWB system in a column with and without decanter as well as for different sets of parameters (UNIQUAC activity coefficient model). They found three steady states for the parameter set and column design of Magnussen et al. (1979) through dynamic simulations ignoring the decanter. Moreover, the three solutions still exist when the decanter is included. The profiles of the three solutions follow different paths in the composition triangle and all have trays lying in the two-liquid phase region. Since two of the three solutions were unstable, the authors conclude that even more steady states should exist, a result consistent with the five steady states reported by Kovach III and Seider (1987b).

Rovaglio et al. (1991) [heterogeneous simulations]: Rovaglio and co-workers verified the three solutions found by Rovaglio and Doherty (1990) for the second column design and the PAGE80 parameter set. They were able to show that the solutions persist even when the entrainer recovery column and the benzene recycle stream is included in the model (MSS in a column sequence).

2.1.3. From Homogeneous to Heterogeneous System Analysis

Rovaglio et al. (1993) [heterogeneous simulations]: The authors verified the existence of MSS reported by various groups for the EWB system through dynamic simulations. They offered an explanation for the multiplicities reported by Rovaglio and Doherty (1990) and Rovaglio et al. (1991) based on the observation, that the entrainer inventory in the stripping section is different for the three solutions reported. Although these steady states satisfy the convergence criteria, “there may be small differences in the necessary make-up flowrates needed to keep these states constant and stable”. Therefore, they concluded that (1) the three solutions are not real multiplicities but one real (converged) solution and two “pseudo” solutions caused by not tight enough convergence criteria, and (2) that “the problem of MSS seems to be associated with the numerical aspects related to the relative small amount of entrainer make-up.” However, the second conclusion is much too general when compared to the evidence given and counter-examples have been reported.

Bossen et al. (1993) [heterogeneous simulations]: Bossen and co-workers also studied the heterogeneous EWB mixture for a column including the decanter and the UNIFAC model. In one of four steady states they found, the whole profile as well as the decanter compositions lie in the homogeneous region. The products of the remaining three profiles have exactly the same compositions and flowrates. The only difference between these three profiles is the location of

the front of sharp ethanol-benzene composition change (internal state multiplicities). Since these three profiles are in very good agreement with the results of Rovaglio et al. (1993), which were obtained for UNIQUAC, it is highly probable that the convergence criteria applied in this study were not tight enough and thus, only two of the four steady states might be real.

Gani and Jorgensen (1994) [heterogeneous simulations]: Next, Gani and Jorgensen calculated as many as ten solutions for the EWB column from above. However, they do not indicate their convergence tolerance, thus not providing sufficient evidence that the solutions were fully converged (Widagdo and Seider, 1996).

Bekiaris et al. (1996) [heterogeneous analysis]: Bekiaris and co-workers extended their analysis, which was originally developed for homogeneous systems (Bekiaris et al., 1993), to multicomponent heterogeneous azeotropic distillation. They present the first theoretical framework to investigate the physical causes of MSS in heterogeneous distillation and to obtain quantitative and qualitative predictions of those multiplicities by a necessary and sufficient graphical condition. Moreover, they locate the region of feed compositions which will lead to MSS in the limiting case used for the analysis. They demonstrate how particular configurations (e.g. the presence or absence of a decanter, total or partial reboiler and condenser, tray efficiencies. . .) affect the presence or absence of multiplicities. Finally, the multiplicities for the EWB mixture are analyzed and the most important results are verified by simulation. It was shown that three steady states exist in some interval of the product flowrates (one homogeneous and two heterogeneous).

2.1.4. Experimental Verification of Multiple Steady States

Up to this point, two general classes of multiplicities have been analyzed and supported by simulation studies: those analyzed by Jacobsen and Skogestad (1991) and those by Bekiaris and co-workers (1993; 1996). In this section, experimental evidence is reported for both types.

Kienle et al. (1995) [homogeneous experiments]: Kienle and co-workers exclusively study the first type of the multiplicities reported by Jacobsen and Skogestad (1991). Consequently, they apply their methods from nonlinear wave propagation theory to the $[L^V, V^N]$ configuration of a column separating an ideal mixture of methanol and propanol. For single column sections of infinite length, a unique steady state is reported for molar inputs but three steady states may exist for volumetric inputs. Unfortunately, the procedure for combining the results from the rectifying and stripping sections is not reported and only a numerical analysis is performed. By this, a region with MSS is elaborated in the two- parameter space by stage-by-stage calculations of a model including heat effects and using the volumetric reflux, L^V , and the reboiler heat duty, Q_r , as the parameters. Then, this type of MSS was verified in an experiment. Using the $[L=D, Q_r]$ configuration, it was demonstrated that the same value of a volumetric reflux flowrate corresponds to three different values of the reflux ratio (nonlinearity in the input transformations). Operating the column in $[L^V, Q_r]$, they were able to start the plant up to one of the two stable steady states in the flowrate multiplicity interval. During the experiment, the plant was temporarily disturbed to obtain the second of the two stable steady states. Finally, the original operating point was recovered. Therefore, the existence of two stable steady states for the same specifications, caused by nonlinearities in the input relationship, was experimentally verified.

Koggersbøl et al. (1996) [homogeneous experiments]: The authors also study multiplicities caused by the nonlinear input transformations in the $[L^V, V^N]$ configuration (Jacobsen and Skogestad, 1991). They argue that instability may not necessarily lead to output multiplicities. In the experiments, two branches of steady states were measured over some interval of the operating parameter, but instability of either of these branches could not be verified.

Güttinger et al. (1997) [homogeneous experiments]: Güttinger and co-workers presented the first experimental study showing the existence of MSS caused by the VLE for the homogeneous mixture of methanol, methyl butyrate, and toluene (MMBT system). The experiments on an

industrial pilot column show two stable steady states for the same feed flowrate, composition and quality and the same set of the operating parameters (output multiplicities). The measurements are in excellent agreement with the predictions obtained from the ∞/∞ analysis (Bekiaris et al., 1993), as well as with stage-by-stage simulation results. For more details on the experiments the reader is referred to Chapter 5.

Wang et al. (1997) [heterogeneous experiments]: The authors perform experiments using a laboratory sieve plate distillation column operating on a heterogeneous mixture of isopropyl alcohol, cyclohexane and water. Unfortunately, the plant made use of an organic surge tank in the entrainer reflux flow whose level was controlled by varying the entrainer make-up flowrate. Therefore, the entrainer make-up is not the same for the steady states measured, i.e., constant inputs are not achieved and consequently, the conclusion that steady-state multiplicities have been measured is erroneous. Instead, the simulations and the laboratory experiments show high parametric sensitivity to the entrainer make-up (Rovaglio et al., 1993). Moreover, oscillations in the closed-loop operation of the plant were observed but could not be verified by dynamic simulation.

Müller and Marquardt (1997) [heterogeneous experiments]: In their work, the authors apply the procedure (analysis, simulation and experiments) reported by Güttinger et al. (1997) to the heterogeneous mixture of ethanol, water and cyclohexane (instead of a homogeneous mixture). First, the ∞/∞ analysis for heterogeneous mixtures was applied to predict the existence of MSS caused by the VLLE (Bekiaris et al., 1996). In comparing the MSS interval for volumetric and molar specification of the distillate flowrate, it can be seen that singularities in the input relationship cause the MSS interval to be smaller (Jacobsen and Skogestad, 1991), but still significant enough to be measured on a volumetric basis. In the experimental part, Müller and Marquardt tracked the two stable solution branches whose compositions favourably compare to the results obtained from the steady-state simulations. The unstable branch was not measured due to operational problems in the decanter. Moreover, they report dynamic measurements of the hysteresis behaviour induced by the existence of MSS.

Dorn et al. (1998) [homogeneous experiments]: Dorn and co-workers continued the experimental investigation by Güttinger et al. (1997) for the same homogeneous mixture (MMBT). Despite of the two stable solutions already reported, their experiments on a different pilot plant verified the existence of a third, unstable steady state, which was stabilized with PI-control. The steady-state experiments are shown to be in good qualitative agreement with the theoretical predictions and the stage-by-stage simulation results. Furthermore, the transition from an unstable to a stable operating point was realized in the pilot plant when the control action was removed.

2.1.5. Various Studies on Multiple Steady States

Sridhar (1997) [heterogeneous analysis]: Sridhar's second study is based on Sridhar (1996) and concludes that "rigorous analysis is used to demonstrate that the cause for the existence of solution multiplicities in multistage separation process problems involving the standard specification is the tendency of the mixture to exhibit a second liquid phase". This conclusion is objected here because (1) the analysis, specifically the transformation from the "multistage VP problem" to the "standard specification", is not rigorous; and (2) parts of the analysis are contradicted by other literature results.

Bekiaris et al. (1998) [heterogeneous analysis]: Bekiaris and co-workers study the influence of the VLLE on the existence of MSS with the primary focus on the heterogeneous EWB mixture. The sometimes contradicting reports on MSS in this system are shown to be caused by the different thermodynamic models used and by the fact, that the existence of MSS for this system is highly sensitive to the VLLE description. These reports are compared with the ∞/∞ predictions, which can directly be obtained from VLLE data without using a probably restricted thermodynamic model. Moreover, parameter sets are identified which do not allow a reliable

analysis of the EWB system, since fundamental properties of the VLLE are not covered correctly (existence of azeotropes and size of the two-phase region).

For the case of the multiplicities reported by Magnussen et al. (1979), the column profiles excellently compare to those predicted for a ∞/∞ tray column without decanter. The differences between Magnussen's results and the predictions can be explained from a thermodynamic point of view and hence, the authors conclude that the multiplicities Magnussen reported are of the same type as those analyzed by Bekiaris et al. (1996).

Moreover, they show that two of the three operating regimes reported by Prokopakis and Seider (1983b) for a column with decanter are similar to the profiles obtained from the ∞/∞ predictions including a decanter. In addition, the study enlightens the results published by Kovach III and Seider (1987a; 1987b), Venkataraman and Lucia (1988), and Kingsley and Lucia (1988).

2.2 MSS in Reactive Distillation

Pisarenko et al. (1987) and Karpilowski et al. (1997) [analysis and simulations]: The first report on output multiplicities in reactive distillation was published by Pisarenko et al. (1987) who analyzed a single-product reactive distillation column. They were able to obtain three steady-state solutions for the same inputs and operating parameters by simulation; two of them were stable and one unstable. Recently, Karpilowski et al. (1997) continued their study and developed a mathematical analysis of single-product column multiplicities which is based on the limiting case of infinite reflux. However, their method is not likely to be extendible to classical two-product columns. It was successfully applied, however, to the production process of butyl acetate.

Nijhuis et al. (1993) and Jacobs and Krishna (1993) [simulations]: In 1993, two simulation studies appeared at almost the same time showing multiple steady states for the reactive distillation process of MTBE and two similar industrial column setups. By variation of the methanol feed tray location, Nijhuis et al. (1993) were able to find several feed tray locations where two different steady states exist (using a steady-state process simulator). Further simulations for constant feed locations but varying reflux flowrate or varying catalyst amount confirmed that the multiplicities obtained were not an artifact.

Both contributions made a first attempt to address the physical causes responsible for the existence of output multiplicities in this process. These arguments have been questioned by Güttinger and Morari (1997) where a more detailed analysis of the physical causes can be found.

Ciric and Miao (1994) [simulations]: Ciric and Miao turned the attention to the irreversible production of ethylene glycol in a single-product reactive column. Their bifurcation calculations showed a large regime with three steady states and a small region of switch-back multiplicities. Extensive case-studies showed that the existence of MSS for the glycol process is quite robust against variations of the feed location, the hold-up distribution, the presence of the side-reactions, and the heat of reaction.

Hauan et al. (1995) [simulations]: Then, the attention turned back to the MTBE process where Hauan and co-workers were able to reproduce the results of Jacobs and Krishna (1993) under the assumption of chemical reaction equilibrium. They presented a very detailed mechanistic explanation of the phase behaviour at the stable steady states for feed tray locations in the interval showing the multiplicity. Moreover, they rigorously explained the resulting behaviour on the two steady-state branches but were not able to predict why a steady-state multiplicity exists in this process.

Sundmacher and Hoffmann (1995), Schrans et al. (1996) and Hauan et al. (1997) [simulations]: At about the same time, Sundmacher and Hofmann observed oscillations in their laboratory column operating on the MTBE reactive distillation system. Surprisingly, even the non-reactive binary mixture methanol-isobutene showed similar oscillations and the authors associated the thermodynamics of this binary mixture with the occurrence of the oscillations. Oscillations for feed composition steps and steady-state multiplicities for the reactive MTBE system have further

been demonstrated by dynamic simulations of the “Nijhuis” column (Schrans et al., 1996; Huan et al., 1997). Schrans et al. (1996) first reported that there are three steady states possible for the MTBE system, two of them stable and one unstable.

Bravo et al. (1993) and Mohl et al. (1997) [simulations]: Recently, Mohl et al. (1997) did bifurcation calculations for the “Nijhuis” column and showed that MSS disappear at low reflux values but still exist at high reflux. However, no oscillations were observed in the dynamic transitions between the different steady states in the multiplicity interval. This contradicts the previous results since both studies performed step disturbances in the feed composition. MSS have further been demonstrated for the industrial production of TAME (Bravo et al., 1993; Mohl et al., 1997).

Pilavachi et al. (1997) [simulations]: The effect of different thermodynamic models and parameters on the existence of MSS for the “Nijhuis” and the “Clausthal” columns was studied by Pilavachi et al. (1997). Accordingly, MSS in the MTBE process depend critically on the correct representation of the reactive equilibrium but are more robust against the VLE model, see also Okasinski and Doherty (1997b).

After those simulation studies two approaches have been published for the prediction of multiple steady states in reactive distillation.

Gehrke and Marquardt (1997) [analysis]: Gehrke and Marquardt presented a numerical method to calculate column multiplicities based on a single-stage model by a singularity theory approach. Qualitatively correct predictions were obtained for the ethylene glycol column studied by Ciric and Miao (1994). However, their approach is computationally intensive, especially if high-order singularities must be found.

Güttinger and Morari (1997) [analysis]: Conversely, Güttinger and Morari (1997) presented a first approach to extend the ∞/∞ analysis of Bekiaris et al. (1993) to reactive distillation systems. By the use of reactive residue curves and the transformation of Ung and Doherty (1995e), they were able to predict the existence of MSS by graphical methods. They demonstrated that the multiplicities in the MTBE process can either be caused by the nonlinear relationship of the input transformations or by the reactive vapour-liquid- equilibrium. The ∞/∞ singularity analysis provides the necessary tools for determining the influence of the column configuration on the existence of MSS.

Sneesby, Tadó and Smith (1997) and Bartlett and Wahnschafit (1997) [simulations]: The existence of type Ia MSS in the MTBE process has further been shown by Sneesby and co-workers. Moreover, Bartlett and Wahnschafit performed a control study for an MTBE column operating in the multiplicity interval.

Güttinger and Morari (1998a; 1998b) [analysis]: In a series of two papers, the ∞/∞ analysis to predict multiple steady states in equilibrium reactive distillation has been developed for columns where the reactions take place in the entire column (“non-hybrid” columns) and for columns with a reacting core (“hybrid” columns). Using the transformation of Ung and Doherty (1995e), a method was presented to predict the existence of output multiplicities based on the reactive vapour-liquid equilibrium for the limiting case of non-hybrid columns of infinite length operated at infinite internal flows. By locating all possible profiles and products through a bifurcation analysis, qualitative and quantitative predictions have been obtained. The region of feed compositions leading to multiple steady states can be constructed graphically applying a necessary and sufficient geometrical condition. Through the ∞/∞ singularity analysis, the predictions have been extended to cover multiplicities introduced by the nonlinear relationships between transformed, molar, mass and volumetric flowrates.

Moreover, Güttinger (PhD thesis, 1998) has introduced two procedures to extend the predictions to hybrid columns: by an exact method, similar results were obtained for hybrid columns as for non-hybrid ones: prediction of the product paths, of the existence of output multiplicities and of the region of feeds leading to multiple steady states. The applicability of this method to finite columns was demonstrated for an example system where the existence of a new type of multiplicities, which is caused by the interactions of reactive and non-reactive column sections.

An approximate method estimates the hybrid product paths and can be used to draw conclusions on the steady-state behaviour of a finite hybrid column. However, the procedure of infinite/infinite analysis has not been applied to non chemical equilibrium systems, which is the object of the present study.

Chapter 3. Multiple Steady States in Reactive Distillation - Non-Hybrid ∞/∞ Analysis

A method is presented to predict the existence of output multiplicities for reactive equilibrium distillation columns, where the reactions take place in the entire column (“non-hybrid” columns). As necessary prerequisites for this method, conditions for feasible reactive column profiles in the ∞/∞ case need to be derived. Then, the reactive ∞/∞ analysis can be formulated analogously to the non-reactive cases (Güttinger and Morari, 1998a).

3.1 Introduction to Reactive Distillation

3.1.1 Motivation

During the last decade, the reactive (catalytic distillation (RD)) has gained increasing importance. Some processes in the chemical and petrochemical industries have been significantly improved by the use of reactive distillation technology, e.g. the production of fuel ethers (DeGarmo et al., 1992). In the end, the motivation for implementing RD processes in industry is always of an economical nature, since capital and operating costs of a plant must be minimized.

The synergies encouraging the combined use of reaction and separation can be assigned to either chemistry or separation in most cases. In terms of chemistry, conversion and yield of the desired product can often be improved by RD. This is achieved by carrying equilibrium limited reactions to completion or by the boiling point temperatures shifting the chemical equilibrium (Venkataraman et al., 1990; DeGarmo et al., 1992; Doherty and Buzad, 1992). Side-reactions can be suppressed by feeding one reactant in excess (increasing yield) and unfavourable thermodynamics may be overcome (Doherty and Buzad, 1992; Isla and Irazoqui, 1996; Okasinski and Doherty, 1997a). Examples of processes which have profited from chemistry-based synergies are the production of MTBE (methyl-tert-butyl-ether), TAME (tert-amyl-methyl-ether) and esterification reactions (methyl- or ethyl-acetate). In terms of separation, close-boiling mixtures have been one of the driving forces in the development of RD processes. Additionally, these processes often allow to overcome non-reactive azeotropes and distillation boundaries (Barbosa and Doherty, 1988c). The inherent direct heat integration of a distillation column utilizes the heat of reaction for evaporating the liquid phase (Grosser et al., 1987; Sundmacher et al., 1994). However, there are certainly other issues to consider in the evaluation of RD processes, e.g. control problems (Bartlett and Wahnschafit, 1997).

3.1.2 Assumptions, Definitions and Literature

All RD processes are rate-based in nature and kinetic considerations may have to be included in the design of processes undergoing slow reactions. Comparisons of the applicability of rate-based and equilibrium models to reactive distillation have been given by Serafimov et al. (1993) and Pilavachi et al. (1997).

Hybrid columns are distillation columns with a reactive core, i.e., they are built from a reactive column section where the catalyst is present and one or more non-reactive sections (rectifying and/or stripping sections). Consequently, non-hybrid columns denote columns where all trays including condenser and reboiler are reactive (Figure 3.1). Commonly, hybrid columns are resulting from the use of a heterogeneous (solid) catalyst, whereas a homogeneous (liquid) catalyst would lead to a non-hybrid column design.

Most of the pioneering work in the areas of equilibrium RD thermodynamics and design is based on transformations of the physical compositions (Zharov, 1970; Barbosa and Doherty, 1988c). Barbosa and Doherty (1988a) presented design and minimum reflux calculations for single-

reaction systems. Using a generalized version of the composition transformations Ung and Doherty (1995d) extensively analyzed the synthesis of RD systems with multiple reactions by graphical design methods based on reactive residue curves.

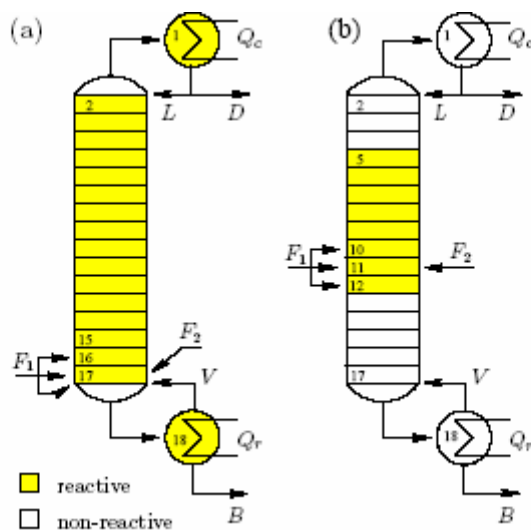


Figure 3.1: Non-hybrid (a) and hybrid (b) reactive distillation columns. The hybrid column corresponds to the design used by Nijhuis et al. (1993).

Espinosa and coworkers studied the design of reactive columns with inerts present and columns with a reacting core, i.e., hybrid columns (Espinosa et al., 1995a, b; 1996).

3.1.3 Multiple Steady States in Reactive Distillation

Because of the occurrence of reactive azeotropes, many characteristics of RD processes are very similar to those observed in (non-reactive) azeotropic distillation. Among the unusual features of both azeotropic and reactive columns, multiple steady states (MSS) have been discovered. Definition 1 of “Multiple Steady States in Single Columns” (chapter 1) can equally be applied to reactive distillation systems. Moreover, the definitions of input and (internal) state multiplicities as well as the concept of column configurations carry over to reactive distillation.

This approach comprises of a description of the thermodynamic requisites for the reactive ∞/∞ analysis. The methods sketched by Güttinger and Morari (1997) are extended and presented in detail by Güttinger (PhD thesis, 1998) for non-hybrid columns, developing also prediction methods for hybrid columns. The ∞/∞ case refers to distillation columns of infinite length (with an infinite number of equilibrium stages) operated at infinite internal flows (Petlyuk and Avet'yan, 1971; Bekiaris et al., 1993). For reactive ∞/∞ columns there is the additional requisite of infinite catalyst activity on each tray of the reactive section to achieve equilibrium reactions. The ∞/∞ analysis can be fully expanded to reactive systems, and prediction tools for the occurrence of multiplicities are developed.

So far, four physical phenomena have been found to give rise to output multiplicities in azeotropic and reactive distillation:

I. Jacobsen and Skogestad (1991) reported two different types of multiplicities in binary distillation columns with ideal vapour-liquid-equilibrium (VLE):

- a) For constant molar overflow (CMO) and the $[L^M, V^N]$ configuration, multiplicities can occur due to the nonlinear relationship between mass and molar flowrates (or volumetric and mass flowrates or heat duties and molar flowrates). This behaviour is not expected for binary systems with configurations involving a product flowrate, e.g. $[D^M, V^N]$. Experimental studies have been reported by Kienle et al. (1995) and Koggersbøl et al. (1996).

b) Multiplicities can further be caused by the presence of energy balances in the [LN, V N] configuration of ideal binary columns (Jacobsen and Skogestad, 1991; Häggblom, 1996). Type I multiplicities have also been shown for more complex distillation systems, e.g. multicomponent azeotropic or even reactive distillation (Güttinger and Morari, 1997; Güttinger and Morari, 1998b).

II. This type of output multiplicities is caused by the underlying reactive or non-reactive VL(L)E and also occurs for CMO conditions.

- a) The existence of output multiplicities caused by the non-reactive VL(L)E was studied by Bekiaris et al. (1993) for homogeneous and by Bekiaris et al. (1996) for heterogeneous mixtures (∞/∞ analysis). These multiplicities have been verified experimentally for a ternary homogeneous and a heterogeneous system (Güttinger et al., 1997; Müller and Marquardt, 1997; Dorn et al., 1998). In reactive distillation, this type of MSS is caused by the reactive VLE and can occur in non-hybrid as well as in hybrid columns (Güttinger and Morari, 1998a; 1998b).
- b) In hybrid reactive distillation columns, MSS can occur due to the interactions between reactive and non-reactive column section (or the reactive and non-reactive VLE). This type of MSS was analyzed by Güttinger and Morari (1997; 1998b).

3.2 Non-Hybrid Column Profiles

3.2.1 Reactive Composition Transformation

In reactive equilibrium of a c component mixture, the reachable compositions form a subspace of lower dimension in the physical composition space, the “reaction space” (Bessling et al., 1997). The dimension of the subspace is given by the degrees of freedom from the extended Gibbs phase rule (Smith et al., 1996):

$$\text{Degrees of freedom} = 2 - \pi + c - r \quad (3.1)$$

where π is the number of phases and r the number of reactions present. Thus, a homogeneous non-reactive system in vapour-liquid equilibrium has c degrees of freedom. Each linearly independent reaction reduces the dimension of the reaction space by one. Bessling et al. (1997) presented illustrations of the physical space and the reaction space for a variety of topologically different reactive systems.

The basic idea to obtain a convenient description of the reactive VLE is to find a set of transformed composition variables X which can be used as a basis for the reaction space. The new variables should exhibit similar properties as the mole fractions in the physical composition space (e.g. sum to unity). Such a transformation has first been published by Zharov (1970) for isothermal open-evaporation processes. The transformations were rediscovered by Barbosa and Doherty (1988c) and refined by Ung and Doherty (1995e) and Espinosa et al. (1995a). This work is based upon the transformation of Ung and Doherty (1995e), which can be applied to any number of reactive and inert components and to any number of independent reactions r :

$$D: [0..1]^c \rightarrow \mathfrak{R}^{(c-r)}$$

$$X_i = \frac{x_i - \nu_i^T (\nu_{ref})^{-1} x_{ref}}{1 - \nu_{tot}^T (\nu_{ref})^{-1} x_{ref}} \quad (3.2)$$

In a similar way, molar flowrates can be transformed (P denotes any of the streams D, B, F_i, L or V , see Figure 3.1):

$$P^D = P^N \left(\mathbf{1} - \nu_{tot}^T (\nu_{ref})^{-1} x_{ref}^P \right) \quad (3.3)$$

The transformed compositions X exhibit the following properties (Ung and Doherty, 1995c; Ung and Doherty, 1995e):

1. X expresses the conservation of mass for any value of the extent of reaction; they are reaction-invariant compositions. Therefore, X takes the same value for any reaction extent of a given liquid mixture.
2. The X – vector sums to unity.
3. The transformed representation is canonical in the sense that it does not depend on the combination of the reaction equations chosen (as long as this combination is linearly independent).
4. Reactive azeotropes occur if and only if X=Y (the transformed liquid composition is equal to the transformed vapour composition). A physical explanation of reactive azeotropes was given by Barbosa and Doherty (1988b).
5. The reaction space is always a convex polyhedron but not necessarily a “regular” simplex.

Zharov (1970) and Ung and Doherty (1995a) derived the equations describing the simple distillation (open-evaporation) of an equilibrium reactive system. The reactive residue curves are obtained by solving the following differential equation in transformed compositions:

$$\frac{dX_i}{d\tau} = X_i - Y_i \quad i = 1..(c-r) \quad (3.4)$$

where τ is the dimensionless “warped” time. Equation (3.4) is identical with the residue curve equation for non-reactive systems if the transformed compositions are replaced by molar ones. Therefore, the properties of reactive and non-reactive residue curves are very similar (Ung and Doherty, 1995a). The singular points with X=Y correspond to reactive azeotropes, “surviving” non-reactive azeotropes or to pure components. They can either be stable or unstable nodes or saddles. In addition, reactive distillation regions, reactive boundaries, and reactive distillation lines can be defined in an analogous manner (Bessling et al., 1997).

3.2.2 Feasible Non-Hybrid ∞/∞ Profiles

The following feasibility analysis of profiles in the ∞/∞ case is based on a non-hybrid reactive distillation column (Figure 3.1a). Ung and Doherty (1995d) derived the equations describing the operating lines (material balances) of such a non-hybrid column. They showed that the equations for the rectifying and stripping sections are identical to those for non-reactive columns if all molar compositions and flowrates in the latter are replaced by their transformed analogues. Moreover, the overall material balances maintain their form in transformed coordinates (the unit base of flow will be denoted by superscript D for transformed, N for molar, M for mass or V for volumetric flowrates):

$$\begin{aligned} F^D &= D^D + B^D \\ F^D X^F &= D^D X^D + B^D X^B \end{aligned} \quad (3.5)$$

Thus, most of the standard tools for column design and sequencing can be applied directly to equilibrium reactive systems.

A **reactive distillation column profile is feasible**, if the feed, distillate and bottom compositions, in transformed coordinates, all lie on a straight line. This necessary condition corresponds to the

well-known *lever rule*. At *infinite reflux*, the composition profile of a packed non-reactive distillation column must coincide with some part of a non-reactive residue curve, the profile of a tray column with some part of a non-reactive distillation line. Since all column material balances have the same form as for non-reactive columns, the following important result carries over by analogy: The transformed composition profiles of packed reactive columns coincide with the reactive residue curves (Barbosa and Doherty, 1988a), and those of reactive tray columns coincide with reactive distillation lines. Moreover, the results of Bekiaris et al. (1996) can be easily adapted to reactive systems to study the influence of the condenser and reboiler types (partial or total). Since residue curves are a good approximation for distillation lines the analysis is based upon on the former (Widagdo and Seider, 1996).

If a distillation column has *infinite length*, i.e., an infinite number of equilibrium stages, its column profile must contain at least one pinch point (Petlyuk and Avet'yan, 1971). From the analogy described above it is obvious that this fact does carry over to reactive columns. Thus, the transformed composition profile of a reactive column (section) of infinite length must contain at least one pinch point. The only candidate pinch points for reactive columns at infinite reflux are the singular points of the reactive residue curve diagram as shown for non-reactive distillation by Bekiaris et al. (1993). Therefore, the following *conditions are necessary and sufficient for a feasible reactive column profile* in the ∞/∞ case of a non-hybrid column:

Conditions 1 (Feasibility of Non-reactive ∞/∞ Profiles)

1. a packed column profile coincides with a part of a residue curve and the profile of a tray column coincides with a part of a distillation line;
2. the distillation lever rule is fulfilled;
3. the column profile contains at least one pinch point (singular point).

Conditions 2 (Feasible ∞/∞ Non-Hybrid Profiles):

1. the transformed profile coincides with a part of a reactive residue curve;
2. the transformed profile contains at least one pinch point (reactive singular point);
3. the transformed lever rule (3.5) holds.

Note that these conditions are necessary but not sufficient for hybrid columns.

Since the conditions derived above are completely analogous to those of non-reactive columns, the description method for non-reactive column profiles of Bekiaris et al. (1993) can be applied directly to reactive profiles. In the ∞/∞ case of a non-hybrid column all feasible column profiles (fulfilling the conditions above) belong to one of the following three types:

- I. the light-boiling end (distillate) of the reactive profile is located at a reactive unstable node,
- II. the heavy-boiling end (bottoms) of the reactive profile is located at a reactive stable node,
- III. the reactive profile contains at least one reactive saddle singular point.

It was shown above that the lever rule holds in the transformed composition space (3.5). Obviously, such a lever rule does not hold in molar units since the number of moles of the components are altered by the reactions. Even the total number of moles will change in the general case of non-equimolar reactions, $\nu_{tot} \neq 0$:

$$\begin{aligned} F^N &= D^N + B^N - \nu_{tot}^T \in \\ F^N x^N &= D^N x^D + B^N x^B - \mathcal{G} \in \end{aligned} \tag{3.6}$$

The overall material balance in mass units can be written without a reaction term as mass is conserved:

$$F^M = D^M + B^M \tag{3.7}$$

However, the mass fractions will be altered by the reactions as the mole fractions and the component balances in mass units contain a reaction term. Hence, there is no lever rule in mass units for reactive columns. In conclusion, the only units where the lever rule holds are the transformed compositions and flowrates. These are the units of choice for the description of non-hybrid reactive distillation columns in the ∞/∞ case.

3.3 Non-Hybrid Reactive ∞/∞ Analysis

3.3.1 Non-Hybrid ∞/∞ Bifurcation Analysis

Next, it is demonstrated that the non-reactive prediction tools of Bekiaris et al. (1993) can be extended to non-hybrid reactive distillation columns. The only requisites for the existence of an analogous theory are the availability of a lever rule and a method to describe all possible composition profiles in the ∞/∞ case of a reactive distillation column. Actually, the conditions for feasible column profiles derived in the previous section fulfill these requirements. It is important to note that the analysis presented here is only applicable to non-hybrid reactive columns (Figure 3.1a), a restriction which will be relaxed later. A homogeneous two-product distillation column has two operational degrees of freedom for a given design and given feed composition, flowrate and quality. In the ∞/∞ case, the reflux is specified to be infinite and as a result, all internal flows are infinitely large. Thus, there is one degree of freedom remaining which is chosen to be a product flowrate, e.g. the distillate flowrate. Since transformed units are the base for the description of non-hybrid columns, the transformed distillate flowrate D^D is chosen (B^D is determined by equation 3.5).

The ∞/∞ bifurcation analysis is used to predict output multiplicities of type IIa. By adaptation of the definition of the MSS types, these multiplicities are now caused by the reactive VLE. First, the limiting case of a distillation column with zero distillate flow is examined, $D=0$ ($D^D=D^N=D^M=0$). By equations (3.5), (3.6) and (3.7), the following statements about the bottoms flow can be derived: $B^D=F^D$, $B^M=F^M$, but $B^N=F^N$. In all cases, no distillate is taken out and all feeds entering will be leaving in the bottoms after they have reached chemical equilibrium in the reactive column. Therefore, the transformed bottoms composition X^B will be equal to the transformed feed composition X^F (by equation 3.5). In molar units, the bottoms composition will not be that of the feed but of the feed mixture in chemical equilibrium. For a feasible reactive profile the distillate must be located on the low-boiling part of the reactive residue curve containing the bottoms (and the feed) such that the profile also contains a reactive pinch point.

Thus, the distillate is located at the lightest-boiling reactive node of the distillation region containing the feed – similarly as for non-reactive columns (Bekiaris et al., 1993). Hence, the initial column profile is of type I.

Second, the following equations hold for the limiting case of zero bottoms product flowrate: $B^D=B^N=B^M=0$ and $D^D=F^D$, $D^M=F^M$. The bottoms composition X^B is that of the heavy-boiling reactive node of the distillation region containing the feed, and the transformed distillate composition X^D is equal to X^F , the composition of the feed mixture in equilibrium. The resulting column profile is of type II.

Third, a *bifurcation study* (continuation of solutions) is performed by tracking the distillate and bottoms compositions in the transformed composition space, starting from the profile with $D^D=0$ and ending at the profile with $D^D=F^D$. By this procedure, *all feasible transformed composition profiles* are obtained for the ∞/∞ case of a non-hybrid reactive column. This continuation of solutions can be constructed based on physical arguments only, i.e., applying the feasibility conditions for reactive profiles and using the reactive residue curve diagram. The *continuation path* is defined as the path generating all possible column profiles. The distillate and bottoms compositions along this path form the *distillate product path* and the *bottoms product path*. Each pair of distillate and bottoms locations, X^D and X^B , is assigned to a value of the

transformed flowrate D^D by the lever rule (3.5). Therefore, the distillate and bottoms product paths are parameterized by a product flowrate, $X^D(D^D)$, $X^B(D^D)$. By plotting the transformed compositions X^P against the transformed distillate flowrate D^D , a series of *bifurcation diagrams* can be constructed.

If the transformed distillate flowrate is varying non-monotonically along the continuation path, *multiple steady states* exist for the ∞/∞ case of a non-hybrid column and for the transformed feed composition studied. Precisely, MSS will then exist for all feeds resulting in the same composition in chemical equilibrium, i.e., having the same value X^F .

Because of the analogy described above, the following result from Bekiaris et al. (1993) is straightforward for non-hybrid columns. Starting at the initial point (type I profile), the distillate flowrate D^D is monotonically increasing as all type I profiles are tracked. For the same reason, D^D is also monotonically increasing as all type II profiles are tracked, ending at the final point with $D^D=F^D$. Therefore, a decrease of D^D can only occur for type III column profiles. Furthermore, if D^D is varying non-monotonically along the product path, the bottoms flowrate B^D will also vary non-monotonically (by equation 3.5). Note again that the whole bifurcation analysis must be done using transformed compositions and flowrates. To obtain the product paths in molar compositions and flowrates, the inverse of the transformation (3.2) and (3.3) must be applied (“back-transformation”). Unfortunately, this is a procedure involving numerical iteration.

Importantly, the existence of multiple steady states in transformed flowrates has not been shown yet to be necessary and sufficient for multiplicities to exist in other units, i.e., molar or mass flowrates. However, the predictions can be extended to cover other units by applying the ∞/∞ singularity analysis described below.

3.3.2 Non-Hybrid MSS Feed Region Condition

Multiple steady states exist if the transformed distillate flowrate, D^D , is decreasing somewhere along the continuation path. A decrease in D^D , i.e., the existence of MSS, can be detected by the geometrical, necessary and sufficient multiplicity condition. Essentially, this condition takes the same form as those developed for single azeotropic columns and column sequences, if the reactive continuation path and transformed compositions for the feed and the products are used.

From the bifurcation procedure and the geometrical condition it is clear that the existence of MSS depends strongly on the feed composition X^F . All possible transformed feed locations leading to multiple steady states in the ∞/∞ case of a non-hybrid column can be determined by the MSS feed region condition. The condition is also adapted from the non-reactive ∞/∞ analysis. The MSS feed region is defined in the transformed composition space and is suitable to test a candidate feed composition x^F with respect to the occurrence of MSS. With equations (3.2) the transformed feed composition $X^F(x^F)$ is obtained and it can be easily checked if it is located in the MSS feed region.

However, sometimes it may be necessary to represent the feed region in the physical composition space. Since the transformed feed composition X^F is invariant for all mixtures reaching the same composition in chemical equilibrium, the equations (3.2) must be fulfilled for all physical compositions x^F leading to X^F . These $c-r-1$ linearly independent restrictions on the c independent physical compositions x^F leave $c-1-(c-r-1)=r$ degrees of freedom in x^F . By multiplication with the denominator of (3.2) a system of equations linear in x is obtained. Since all these equations are coupled by the reference components, it is always possible to reduce the system by substitution of some x . It can be shown that the system can be reduced to one single linear equation relating $r+1$ of the remaining mole fractions x^F and containing the known transformed composition X^F . Therefore, for each transformed composition X^F this equation describes a linear geometrical object of dimension r (equal to the degrees of freedom obtained above). A straight line is obtained for $r=1$, a plane for $r=2$. . . Hence, the MSS feed region in the physical composition space is built from straight lines (or planes), each of those belonging to one

transformed composition X^F contained in the feed region. From the properties of these stoichiometric lines it can be concluded that it is sufficient to evaluate the X^F on the boundary of the MSS feed region to obtain the convex hull of the feed region in physical coordinates

3.3.3. ∞/∞ Singularity Analysis

3.3.3.1 A United Approach to the Prediction of MSS

The ∞/∞ analysis was originally designed to predict output multiplicities for single azeotropic columns under the assumption of CMO (Appendix B) and for specifications involving a molar product flowrate (Bekiaris et al., 1993; 1996). There are basically two reasons why the prediction of MSS needs to be extended to other units than molar ones: First, it is mostly more economical to control a flow on a mass or volumetric basis instead of a molar basis for the cost of the equipment involved in practice (valves, measurement devices and composition analyzers). Second, Jacobsen and Skogestad (1991) demonstrated in their analysis that singularities in the input relationships can alter the number of steady states present in CMO columns when comparing specifications involving molar, mass or volumetric flowrates (MSS of type Ia). For the cases where MSS were argued to be undesirable, there is the possibility that they could be avoided by selecting an appropriate control configuration, e.g. controlling a mass or volumetric product flowrate instead of a molar one.

Because of the lever rule involved in the bifurcation analysis, the ∞/∞ analysis requires an (external) product flowrate in the column configuration. However, the information obtained from the ∞/∞ analysis can be used to extend the predictions to column configurations involving a mass or volumetric product flowrate. Even though Jacobsen and Skogestad concluded that MSS are unlikely in such configurations for ideal binary systems, e.g. for $[D^M, V^N]$, there is no evidence that this finding carries over to multicomponent or azeotropic systems. The combination of the original ∞/∞ analysis with its extension to non-molar flowrates, the ∞/∞ singularity analysis, results in a unified method to predict MSS of types Ia and II for the ∞/∞ case of a column under CMO (Güttinger and Morari, 1997).

3.3.3.2 The Product Singularity Functions

For column configurations involving a molar product flowrate, the feasible product paths can be determined in the molar composition space for ∞/∞ columns and a (ternary) homogeneous or heterogeneous mixture by the ∞/∞ bifurcation analysis (Bekiaris et al., 1993; 1996). Using these ∞/∞ predictions, specifically the compositions x^D and x^B as functions of D^N (or B^N), a bifurcation diagram can be constructed with one product flowrate, D^N , as the bifurcation parameter. MSS exist if the product flowrate varies non-monotonically along the continuation path. Hereafter, a product path parameterized by a molar product flowrate is denoted by x^P (P^N), where P is any column product (D or B).

In principle, the molar, mass and volumetric product flowrates are related by:

$$P^M = P^N W(x^P) \quad (3.8)$$

$$P^V = P^M / \rho_l(x^P, T^P) \quad (3.9)$$

where $W(x^P)$ is the molar weight of a mixture and $\rho_l(x^P; T^P)$ the liquid density. Note that x^P and T^P on a bifurcation path are functions of the product flowrate P. The derivatives of equations (3.8) and (3.9) are the product singularity functions:

$$\Sigma_{M,N} = \frac{dP^M}{dP^N} = W(x^P) + P^N \frac{dW(x^P)}{dP^N} \quad (3.10)$$

$$\Sigma_{V,M} = \frac{dP^V}{dP^M} = \frac{1}{\rho_l(x^P, T^P)} - \frac{P^M}{\rho_l(x^P, T^P)^2} \frac{d\rho_l(x^P, T^P)}{dP^M} \quad (3.11)$$

In Figures 3.2 and 3.3, the four possible types of singularities are illustrated. On the left, the product path of a product P obtained from the ∞/∞ predictions is plotted versus the flowrate of the stream in two different units of measure, P^1 and P^2 . For example, P^1 and P^2 could be D^M and D^N , respectively, to depict the distillate product path $x^D(D^N)$ versus the mass and molar distillate flowrates

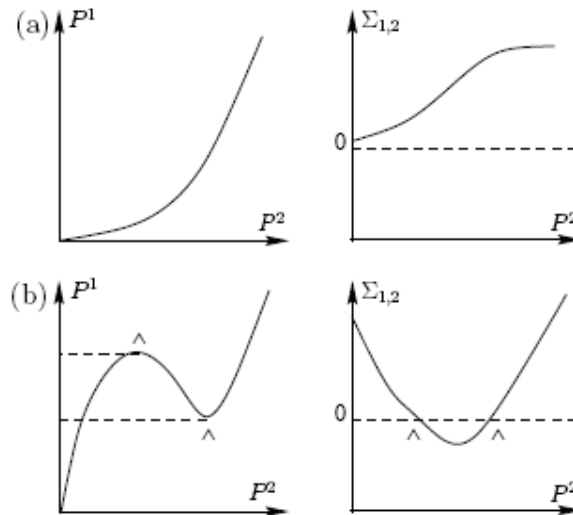


Figure 3.2. Illustration of the first two of four possible types of singularity functions Σ

The derivative of this curve is the product singularity function $\Sigma_{1,2}$, e.g. equation (3.10), which is shown on the right of the Figures. Each of the two product paths can be analyzed with respect to specification of either the flowrate P^1 or P^2 or the four cases shown in Figures 3.2 and 3.3 can be distinguished:

- No singularities occur and no MSS exist for either specification of P^1 or P^2 . The qualitative behaviour remains unchanged and the singularity function $\Sigma_{1,2}$ does not intersect zero.
- Singularities occur and MSS exist for P^1 but not for P^2 . The multiplicities disappear or reappear depending on the direction of the input transformation. The singularity function crosses zero at the limit (turning) points \wedge .
- Singularities occur and MSS exist for both specifications, but with different limit points $*$ and \wedge . The singularity function crosses zero four times: At the limit points $*$ it jumps from $+\infty$ to $-\infty$, and at the limit points \wedge it is continuous and intersects zero. The multiplicities are qualitatively different in units of P^1 and P^2 because the limit points do not coincide.
- Degenerated case (c) with identical limit points and MSS existing in both flowrate units. The singularity function is not intersecting zero but jumping from a positive finite value to a negative finite value and vice versa. The multiplicity intervals are identical from a physical point of view.

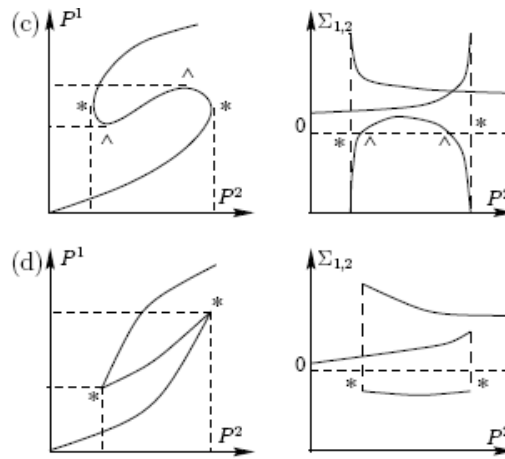


Figure 3.3. Illustration of the last two of four possible types of singularity functions Σ

3.3.3.3 Calculating Singularities in Practice

The results above lead to the question how the singularity analysis would be performed in practice. In order to obtain the ∞/∞ predictions for a column configuration involving a mass product flowrate, $\Sigma_{M,N}$ from equation (3.10) has to be evaluated. This requires information about x^P and P^N for both products D and B, i.e., it needs exactly the information obtained from the original ∞/∞ analysis. By plotting the singularity function $\Sigma_{1,2}$ versus D^N and B^N , respectively, one can determine which of the four cases from Figures 3.2 and 3.3 applies. Therefore, the existence of MSS and the multiplicity interval can be predicted for specifications involving a mass product flowrate.

After having obtained the predictions for mass flowrates, the second singularity function, $\Sigma_{V,M}$ from equation (3.11), can be evaluated. Here, care has to be taken since the density ρ_i not only depends on the composition x^P , but also on the temperature T^P at the location of the flowrate measurement. Therefore, T^P is often not the boiling-point temperature, but a known temperature of a sub-cooled liquid. By sequentially evaluating equations (3.10) and (3.11), each of the resulting singularity functions will show the behaviour of one of the four cases (a) to (d), and the existence of MSS as well as the product flowrate intervals where they occur can be determined for the ∞/∞ case of a column.

The following properties of the singularity analysis are noteworthy:

1. It is often difficult to detect a zero intersection when the singularity function rises to infinity and switches to minus infinity, e.g. at * in case (c) of Figure 3.3. However, by evaluating the inverse, $\Sigma_{M,N} = \Sigma_{M,N}^{-1}$, these limit points will take the much simpler form of the continuous zero intersections at ^ in case (b). Therefore, it is numerically advantageous to simultaneously evaluate $\Sigma_{M,N}$ and $\Sigma_{N,M}$ to correctly identify the type of a singularity.
2. In general, the ∞/∞ singularity analysis must be performed for each product flow independently to obtain the predictions for specifications involving volumetric flowrates, since the overall mass balance does not hold on a volumetric basis (influence of temperature). For mass flowrates, however, holds and evaluation of one product flow is sufficient. Special care has to be taken for reactive distillation systems.
3. The ∞/∞ singularity analysis studied can be applied to single (non-reactive) columns, to column sequences and to reactive distillation columns, as it only depends on the product paths and not on the detailed prediction method used to generate these paths. It will be

shown that the results of a singularity analysis play a key role for the existence of MSS in the MTBE reactive distillation process.

4. There is an alternative procedure without direct evaluation of the singularity functions. With a similar effort as it is necessary to obtain the singularity functions, the product path $x^P(P^N)$ can be recalculated to get $x^P(P^M)$ by application of equation (3.8) and by a diagram as on the left of Figure 3.2. Then, the multiplicity behaviour could be evaluated graphically.
5. The existence of MSS for different specifications could also be directly studied by simulation of a column, but at the cost of much more data and effort needed. The ∞/∞ singularity analysis is based solely on the ∞/∞ prediction results obtained from the application of graphical methods.

3.3.4. Reactive ∞/∞ Singularity Analysis

The ∞/∞ singularity analysis for non-reactive systems described above, the results, the singularity functions (equations 3.10 and 3.11) and the different types of singularities from Figures 3.2 and 3.3, directly carry over to reactive columns. Preliminary to the evaluation of the singularity functions for the relationships between molar and mass, as well as mass and volumetric flowrates, there is one additional relationship to be evaluated in the case of the reactive ∞/∞ predictions. From the ∞/∞ analysis the product paths as functions of the product flowrates are obtained in transformed variables, $X^D(D^D)$ and $X^B(D^D)$, and the existence of MSS can be predicted for transformed flowrates. Even though transformed units can hardly be implemented in a real distillation column, this result is still useful. In the ∞/∞ case, multiplicities of type IIa (caused by the reactive VLE) are mainly governed by the material balances, i.e., by the lever rule. For reactive columns, the lever rule is only applicable in the transformed space and thus, transformed units are the units of choice to appropriately describe a reactive ∞/∞ column. Currently, only the analysis in the transformed space allows to predict whether MSS of type IIa are possible for a given feed (MSS feed region condition).

In order to avoid MSS, one can possibly shift the feed location out of the non-hybrid MSS feed region. However, if the feed cannot be changed for some reason, if MSS are unavoidable to match the product specifications or if MSS are economically attractive, it would be more important to predict the existence of MSS for practical relevant specifications, e.g. for molar, mass or volumetric flowrates. This is where the singularity analysis comes in. Without loss of generality, any of the distillate and bottoms products will be denoted by P and the corresponding reactive product paths by $X^P(P^D)$.

Starting from the results of the bifurcation analysis with respect to P^D , it is possible to predict MSS for molar (P^N), mass (P^M) or volumetric flowrates (P^V) for the ∞/∞ case of a reactive column. This means that the ∞/∞ predictions are extended to cover also type Ia multiplicities, i.e., singularities in the input relationships (Jacobsen and Skogestad, 1991). In addition to the equations relating molar, mass and volumetric flowrates, (3.8) and (3.9), the following relation between transformed and molar flowrates is obtained from the transformation equation (3.3):

$$P^N = \left(1 - \nu_{tot}^T (\nu_{ref})^{-1} x_{ref}^P\right)^{-1} P^D \quad (3.12)$$

Again, x^P on a bifurcation path is a function of the product flowrate P^D . By taking the derivative of the equation, a product singularity function in addition to (3.10) and (3.11) is obtained:

$$\Sigma_{N,D} = \frac{dP^N}{dP^D} = \left(1 - \nu_{tot}^T (\nu_{ref})^{-1} x_{ref}^P\right)^{-1} - \frac{P^D}{\left(1 - \nu_{tot}^T (\nu_{ref})^{-1} x_{ref}^P\right)^2} \cdot \frac{d}{dP^D} \left(\nu_{tot}^T (\nu_{ref})^{-1} x_{ref}^P\right) \quad (3.13)$$

Note that the complexity of expression (3.13) is caused by its general formulation and that the equation is much simpler for a specific transformation. Importantly, the four possible types of singularities shown in Figures 3.2 and 3.3 and the corresponding argumentation can equally be applied to $\Sigma_{N,D}$.

These results lead to the question how the procedure to calculate singularities in practice from non-reactive systems has to be changed for reactive columns. First $\Sigma_{N,D}$ has to be evaluated to obtain the ∞/∞ predictions for specifications involving a molar product flowrate. However, the evaluation of equation (3.13) requires the knowledge of the physical compositions x and hence, back-transformation has to be carried out. This is a major drawback of the singularity analysis for reactive systems.

After having obtained the predictions for molar flowrates, the procedure continues completely identical as for non-reactive systems: The singularity functions $\Sigma_{M,N}$ and $\Sigma_{V,M}$ are evaluated one after the other. Note that the physical compositions x and the temperature T are known (either by design or from the back-transformation).

Important properties of the singularity analysis have been studied for non-reactive systems and apply to reactive systems as well. Most important, the singularity analysis has to be done for each product flow independently to obtain the predictions for specifications involving molar flowrates, since the reaction term in (3.6) can cause MSS to exist in one product flow but not in the other.

3.3.5. Non-Hybrid ∞/∞ Predictions: Inputs and Results

Prior to summarizing the results obtained from the reactive ∞/∞ bifurcation and singularity analyses, the necessary information to obtain the ∞/∞ predictions is discussed. Basically, the information needed is of the same type as for the non-reactive analysis, i.e., the boiling points and locations of the azeotropes and the distillation boundaries (if there are any). However, in contrast to the widely available databases for non-reactive azeotropes, the existence and location of reactive azeotropes is rarely known in advance, because they depend not only on the VLE but also on the reaction equilibrium (Okasinski and Doherty, 1997b). Therefore, a reliable VLE and reaction equilibrium model has to be available and a reactive residue curve diagram has to be calculated for a mixture of interest. Moreover, a composition transformation has to be found for the stoichiometry of the reactions in the mixtures. After having solved the differential-algebraic equation system, all necessary information can be read from the reactive residue curve diagram. It is important to note that the predictions depend only mildly on the specific column design.

The only information needed is the type of the column internals (trays or packing) as well as the types of condenser and reboiler to appropriately select reactive distillation lines or residue curves.

From the ∞/∞ analysis for non-hybrid reactive systems, the following information can be obtained:

Existence of Multiplicities: The existence of multiple steady states caused by the reactive VLE can be predicted in the ∞/∞ case of a non-hybrid reactive distillation column and a given feed by the geometrical, necessary and sufficient multiplicity condition.

Non-hybrid MSS Feed Region: For any non-hybrid system, the region of feeds that lead to output multiplicities in the ∞/∞ case can be predicted in transformed coordinates. Determining the

corresponding region in the physical composition space is straightforward and does not require back-transformation.

Quantitative Predictions: For any non-hybrid system and a given feed all possible column profiles can be located in the transformed composition space by performing a continuation of solutions. From the product paths obtained by the continuation, bifurcation diagrams can be constructed and the limit points as well as the product flowrate multiplicity range (the interval of the product flowrate where MSS exist) can be determined.

Singularity Analysis: By performing a series of singularity analyses, the predictions obtained for transformed flowrates are extended to specifications involving molar, mass or volumetric flowrates. Qualitative and quantitative changes in the multiplicity behaviour are detected. This means that the ∞/∞ predictions are expanded to also cover the type Ia multiplicities studied by Jacobsen and Skogestad (1991). However, since the analysis requires that one product flowrate is used for the specification, the [L; V] configurations studied by Jacobsen and Skogestad (1991) cannot be taken into account.

Hence, the methods presented allow the simultaneous prediction of output multiplicities caused by the reactive VLE (type II) and by the nonlinearities in the flowrate relationships (type Ia).

3.3.5 Implications for Finite Reactive Columns

The ∞/∞ case is the limiting case of *high reflux, fast reactions* and a *large number of equilibrium stages*. Therefore, if MSS are predicted by the geometrical condition for a given feed, these multiplicities will also exist for columns with sufficiently large reflux, sufficiently fast reactions and a large number of stages. However, the “critical design” where MSS disappear can not be predicted. Since the geometrical condition is only sufficient for finite columns, there may be multiplicities in finite columns which cannot be predicted using the ∞/∞ analysis, e.g. those related to heat effects (type Ib). Similarly, the MSS feed region is affected for finite columns. From experience, the feed region for finite but large columns is smaller than in the ∞/∞ case. If the reflux and the number of equilibrium stages are decreased, the MSS feed region collapses and the multiplicities disappear (Bekiaris and Morari, 1996).

These observations have the following consequences if the existence of MSS is questioned for a given finite non-hybrid column and a given feed. First, if the feed lies inside the non-hybrid MSS feed region, MSS will exist for transformed flowrates and a sufficiently large column operated at large internal flows. In principle, they could disappear for molar or mass flowrates by singularities in the corresponding relationships although this has not been observed in any of the studies. Secondly, MSS of type II will not exist for a feed outside the non-hybrid MSS feed region (in transformed coordinates). However, singularities in the relationship between transformed and molar flows seem to play an important role if the feed is located close to the non-hybrid MSS feed region and can result in a MSS feed region in molar coordinates different from the transformed one. Even though they are theoretically possible, singularities between molar and mass flows have not been reported for points outside the MSS feed region (in transformed coordinates) and for non-hybrid columns. Nevertheless, the existence of MSS of type Ia strongly depends on the column configuration.

3.4. Reactive ∞/∞ Procedures

3.4.1 Reactive Geometrical Multiplicity Condition

In this section the *geometrical, necessary and sufficient, multiplicity condition* is adapted from the case of single columns. The extension of the condition to reactive systems is straightforward if the transformed continuation paths and the transformed feed composition are used. If a continuation path is defined as the path generating all possible column profiles starting at $D^D=0$ and ending at $D^D=F^D$, MSS result when the transformed distillate flowrate is decreasing

somewhere along this path. Note that subscripts are used for indexing different steady states in this case.

Pick a pair of transformed product compositions X_1^D and X_1^B from the path which are connected by a type III profile, i.e., the profile runs over at least one reactive saddle singular point. Thus, these product locations will be located on a reactive distillation boundary or on the edges of the transformed composition space (Figure 3.4). Now pick X_2^D and X_2^B sufficiently close to X_1^D and X_1^B such that the new column profile corresponds to a “later” profile on the continuation path. For the existence of multiple steady states it is required, as one moves along the continuation path from the product locations 1 to 2, that the line passing from X_1^D parallel to $X_1^B X_2^B$ crosses the $X_2^D X_1^B$ line segment at I.

This formulation of the geometrical multiplicity condition can be applied to four entirely different column types with minor modifications: homogeneous and heterogeneous azeotropic columns, column sequences and non-hybrid as well as hybrid reactive distillation columns.

3.4.2 Non-Hybrid MSS Feed Region Construction

The construction procedure for the MSS feed region was adapted from Bekiaris et al. (1996). From all possible product paths in the ∞/∞ case the segments for which the products are connected by a type III profile are investigated. It is sufficient to consider type III profiles only for the construction of the MSS feed region, since the product flowrates can only vary non-monotonically for such profiles.

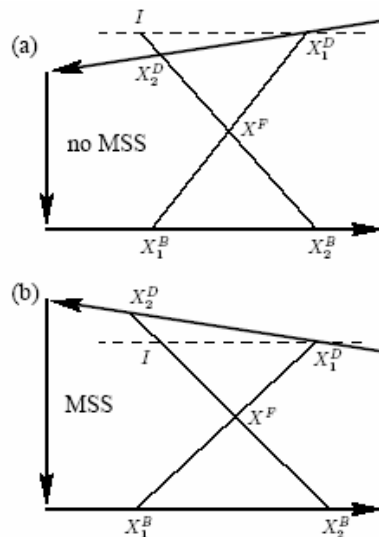


Figure 3.4. Illustration of the geometrical, necessary and sufficient multiplicity condition for reactive distillation columns.

For each possible segment of the path of type III profiles the procedure is performed as following:

1. Pick a transformed product location from a product path, e.g. X^D .
2. Find the set containing all other product compositions X^B such that the geometrical condition is satisfied for the picked X^D and name this set $S(X^D)$. Note that $S(X^D)$ is always part of a reactive distillation boundary or the edges of the transformed composition space and that it may contain an inflexion point and/or it may consist of more than one non-connected boundary segments.
3. Draw the straight lines connecting X^D with the end points of each of the boundary segments belonging to $S(X^D)$.
4. For the X^D chosen, the appropriate feed composition is the union of the areas enclosed by each boundary segment that belongs to $S(X^D)$ and the corresponding straight lines connecting the end points of the segment with X^D . Name this union $A(X^D)$.

5. Choose another X^D and repeat from 1 for any X^D on the continuation path.
6. Finally, the transformed feed compositions X^F that lead to output multiplicities lie in the union of all the areas $A(X^D)$, i.e., in the union of all areas enclosed by the boundary segments that belongs to some $S(X^D)$.

3.4.3 Back-transformation of the ∞/∞ Predictions

The non-hybrid ∞/∞ theoretical predictions are obtained in transformed compositions and flowrates, X^P (P^D) (where P stands for any product flow D or B). To obtain the predictions using molar compositions, X^P has to be transformed back. This means, that the $c-r-1$ independent transformation equations (3.2) have to be solved simultaneously with the r chemical equilibrium equations. In general, the latter take the form (for each reaction):

$$K(T) = \prod_{i=1}^c a_i^{v_i} = f(x_i, \gamma(x_i, T)) \quad (3.14)$$

where f is nonlinear. This equation is problematic because the boiling point temperature T is involved in an implicit and nonlinear manner. T is determined by a bubble-point calculation at a given pressure p which involves x and, is nonlinear and implicit in T :

$$\text{Find } T \text{ such that } \sum_i x_i p_i^o(T) \gamma_i(x, T) = p \quad (3.15)$$

Therefore, it is obvious that the back-transformation problem can only be solved numerically for each X^P . If the equilibrium constant K is not temperature dependent and the relationship (3.14) does not involve the activity coefficients, then an analytical solution would be possible.

For type III profiles it was shown that the products either lie on the edges of the triangle or on interior boundaries. Normally, the back-transformation of compositions lying on the edges of the transformed space is rather simple since some components are missing. Moreover, the interior boundaries are reactive residue curve boundaries which are obtained by integration of equation (3.4). In order to get $Y(X)$, a bubble-point calculation has to be done and hence, the molar compositions x and y are known. By storing x together with the transformed compositions on the boundary the back-transformation can be simplified using a look-up table and interpolation methods.

Chapter 4 - Hybrid ∞/∞ Analysis

The ∞/∞ analysis from the Chapter 3 can be applied to columns with a reacting core (“hybrid” columns). They are built from a reactive column section, where the catalyst is present, and one or two non-reactive sections (rectifying and stripping sections). In some cases a higher performance can be obtained by the use of hybrid columns.

4.1 Hybrid ∞/∞ Profiles

4.1.1 Preliminaries

First, note that the definitions introduced for non-hybrid columns (MSS, column configurations etc) carry over to hybrid columns. By feasible hybrid profiles steady-state column profiles of a hybrid equilibrium reactive distillation column are denoted. Again, such profiles can be assigned to a real distillation plant (measured profiles) or to a distillation column model (steady-state solutions). In this chapter, the “model” of interest for the analysis is the ∞/∞ limiting case of a hybrid column (to be described).

In Chapter 3, feasibility conditions were developed for profiles in the ∞/∞ case of a non-hybrid equilibrium reactive column: The (packed) column profile must coincide with a reactive residue curve, it must contain at least one reactive pinch point and the lever rule in transformed units must be fulfilled (simplified formulation). At a first glance, the extension of these conditions to hybrid ∞/∞ columns might appear rather simple: The reactive residue curves have to be replaced by their non-reactive counterparts for the column sections where no reactions take place (rectifying and stripping sections).

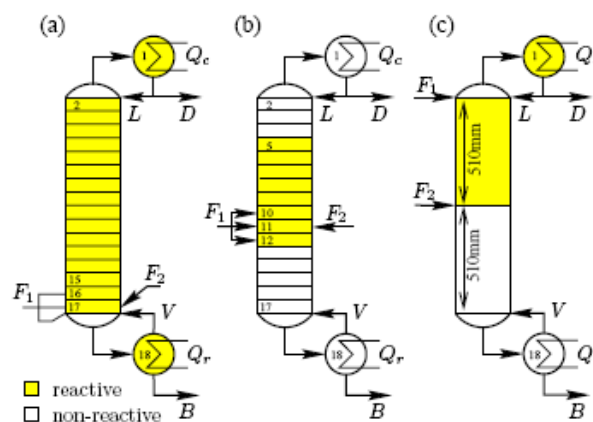


Figure 4.1 Three reactive distillation columns: (a) a non-hybrid column, (b) the hybrid “Nijhuis” column (Nijhuis et al., 1993), and (c) the hybrid “Clausthal” column (Sundmacher and Hoffmann, 1995).

The necessity of a pinch point and of the lever rule to be fulfilled in transformed units remains. However, there are several problems which make the extension non-trivial: The lever rule in transformed units is necessary but not sufficient to guarantee feasibility of a hybrid column profile. Moreover, it is non-trivial to extend the concept of infinite length to a hybrid column, which consists of multiple sections of physically different nature (reactive and non-reactive). One can imagine that the whole column is of infinite length or, for example, that each of the reactive and non-reactive sections has infinite length. Therefore, a closer look at necessary and sufficient conditions for feasible hybrid profiles in the ∞/∞ case is needed.

4.1.2 ∞/∞ Assumptions for Hybrid Columns

By definition, a hybrid reactive column consists of up to three column sections: a non-reactive rectifying section, a reactive section and a non-reactive stripping section. Sometimes, one of the non-reactive sections can be missing as shown in Figure 4.1, where a non-hybrid (a) and two hybrid column designs (b, c) are illustrated. As indicated above, the assumption of infinite column length (an infinite number of equilibrium stages) can be realized in different ways in the ∞/∞ case of a hybrid column. Hereafter, two approaches (or ∞/∞ “models”) are studied: In one approach, each of the sections present (rectifying, reactive and stripping section) is assumed to have infinite length. This realization is the basis for the hybrid analysis referred to as the exact method. Feasibility conditions for such hybrid profiles will be developed later in this section. In the other approach, it is assumed that only the reactive section has infinite length, and that the other sections are of finite length.

The following assumptions are made for the ∞/∞ analysis of hybrid reactive columns:

Assumptions 1 (∞/∞ Assumptions for Hybrid Columns):

1. *Reactions take place in the liquid phase of the reactive section and reach chemical equilibrium instantaneously, i.e., simultaneous chemical and vapour-liquid equilibria are established;*
2. *a. for the exact method, each of the rectifying, reactive and stripping sections of a hybrid column have infinite length (an infinite number of stages);*
2. *b. for the approximate method, the reactive section has infinite length, but both rectifying and stripping sections are considerably smaller;*
3. *the column operates at infinite internal flows (infinite reflux and boil-up);*
4. *the column pressure is constant (negligible pressure drop);*
5. *all column feeds enter the reactive section.*

The fourth assumption is not fundamental to the following analysis and could be relaxed, but at the cost of a more complex formulation of the procedure to construct the MSS feed region. Note that in the limiting case of infinite reflux, the number and location of the feeds within a section have no influence on the product compositions as long as the overall feed flowrate and composition remain the same (Laroche et al., 1992a).

Anyway, feeding to the reactive section also makes sense intuitively. The task of the reactive section is to convert the reactants to the desired products and to remove the latter from the section. Conversely, the rectifying and stripping sections separate products and inerts from the reactants, which are recycled to the reactive section. An unreacted feed only contains reactants and inert components and should therefore be fed to the reactive section. Feeding to a non-reactive section would cause additional traffic (and heat requirements), since the reactants have to be transported to the reactive section first.

4.1.3 Infinite Internal Flows and Infinite Column Length

At infinite internal flows (infinite reflux and boil-up), the profile of a packed non-hybrid reactive column coincides with a part of a reactive residue curve (Chapter 3). The profile of a packed non-reactive column coincides with some part of a non-reactive residue curve (Chapter 3). Similar conditions were found for tray columns including different types of condenser or reboiler equipment. The formulation used here rests upon residue curves since they are reasonable approximations to describe profiles of tray columns (Widagdo and Seider, 1996). Therefore, the rectifying and stripping profiles of a hybrid column operated at infinite internal flows have to coincide with some parts of non-reactive residue curves, and the reactive section profile in transformed units has to coincide with some part of a reactive residue curve.

If any column section has infinite length, there must be at least one pinch point in the column profile of that section (Petlyuk and Avet'yan, 1971). At infinite internal flows, the only candidate pinch points are the singular points of the corresponding (reactive or non-reactive) residue curve map. Therefore, in the case where each of the column sections has infinite length (assumption 1.2a), the reactive section profile has to contain at least one reactive singular point and each of the rectifying and stripping profiles has to contain at least one non-reactive singular point. In the case of assumption 1.2b, only the reactive section must contain at least one reactive pinch, the other sections have finite length.

4.1.4 Material Balances for Hybrid Columns

So far, the extension of the feasibility conditions from non-hybrid to hybrid columns was rather straightforward. The crucial point is the global material balance and thus the lever rule for hybrid columns. Ung and Doherty (1995d) derived the equations describing the operating lines (material balances) of a non-hybrid column. They showed that the equations for the reactive sections are identical to those of non-reactive columns if all molar compositions and flowrates are replaced by their transformed analogues (for the transformation equations see Chapter 3). Moreover, the overall material balances maintain their form in transformed coordinates. Note that F_{tot} , x_{tot}^F and X_{tot}^F are the overall (total) feed flowrate, the overall molar and the overall transformed feed compositions, respectively. From Figure 4.2, the transformed material balances of the reactive section can be written as:

$$\begin{aligned} F_{\text{tot}}^D &= L_3^D + V_2^D - L_2^D - V_3^D \\ F_{\text{tot}}^D X_{\text{tot}}^F &= L_3^D X_3 + V_2^D Y_2 - L_2^D X_2 - V_3^D Y_3 \end{aligned} \quad (4.1)$$

From material balances around the non-reactive rectifying section (including the condenser) and the stripping section (including the reboiler) one obtains:

$$\begin{aligned} \text{Rectifying section : } \quad V_2^N &= L_2^N + D^N \\ V_2^N y_2 &= L_2^N x_2 + D^N x^D \end{aligned} \quad (4.2)$$

$$\begin{aligned} \text{Stripping section : } \quad L_3^N &= V_3^N + B^N \\ L_3^N x_3 &= V_3^N y_3 + B^N x^B \end{aligned} \quad (4.3)$$

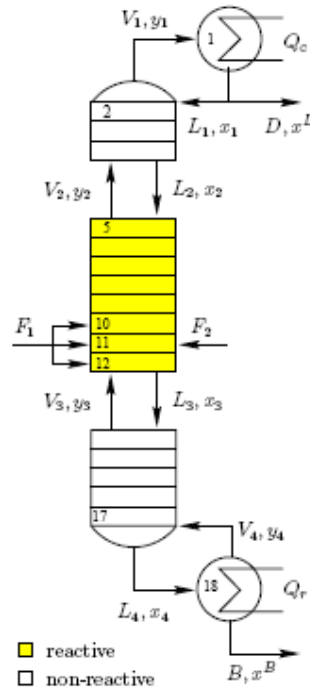


Figure 4.2. Illustration of a hybrid reactive distillation column with two non-reactive and one reactive section (“Nijhuis” column). Note that the indexes do not correspond to tray numbers.

Importantly, the transformed composition variables X are reaction-invariant compositions and take the same value for any reaction extent of a given liquid mixture (Ung and Doherty, 1995e). Hence, X takes the same value for an unreacted mixture and the same mixture in chemical equilibrium. Consequently, the non-reactive material balances of the rectifying and stripping sections in molar units are also fulfilled in transformed units:

$$\begin{aligned} \text{Rectifying section : } V_2^D &= L_2^D + D^D \\ V_2^D Y_2 &= L_2^D X_2 + D^D X^D \end{aligned} \quad (4.4)$$

$$\begin{aligned} \text{Stripping section : } L_3^D &= V_3^D + B^D \\ L_3^D X_3 &= V_3^D Y_3 + B^D X^B \end{aligned} \quad (4.5)$$

By combining equations (4.1), (4.4) and (4.5), the flows at the section borders can be eliminated and the global material balance of a hybrid column in transformed units is obtained (after some rearrangement):

$$\begin{aligned} F_{tot}^D &= D^D + B^D \\ F_{tot}^D X_{tot}^F &= D^D X^D + B^D X^B \end{aligned} \quad (4.6)$$

Therefore, the lever rule in transformed units does not only hold for non-hybrid, but also for hybrid columns. Any feasible hybrid column profile must fulfill equations (4.6) and thus must follow the transformed lever rule.

The three conditions above, coincidence of profiles with residue curves, necessity of pinch points, and the transformed lever rule, are necessary but not sufficient for feasibility of a hybrid column profile under assumption 1.2a, although they are necessary and sufficient conditions for non-hybrid columns. The reason is that the transformed composition space has a lower

dimension ($c - r$) than the physical space (c). Thus, the transformed lever rule consists of $c - r$ linear independent equations ($c - r - 1$ for the compositions X and one overall balance). Such a description is adequate for the reactive column section or for a non-hybrid column, which is part of the reaction space and thus exhibits $c - r$ degrees of freedom. However, the non-reactive sections exist in the physical space and have c degrees of freedom. Therefore, r equations are missing if non-reactive sections are described by the transformed lever rule only and thus, r equations from the non-reactive component balances, (4.2) or (4.3), have to be fulfilled in addition (for each non-reactive section).

4.1.5 Feasible Hybrid ∞/∞ Profiles

In conclusion, the necessary and sufficient conditions for feasible hybrid ∞/∞ profiles under assumption 1.2a are:

Conditions 3 (Feasible ∞/∞ Hybrid Profiles):

1. the rectifying and stripping profiles of an ∞/∞ hybrid column must coincide with parts of non-reactive residue curves, and the reactive section profile in transformed units must coincide with a part of a reactive residue curve;
2. each column section contains at least one pinch point (appropriate reactive or non-reactive singular points);
3. the transformed lever rule (4.6) holds;
4. r independent non-reactive material balances hold for each non-reactive section.

Note that for scenarios of infinite column length different from assumptions 1.2a, condition 3.2 may not be necessary.

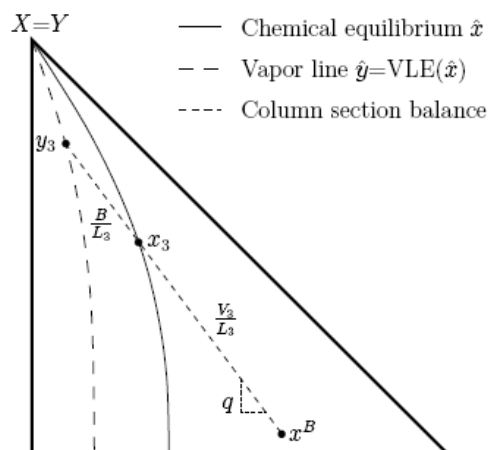


Figure 4.3. Illustration of the graphical interpretation of the feasibility condition 3.4 for a non-reactive hybrid stripping section (notation from Figure 4.2).

4.1.6 Graphical Interpretation

There is a severe problem with mixing rules for column sections in the ∞/∞ case: All internal flowrates L_i and V_i at the section borders are infinite and thus, it is impossible to evaluate the lever rule graphically (Figure 4.2). The ∞/∞ analysis, however, rests upon geometrical methods and requires a lever rule for the graphical determination of all feasible profiles. Thus, there is the need for a graphical interpretation of condition 3.4 which is suitable for the ∞/∞ case. The following approach can be applied to either of the non-reactive sections and is demonstrated for the stripping section hereafter.

In Figure 4.3, the mass balance line of the stripping section is illustrated in the two-dimensional molar composition space ($c = 3$) where a single reaction takes place ($r = 1$). The composition and flowrate of the bottoms product B (a total of three degrees of freedom) are not unique by the transformed lever rule ($c - r = 2$ equations). Rearranging the non-reactive balance around the stripping section (4.3), a mixing rule can be obtained (Figure 4.3):

$$x_3 = \frac{V_3}{L_3} y_3 + \frac{B}{L_3} x^B \quad (4.7)$$

For the limiting case of infinite internal flows (the external flowrate B remains finite and constant):

$$\lim_{L_3, V_3 \rightarrow \infty} \frac{V_3}{L_3} = 1 \quad \text{and} \quad \lim_{L_3, V_3 \rightarrow \infty} \frac{B}{L_3} = 0 \quad (4.8)$$

Geometrically, x_3 approaches y_3 in Figure 4.3 until they coincide in the limit of infinite internal flows. Note that in the limiting case, the distance between B and y_3 is not defined (by the lever rule) and therefore, the exact location of the bottoms product B (covering all three degrees of freedom) cannot be determined. However, it can be determined the direction of the line shown in Figure 4.3 and thus, one obtains a “locus” of all possible x^B compositions. This locus can be understood as the graphical interpretation of the feasibility condition 3.4.

As the next step, it is described how one calculates the properties of this locus of the bottoms product. Since the liquid L_3 is leaving the reactive section, x_3 is in chemical equilibrium and lies on the bold solid line \hat{x} in Figure 4.3. y_3 is the vapour in equilibrium with the liquid composition on the top stage of the stripping section. Therefore, y_3 is not in chemical equilibrium in a finite column. In the limiting case of an infinite number of equilibrium stages in each column section, however, there is a pinch point at the border of the reactive and stripping section (justified below). Therefore, the concentration difference at the border disappears and thus, the liquid composition on the top stage of the stripping section approaches chemical equilibrium. Hence, y_3 is in vapour-liquid equilibrium with a composition in chemical equilibrium, and is therefore located on the “reactive vapour line” \hat{y} (dashed bold in Figure 4.3). In the limit of infinite internal flows (4.8), x_3 and y_3 must coincide. This can only happen at a singular point of both the molar composition space and the reaction space ($X=Y$ in Figure 4.3). Therefore, this singular point will act as a simultaneous pinch point in both the stripping and the reactive section as stipulated.

Next, since x^B must lie on the straight mass-balance line through x_3 and y_3 , the direction of this line needs to be calculated in the ∞/∞ case. This line is referred to as the “q-line”: it starts at $X=Y$ and its slope is denoted by q (Figure 4.3). At the joint singular point, q can be easily computed from the data available for the calculation of the reactive residue curves (the molar compositions \hat{x} in chemical equilibrium and their corresponding vapour compositions \hat{y}). Starting with \hat{x} on any reactive residue curve close to the singular point, the limiting value q is obtained as \hat{x} approaches the singular point. Therefore, the calculation of q requires thermodynamic information only, and the q-line is a property of the chemical and vapour-liquid equilibrium of a mixture. In general, the graphical element resulting from this procedure is not necessarily a line, but a plane in higher dimensions (etc). Nevertheless, the term “q-line” is kept here for simplicity. Note that even though the procedure is exact in the ∞/∞ limiting case, its graphical representation is approximate by the calculation procedure. Therefore, condition 3.4 should be used to determine feasibility of a hybrid profile exactly. Not surprisingly, the procedure requires the non-reactive composition space to be used for the graphical determination of any hybrid ∞/∞ profile.

4.2 Hybrid ∞/∞ Methods

4.2.1 The Exact Method

The non-reactive prediction tools of Bekiaris et al. (1993) were extended to non-hybrid reactive distillation columns (non-hybrid ∞/∞ analysis). Importantly, it was shown that the only prerequisite for extending the ∞/∞ analysis to a new class of distillation systems is the availability of necessary and sufficient feasibility conditions for column profiles in the ∞/∞ case. This prerequisite can be fulfilled for hybrid columns under assumption 1.2a (where each column section has infinite length), since the feasibility conditions 3 are necessary and sufficient in this case. Therefore, under assumption 1.2a all the procedures described in the current section are applicable to ∞/∞ hybrid columns.

The basic idea for the formulation of the hybrid ∞/∞ prediction method is to make use of the analogy to the non-hybrid method by replacing the feasibility conditions for non-hybrid columns with the hybrid equivalents, resulting in a graphical method to determine all possible hybrid column profiles for a given feed. This analogy is possible since a hybrid column of given design with given feed composition, flowrate and quality, has only one operational degree of freedom in the ∞/∞ case, just like a non-hybrid column (Appendix B). Thus, the single degree of freedom can be used to parameterize all possible profiles and to perform a continuation of solutions. Since the lever rule holds in transformed units only, the transformed distillate flowrate D^D is selected as the continuation parameter (B^D is given by equation 4.6). As a result, the formulations of the hybrid prediction methods are very similar to those for non-hybrid columns in Chapter 3. Instead of describing these hybrid formulations in great detail hereafter, the focus will be on the main results, and on the discussion of the differences to the non-hybrid counterparts from Chapter 3.

Hybrid ∞/∞ Bifurcation Analysis: The hybrid bifurcation analysis proceeds analogously to the non-hybrid one. First, the feasible profile in the limiting case of an ∞/∞ hybrid column with zero distillate flow, $D^D=0$, is determined (initial profile). Second, the feasible profile with zero bottoms flow, $B^D=0$ and $D^D=F^D$, must be found (final profile). The properties of the initial and final hybrid profiles are quite different from those of the non-hybrid profiles and are discussed in Appendix 4.5. Third, a bifurcation study (continuation of solutions) is performed by tracking the distillate and bottoms compositions in the transformed composition space, starting from the profile with $D^D=0$ and ending at the profile with $DD=FD$. With this procedure, all feasible transformed composition profiles are obtained for the ∞/∞ case of a hybrid reactive column under assumption 1.2a.

The definitions of the continuation path as well as of the distillate and bottoms product paths carry over from the non-hybrid analysis. Since the graphical interpretation of the feasibility conditions 3 requires to work in the physical composition space, the product paths are generally obtained in molar compositions. However, they are parameterized by the transformed distillate flowrate, D^D , since the lever rule holds in the transformed space only. By plotting the parameterized paths, $x^D(D^D)$ and $x^B(D^D)$, versus the flowrate D^D , a series of bifurcation diagrams can be constructed, and the limit points as well as the interval of the product flowrate where MSS exist can be determined. These product paths are denoted by $x^P(PD)$ hereafter, where P stands for any product D or B. If the transformed distillate flowrate is varying non-monotonically along the continuation path, multiple steady states of type II exist in the ∞/∞ case of a hybrid column (under assumption 1.2a) and for the feed composition studied. Note that only transformed flowrates allow to identify type II multiplicities, since the lever rule does only hold in transformed units. Multiplicities in other flowrate units are detected by the reactive singularity analysis to follow.

Geometrical Multiplicity Condition: The geometrical, necessary and sufficient multiplicity condition is used to detect a decrease in the distillate flowrate on the continuation path as defined above, i.e., the existence of MSS. It takes exactly the same form as for non-hybrid columns if the

non-hybrid product paths are replaced by their hybrid equivalents. Since the lever rule only holds in the transformed composition space, the hybrid product paths $x^P(P^D)$ have to be transformed to obtain $X^P(P^D)$ in advance to applying the condition.

Hybrid MSS Feed Region: All possible feed locations leading to MSS in the ∞/∞ case of a hybrid column under assumption 1.2a can be predicted by the MSS feed region condition. The procedure developed for non-hybrid systems can be applied directly to hybrid columns by replacing the product paths as was done for the geometrical condition above. Since all feeds enter the reactive section of the hybrid column, MSS existing for a transformed feed composition X^F will also exist for all molar feed compositions x^F resulting in the same composition in chemical equilibrium. Therefore, the methods relating the transformed and physical MSS feed region from Chapter 3 carry over, and the physical hybrid MSS feed region can easily be constructed.

Reactive Singularity Analysis: The ∞/∞ singularity analysis was refined for application to reactive columns in Section 3.3.4. Note that the product paths from the hybrid bifurcation analysis are obtained in the physical composition space, parameterized by a transformed flowrate, $x^P(P^D)$. Therefore, no back-transformation is needed to determine $x^P(P^N)$, but singularities in the relationship between transformed and molar flowrates are still possible. Importantly, the reactive singularity analysis applies to hybrid columns without any modification of the formulation. Consequently, the hybrid prediction method can be extended to specifications involving molar, mass or volumetric product flowrates and covers the type Ia multiplicities studied by Jacobsen and Skogestad (1991). Qualitative and quantitative changes in the multiplicity behavior can be detected.

4.2.2 The Approximate Method

Recall the suggestion made earlier, that assumption 1.2a is one, but not the only possible “model” of an hybrid column with infinite length. However, it is the only model for which are derived successfully the necessary and sufficient feasibility conditions for hybrid ∞/∞ profiles (conditions 3). These conditions are the basis of the exact method described above, which is exact in the ∞/∞ case of hybrid columns under assumption 1.2a, i.e., where each of the hybrid column sections has infinite length (or an infinite number of equilibrium stages). The major drawback of the exact method is inherent in feasibility condition 3.2, which requires at least one pinch point in each column section. Since pinch points may be “shared” (at the section borders), at least two pinch points are necessary for a feasible profile under assumption 1.2a. These feasibility conditions are quite restrictive and thus, feasible hybrid ∞/∞ profiles may not exist in some cases, resulting in the non-applicability of the exact method. For an ∞/∞ “model” different from assumption 1.2a, i.e., dropping the assumption that each column section independently must have infinite length, condition 3.2 is no longer necessary and a feasible profile may exist. Even though a “precise” analysis is not possible because necessary and sufficient conditions are not available in this case, the aim of this section is to provide a method to *approximate* the product locations of such an hybrid column.

The approximate procedure is described here for hybrid columns, where only the reactive section is of infinite length, and the non-reactive sections are finite (assumption 1.2b). Moreover, it is assumed that the non-reactive sections are relatively small and consist of a few equilibrium stages only. The approximate method rests upon the information obtained from the non-hybrid ∞/∞ bifurcation analysis (Section 3.3.1), i.e., the non-hybrid product paths in the transformed compositions space, $X^P(P^D)$. Each of these product paths is the *locus* of all possible product locations in a column with a single, reactive section of infinite length. The basic idea of the procedure described hereafter is to “convert” these non-hybrid product paths into an *estimate* of the product paths for a hybrid column with small non-reactive sections (assumption 1.2b).

Beforehand, two well-known computational tools are introduced. By a *boiling-point iteration* we refer to the solution of the recursive expression (counting trays from the top):

$$\begin{aligned} x_{(n-1|n)} &= y_{(n|n)} \\ \left[y_{(n|n)}, T = VLE(x_{(n,n)}, p) \right] \end{aligned} \quad (4.9)$$

Given the liquid composition $x_{(n|n)}$ on tray n, the liquid composition $x_{(n-1|n)}$, which is equal to the vapour composition in equilibrium with $x_{(n|n)}$, is calculated. $x_{(n-1|n)}$ denotes the liquid composition on tray n-1, calculated from the known composition of tray n.

Likewise, a *dew-point iteration* is defined as:

$$\begin{aligned} y_{(m+1|m)} &= x_{(m|m)} \\ \left[x_{(m+1|m)}, T = VLE^{-1}(y_{(m+1|m)}, p) \right] \end{aligned} \quad (4.10)$$

Here, the liquid composition on tray m+1, $x_{(m+1|m)}$, which is based on the information from tray m, is the composition of the liquid in VLE with its vapour of composition $x_{(m|m)}$.

Algorithms for boiling- and dew-point computations can be taken from Smith et al. (1996). First, the distillate product path from the non-hybrid ∞/∞ analysis, $X^D(P^D)$ is back-transformed to obtain the corresponding physical compositions in chemical equilibrium, $x^D(P^D)$ (for the back-transformation see Section 3.4.3). This locus of compositions is assumed to approximate *all possible* liquid compositions at the top of the infinitely-long reactive section, $x_{(n|n)} = x^D(P^D)$.

The parameterization with the product flowrate P^D is removed. It is important to note that this is a very crude approximation, since any liquid composition leading to the same composition in chemical equilibrium should be considered at the entrance of the reactive section (compare with Figure 4.2). Similarly, the non-hybrid bottoms path after back-transformation is taken as the locus of all possible compositions of the liquid leaving the reactive section at its lower end, $x_{(m|m)} = x^B(P^D)$ (again removing the parameterization with P^D). This is accurate since the liquid leaving the section is in chemical equilibrium (from Figure 4.2).

In addition to the reactive section of infinite length, the column consists of N_{rect} non-reactive rectifying trays (excluding a total condenser) and N_{strp} non-reactive stripping trays (including a partial reboiler), which are assumed to be equilibrium stages. Now, the approximate procedure can be formulated:

1. Approximate the loci of all possible compositions at the upper and lower end of the reactive section, $x_{(n|n)}$ and $x_{(m|m)}$, as described above.
2. Map the locus $x_{(n|n)}$ repeatedly N_{rect} times using recursion equation (4.9) to obtain $x_{(n-N_{\text{rect}}|n)}$. In the following it is assumed, that the converted composition path $x_{(n-N_{\text{rect}}|n)}$ is an estimate for all possible liquid compositions on the N_{rect} non-reactive tray on top of the reactive section, i.e., an estimate of the all possible distillate locations of the hybrid column.
3. Map the locus $x_{(m|m)}$ repeatedly N_{strp} times using recursion equation (4.10) to obtain $x_{(m+N_{\text{strp}}|m)}$. Similar to point 2, the converted composition path $x_{(m+N_{\text{strp}}|m)}$ is assumed to estimate all possible liquid compositions on the N_{strp} non-reactive tray below the reactive section, i.e., it estimates all possible bottoms product locations of the hybrid column.
4. Transform the estimates of the hybrid product locations obtained in 2 and 3 to obtain $X_{(n-N_{\text{rect}}|n)}$ and $X_{(m+N_{\text{strp}}|m)}$. Apply the transformed lever rule (4.6) to all points on these

paths (using the given transformed feed location) to recover an estimate of the transformed product flowrates, $D|_n^D$ or $B|_m^D$.

Consequently, the product path obtained from this procedure can be depicted in the transformed composition space in the same way as the non-hybrid product paths. Moreover, bifurcation diagrams can be generated by plotting some $X_{(n-N_{rect}|n)}$ or $X_{(m+N_{strip}|m)}$ versus the flowrate $D|_n^D$.

There is no theoretical reason why the geometrical condition, the procedure to construct the MSS feed region, and the reactive singularity analysis from the non-hybrid analysis cannot be applied to these product paths. Some practical drawbacks, however, are discussed later.

Note that the approximate method is mainly justified by the results and is considered tentative here. There is no mathematical evidence on its preciseness, reliability or robustness except for the examples described later on. Thus, there may be better procedures to determine hybrid product paths for columns under assumption 1.2b. However, there is some physical argumentation supporting the procedure. The basic and somewhat hidden feature is that one removes the parameterization by a product flowrate (prior to step 1) before “mapping” the product paths (steps 2 and 3). Therefore, the distillate-bottoms pairing of compositions is disintegrated during the recursive steps in the procedure, and not re-established until the last step. This is essential since the procedure does not guarantee feasibility of the physical material balances (4.2) and (4.3).

4.2.3 Discussion of the Reactive Methods

In this section, the available methods for the prediction of MSS in reactive distillation are compared and their implications for finite columns are shown. First, the ∞/∞ prediction methods are compared to a “classical simulation approach”. The necessary data to perform a reactive ∞/∞ analysis were described in Chapter 3: The non-hybrid ∞/∞ analysis requires mostly thermodynamic information and depends only little on the specific column design. If residue curves are not only used to describe packed columns, but also tray columns (an approximation discussed earlier), and if special cases of condenser or reboiler equipment are neglected, the predictions do not depend on the column design at all. Since the requirements for the exact and approximate methods are identical to those mentioned here, there is no detailed column model needed in the (reactive) ∞/∞ case, unlike in a simulation approach, where column modeling is work intensive and introduces additional parametric sensitivities.

Even though the exact method needs exactly the same moderate amount of data as the non-hybrid analysis, the data are now represented in the physical composition space instead of the transformed one, i.e., in a space with dimension $c - 1$ instead of $c - r - 1$. Therefore, the graphical procedures can only be applied to systems with up to four components without exceeding common human imagination capabilities. An implementation of the procedures in a computer could potentially overcome this limitation. Because of the use of the physical composition space, back-transformation of the results is superfluous. The implications of the ∞/∞ prediction results from the exact method to columns with sections of finite length are analogous to those studied in the non-hybrid analysis, since both approaches essentially take the same form (geometrical condition, MSS feed region construction. . .).

However, the necessity of at least one pinch point in each column section is a fundamental drawback of the exact method and restricts its applicability to systems which are feasible in such a “multiple infinite” column. The approximate method provides a “heuristic” solution to this problem, since it only requires at least one pinch point in the reactive section, and thus is applicable to all systems where non-hybrid prediction results are available. However, the approximate method suffers from other limitations. First, the whole procedure starts with a crude approximation of the product compositions at the ends of the reactive section. Even worse, it is possible that the errors accumulate because of the iterative procedure. Second, the method turns

out to be highly sensitive to product paths on curved boundaries. Third, it takes some effort to perform the required boiling-point and dew-point calculations. On the other hand, back-transformation does not play a time-critical role since it must only be performed at the initiation step. Finally, the implications of the prediction results from the approximate method to a column with finite sections are similar to those made for non-hybrid columns, since the approximate method rests on the predictions for a reactive section of infinite length.

In conclusion, the exact method is very convenient for systems with up to four components. Unfortunately, it may not be applicable to all systems of interest. The approximate method may be limited from its approximate nature and from the effort required. If the ∞/∞ product paths of the non-hybrid analysis are available in physical compositions (after back-transformation), it is recommended to determine the influence of a few additional non-reactive stages by the approximate method. Note that from experience, the approximate method is often more effective in providing estimates of the transformed hybrid product paths than reliably predict the existence of MSS. For those cases where the exact and the approximate methods cannot be applied for some reason, bifurcation simulations of a specific column design and feed location may be necessary to obtain sound evidence on the existence of MSS for hybrid columns.

4.2.4 Possible Physical Causes

In this section, the focus will be on the types of multiplicities which can occur in hybrid reactive systems.

Type Ia MSS are caused by singularities in the nonlinear relationship between different units of measure for the internal and external flowrates, e.g. between transformed and molar, molar and mass, or volumetric and mass flowrates. This type of MSS was first discovered for ideal binary mixtures and finite columns (Jacobsen and Skogestad, 1991), but was also shown to be frequent in multicomponent azeotropic as well as non-hybrid reactive columns. It can be predicted using the ∞/∞ singularity analysis for non-reactive and reactive multicomponent systems.

Type Ib MSS (multiplicities due to internal heat effects) cannot be predicted by means of any ∞/∞ analytical tool. Clearly they should also exist in equilibrium reactive columns as they do for non-reactive columns.

Type II multiplicities are inherently caused by the underlying thermodynamic equilibrium. In non-reactive columns, they are caused by the VLE of the mixture and can be predicted by the non-reactive ∞/∞ analysis (Bekiaris et al., 1993; 1996). In reactive columns, this type of MSS can occur due to the properties of the simultaneous chemical and vapour-liquid equilibrium. This type of multiplicities exists in non-hybrid reactive columns and can be predicted by the non-hybrid ∞/∞ analysis (Chapter 3). Both phenomena leading to type II MSS, i.e., the VLE or the combined vapour-liquid and reactive equilibrium, occur in the entire distillation apparatus (non-reactive or non-hybrid column). This type of MSS is denoted by IIa. Moreover, it is foreseeable that this type of MSS will also occur in hybrid columns, e.g. if the reactive section is very large and the non-reactive sections very short.

Consequently, MSS of type IIa in a hybrid column must also exist in a non-hybrid column. The opposite, however, is not necessarily true. It is possible that MSS exist in a hybrid column, but not in the corresponding non-hybrid column and also not in the non-reactive system. Therefore, these multiplicities cannot be caused by either one of the physical phenomena leading to type IIa and represent a new type, denoted by IIb. The type IIb MSS are caused by the interactions of non-reactive and reactive equilibrium. Table 4.1 lists all discussed types of physical causes for the classes of distillation systems where MSS can exist.

Table 4.1. Overview on the existence of multiplicities of different types (caused by different physical phenomena), depending on the general class of a distillation system. The entries in brackets are conjectured only.

Type of MSS	Ideal Distillation	Azeotropic Distillation	Reactive Distillation	
			Non-hybrid	Hybrid
I	a	Yes	Yes	Yes
	b	Yes	Yes	(Yes)
II	a	No	Yes	Yes
	b	No	No	Yes

Table 4.2. Pure component Antoine parameters of the example mixture

Pure Component		Antoine Parameters		
Name	Index	A[-]	B[K]	C[K]
Light (n-hexane)	L	20.7121	-2691.08	-48.940
Intermediate (n-heptane)	I	20.7664	-2911.32	-56.514
Heavy (n-octane)	H	20.8022	-3108.08	-63.765

4.3. A Fictitious Example System

4.3.1 Thermodynamic Description

The goals of this section are: to provide a comprehensible example of the application of the exact method to a hybrid system, and to demonstrate the existence of multiplicities of type IIb. Since this example is used for illustrative purposes it is “fictitious” in the sense, that not a real physical system is used but a system is constructed from real data. For simplicity, a system with $c=3$ components is chosen, which will be denoted as the light (L), intermediate (I) and heavy boiling (H) components. The mixture data are selected to obtain a system with ideal VLE as well as “ideal” stoichiometry and chemical reaction equilibrium.

The vapour-liquid-equilibrium description of the ideal mixture of n-hexane, n-heptane and n-octane is used for the example system (all activity and fugacity coefficients are equal to unity). The Antoine parameters for calculating the pure component vapour pressures were taken from the Aspen database and can be found in Table 4.2 (Aspen Plus, 1995).

Since the VLE is ideal, non-reactive azeotropes cannot exist. The calculated non-reactive residue curve diagram is depicted in Figure 4.4. All residue curves originate from the low-boiling (unstable) node L and end at the high-boiling (stable) node H. The intermediate component I forms a saddle singular point.

As a next step in the construction of the reactive system the reaction stoichiometry $L + I = H$ is chosen. The two lighter boiling components add to form the heavy boiling one which makes sense, as heavy-boiling organic components often tend to be “larger” than lighter boiling ones. Therefore, the feed will be a mixture of L and I and the heavy component is to be produced and to be isolated in a hybrid reactive column. The reaction is assumed to reach chemical equilibrium instantaneously and for simplicity, the reaction equilibrium is chosen to be temperature independent (\hat{x} denotes the molar compositions in chemical equilibrium):

$$K = \frac{\hat{x}_H}{\hat{x}_L \hat{x}_I} = e^{0.1} \quad (4.11)$$

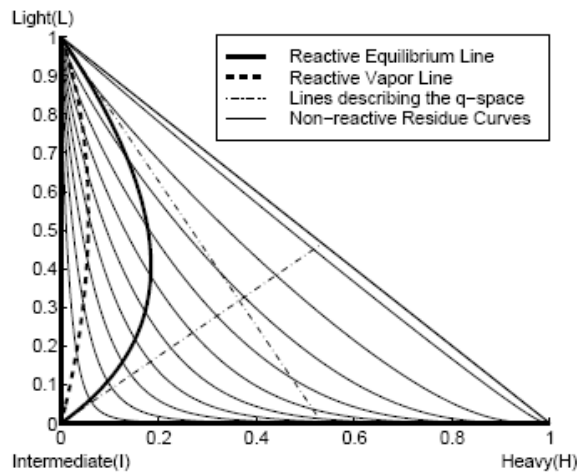


Figure 4.4. Non-reactive residue curve diagram of the example system (physical composition space) including the line of chemical equilibrium compositions (reactive residue curve) and the corresponding vapour-line. Note that the q-lines are not tangent to the reactive equilibrium but tangent to $\hat{y} - \hat{x}$ at the reactive singular points.

Figure 4.4 shows the resulting chemical equilibrium line which represents the single reactive residue curve of the system, originating from pure L and ending at pure I. Note that the maximum achievable molar fraction of H in chemical equilibrium is 0.184, which is far from the goal of a pure component. The line of compositions \hat{y} in vapour-liquid equilibrium with the reactive residue curve compositions \hat{x} is denoted as the “reactive vapour-line”. Finally, the q-line is calculated at each of the reactive singular points and the resulting lines are drawn into Figure 4.4.

In conclusion, there is nothing unusual in the construction of this admittedly fictitious example: the VLE description is taken from real mixture and the reaction is chosen as straightforward and self-evident as possible. Therefore, one could consider the whole reactive system to be “pseudo-ideal” (ideal VLE and “ideal” reactions). Espinosa et al. (1996) use a similar system in their work (Figure 6 in their paper).

4.3.2 Hybrid ∞/∞ Bifurcation Analysis

As a first step in the study of the example system a bifurcation analysis of a hybrid ∞/∞ column by the exact method is performed. The binary feed for the analysis contains 60% L and 40% I prior to reaction, and the molar and transformed feed flowrates are $F^D=F^N=100$, respectively.

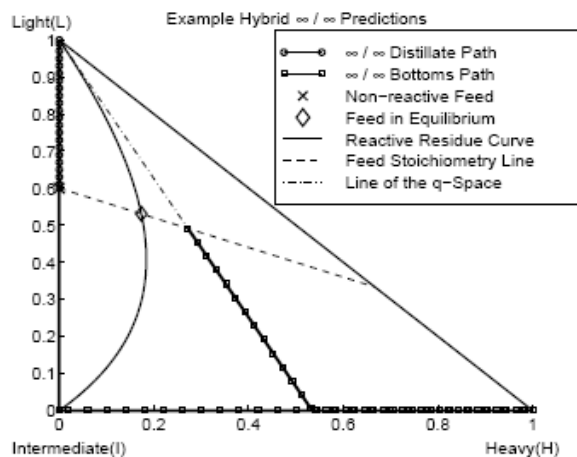


Figure 4.5. Predicted ∞/∞ product paths of the example system (physical composition space) for a feed rich in L as well as the necessary thermodynamic information.

Since the feed enters the reactive section it immediately reaches chemical equilibrium (from assumption 1.1). The feed location is shown in Figure 4.5, together with the main thermodynamic properties of the system. The locus of all molar feed compositions resulting in the same composition in chemical equilibrium is denoted by the “feed stoichiometry line”, and can be best determined from the transformation equations of this system, choosing the heavy component as the reference (Ung and Doherty, 1995e):

$$X_a = \frac{x_L + x_H}{1 + x_H} \quad X_b = \frac{x_I + x_H}{1 + x_H} = 1 - X_a \quad (4.12)$$

$$P^D = (1 + x_H)P^N$$

Using the fact that X_a takes the same value in chemical equilibrium for all feeds on the line, it can be calculated for the given feed, and an expression for the compositions x_L and x_I describing the feed stoichiometry line is obtained (Figure 4.5):

$$X_a^F = \frac{x_L^F + x_H^F}{1 + x_H^F} = 0.6 = \frac{x_L + x_H}{1 + x_H} \quad (4.13)$$

The initial profile is obtained for the limiting case of zero distillate flow, $D^D=0$ and $B^D=F^D$. According to the rules described in Appendix 4.5, the distillate is located at the unstable node L and the bottoms at the intersection of the feed stoichiometry line with the q-line as shown in Figure 4.6a.

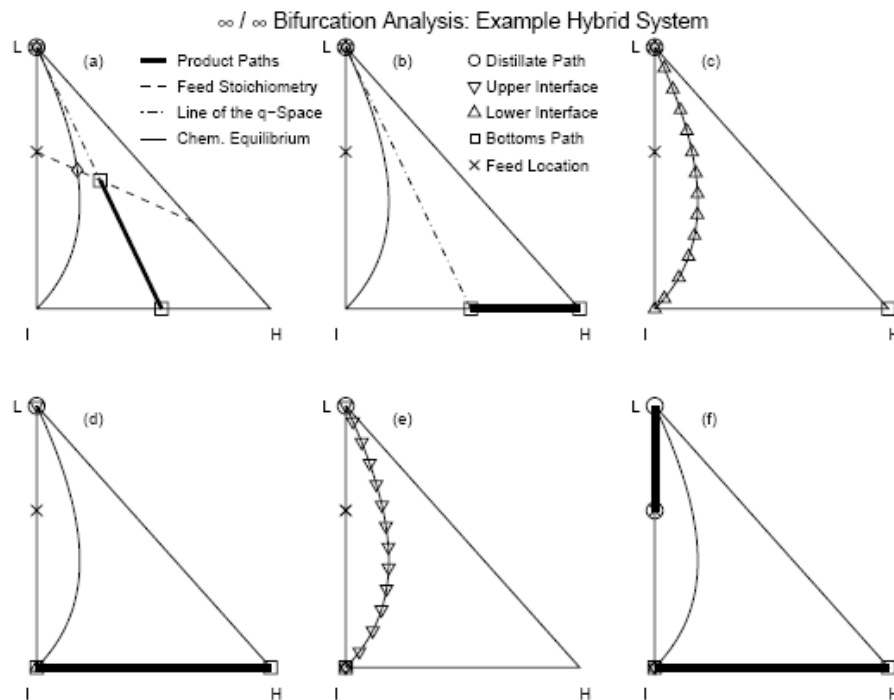


Figure 4.6. Prediction of the ∞/∞ product paths for the example system in the physical composition space for a feed rich in L. The step-wise analysis shows the product locations and the compositions at the section borders.

The stripping section profile coincides with the segment of the non-reactive residue curve through B (between L and B) and contains L as the non-reactive pinch point. Both rectifying and reactive profiles are collapsed at L, which serves as a reactive and non-reactive pinch point.

- (a) If the distillate flowrate D^D is increased, the bottoms moves on the q-line (straight line through L and the initial bottoms composition), a behaviour completely analogous to

∞/∞ non-reactive or to non-hybrid columns. The distillate remains at L as the collapsed section profiles do. The stripping profile still starts at L and coincides with the residue curve through B.

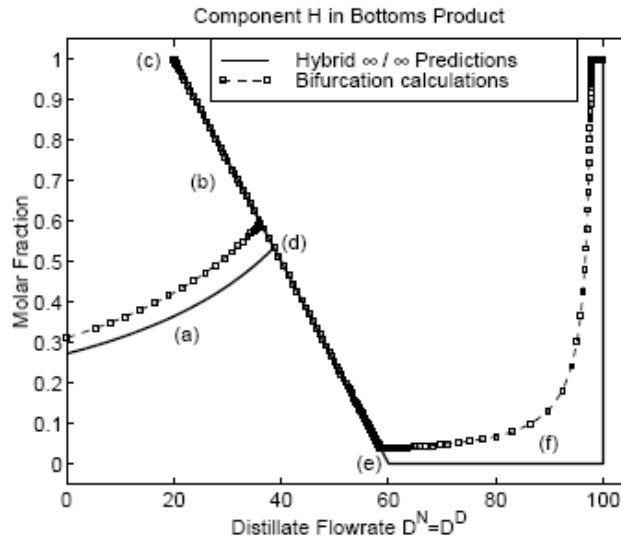


Figure 4.7. ∞/∞ Prediction of the composition of the heavy component H in the bottoms product B compared with the results of the bifurcation computation (example system). The value of the distillate flowrate D^N is identical to D^D and the labels correspond to Figure 4.6.

- (b) As B reaches the I-H edge, the stripping profile contains I as an additional singular point. One can think of three different moves which could happen in the ∞/∞ case: First, the border between stripping and reactive section could detach from pure L and move towards I (along the reactive residue curve since it is in chemical equilibrium). Although there would be a feasible reactive profile for any point on the reactive equilibrium line (from L to this point), no non-reactive residue curve is connecting such a point to the bottoms B and thus, there is no feasible stripping profile (compare Figure 4.4). Second, B could move towards pure I. This would also result in an infeasible profile and is best illustrated using Figure 4.3 and a finite, but large column. A move of B towards I would steepen the mass balance line shown in the Figure. Since both x_3 and y_3 are infinitely close to pure L, this would cause y_3 to leave the composition diagram and no feasible stripping profile could be obtained. Third and last, B could move towards pure H in Figure 4.6b. The distillate still stays at pure L as the collapsed rectifying and reactive section profiles do. The stripping profile now runs from L over I to B and thus, such operating points are feasible. By application of the transformed lever rule, the distillate flowrate D^D is decreasing along this segment of the continuation path and hence, MSS will exist (Figure 4.7).
- (c) As soon as B has reached the heavy component corner, the border between the stripping and reactive profile can leave pure L and move along the reactive residue curve until it reaches I (Figure 4.6c). Since a non-reactive residue curve connects the bottoms at H with any point of the reactive curve, this movement is feasible. L is the pinch point for the rectifying and reactive profiles and H for the stripping profile. At the end of the move, the collapsed rectifying profile stays at L and the reactive profile runs from L along the reactive residue curve to I. Since the product locations do not change during this transition, the distillate flowrate D^D is not changing either (from the lever rule). Hence, an infinite number of profiles result for the same value of D^D , the same inputs and the same outputs (internal state multiplicities). The limit point (c) in Figure 4.7 is the optimal design point: all of the intermediate component contained in the feed is converted to H, which is obtained as a pure bottoms product. The distillate contains

- only the excess of the L component. Since both products are pure, conversion and yield are at their maximum values (100%).
- (d) As the distillate D^D is further increased, other components must show up in the bottoms product and thus, B is moving back towards I (other possibilities are not feasible, Figure 4.6d). The distillate stays at L as the rectifying-reactive border does and all section profiles are feasible. On this move, conversion decreases until zero conversion is obtained as B reaches I.
 - (e) Similarly as for move (c), the border between the rectifying and reactive profiles detaches from pure L and moves along the reactive residue curve towards I (Figure 4.6e). There is always a feasible profile from the distillate at pure L to any point on the reactive residue curve (following a non-reactive residue curve). The reactive profile runs along a segment of the reactive residue curve, the stripping profile is collapsed at I, and all profiles contain a pinch point (L or I). Again, the product flowrates do not change and internal state multiplicities are observed.
 - (f) Finally, the rectifying profile connects the singular points L and I and thus, the distillate can now leave the L component corner and moves towards the feed, still containing I as a pinch point (Figure 4.6). There is zero conversion and basically, the column performs as a non-reactive one. The reactive and the stripping profile are collapsed at pure I. The distillate flowrate D^D increases and becomes equal to the feed flowrate F^D when D has reached the feed location. Since $B^D = F^D - D^D = 0$, the bottoms immediately jumps to the heavy component, establishing a stripping profile between I and H (see Appendix 4.5, only possible in the limiting case).

Now, the final profile is obtained and all possible product locations have been found. The hybrid product paths $x^D(D^D)$ and $x^B(D^D)$ are shown in Figure 4.5 and a bifurcation diagram for the heavy component in the bottoms product is shown in Figure 4.7. Since $x_H^D = 0$ on the whole continuation path, the molar and transformed distillate flowrates are equal. At points (c) and (e) an infinite number of different profiles exist for the same flowrate specification and product compositions (internal state multiplicities). To verify the predictions, a bifurcation computation was performed for the example system and the same feed. The Auto model with constant molar overflow (Güttinger and Morari, 1998a) is used for a column with 20 ideal equilibrium trays in each of the rectifying, reactive and stripping sections. The feed enters in the middle of the column (tray 30), a total condenser and a partial reboiler were used. The reflux flowrate was fixed at $L^N = 1500$ ($L = F = 15$) and a bifurcation study was performed. The computed product paths are compared with the predicted hybrid paths in Figure 4.7. The qualitative agreement is excellent, especially in the region where output multiplicities exist. Comparisons for the other components and for the distillate product show very similar results.

Note that the internal state multiplicities observed in the ∞/∞ analysis (at (c) and (e)) can be compared to the case Bekiaris et al. (1996) described as degenerate multiplicities, where the continuation of solution scans through an infinite number of profiles. To date, the question whether these state multiplicities are an artifact of the ∞/∞ case has not been studied. However, in the bifurcation calculations of the finite column, the steady states in the state multiplicity region do differ by about 10^{-5} (mole fraction). Therefore, extremely tight tolerances have to be used to distinguish between these steady states. Note that this large number of solutions with almost identical inputs and outputs may not be of practical relevance.

The next step is the application of the singularity analysis from Section 3.3.3 to recover the product paths in molar flowrates, $x^D(D^N)$ and $x^B(D^N)$. Since back-transformation is not necessary, this is a fast and simple mathematical operation and the result is depicted in Figure 4.8. Output multiplicities exist for molar or transformed distillate flowrates between 20 and 40, i.e., on 20% of the total flowrate range. A corresponding result is obtained for the transformed bottoms flowrate B^D (from the overall mass balance, 4.6).

Depicting the product path parameterized by B^N , simultaneous output and internal state multiplicities occur for $B^N=40$. Note that a design close to the limit point (c) is the only way of obtaining pure H in a product at reasonable conversion (Figure 4.7). Although pure heavy product could be withdrawn in a finite column at high D flowrates, conversion is extremely low (and so is the bottoms flowrate). The singularity analysis was not performed any further since the determination of flowrates on mass or volumetric bases would require molar weights and liquid densities, which are not available for the example system studied.

4.3.3 Hybrid MSS Feed Region

The hybrid MSS feed region cannot be determined easily using the geometrical condition described for the exact method since the example system has only $c - r - 1 = 1$ dimension in the transformed composition space. But, it is not difficult to determine the region directly from the results of the ∞/∞ bifurcation analysis. For the non-reactive feed F_1 in Figure 4.9, the first steady-state bottoms product is located at point A (compare with Figure 4.5), which is the intersection point of the q-line with the corresponding feed stoichiometry line.

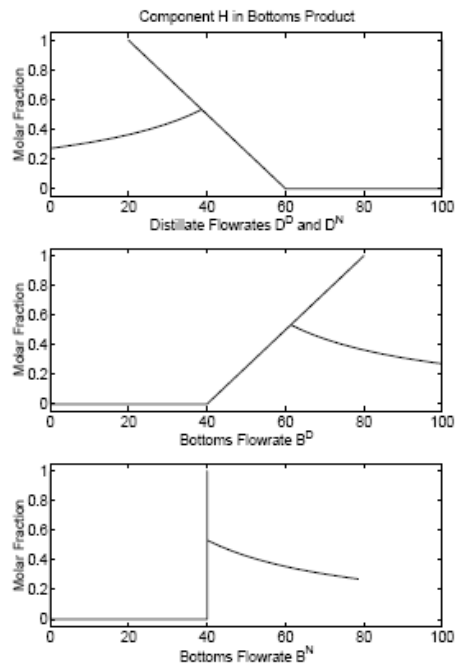


Figure 4.8. ∞/∞ Predictions of the composition of the heavy component H in the bottoms product for the example system and different units of the product flowrates (continuation parameter).

Since the distillate is located at L, the D^D flowrate is increasing for all bottoms locations between A and C (branch denoted by (a) in Figure 4.7), before it starts decreasing on branch (b). Similarly, the first bottoms product for a feed F_2 would be at point B and D^D is increasing for all bottoms compositions between B and C. Therefore, MSS will occur as long as there exists a steady-state solution branch (a) in Figure 4.7 and vice versa: If there is no branch (a), then the branches (b) and (c) will also disappear and the first solution obtained will be at point (d). Hence, no multiplicities would exist.

The critical question is for which non-reactive feed location on the L-I edge branch (a) would consist of a single point, i.e., the limit point?

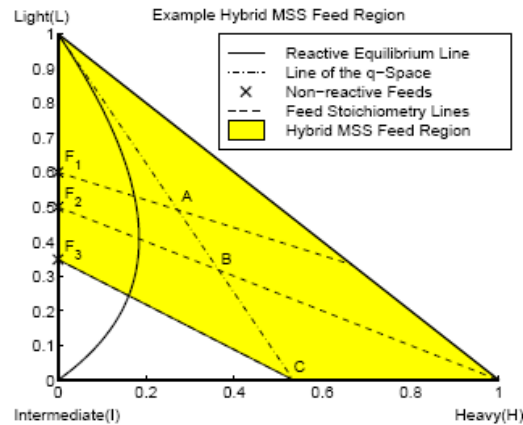


Figure 4.9. Prediction of the MSS feed region for an ∞/∞ hybrid column and the example system. Three non-reactive feed locations used in the study.

From Figure 4.9 it is obvious that the last bottoms location on (a) is at point C where the q-line intersects the stoichiometry line belonging to the critical feed. Therefore, the feed location F_3 is the feed richest in component I for which MSS still exist and all feed locations between L and F_3 on the L-I edge will lead to multiplicities. Since the feed enters the reactive section, all feeds located on the stoichiometric lines corresponding to the feed locations between L and F_3 result in the same composition in chemical equilibrium (where the stoichiometry line intersects the reactive equilibrium line) and will also lead to MSS.

Finally, the hybrid MSS feed region is the union of all stoichiometric lines originating from points between L and F_3 and is shaded in Figure 4.9. The MSS feed region is verified by simulation for different binary feed compositions on the L-I edge. Note that pure component H at maximum conversion (limit point (c) in Figure 4.7) can only be obtained for a feed in excess of the light component (between F_2 and L in Figure 4.9). Therefore, the existence of MSS and the possibility of obtaining a pure reaction product are fundamentally related for this system.

4.3.4 Discussion of the Physical Cause

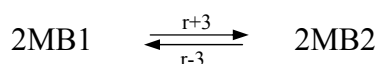
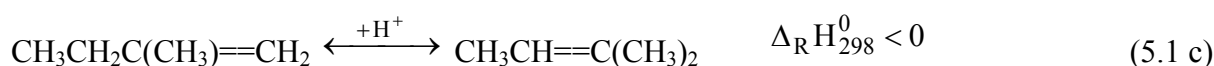
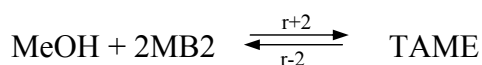
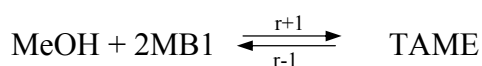
In the previous sections the application of the exact method to a hybrid reactive distillation system was demonstrated. The multiplicities predicted have been verified by bifurcation simulations of a finite column at finite reflux. Since the non-reactive ternary system studied is ideal (VLE), MSS are not possible in any non-reactive column with molar specification of the flowrates (Bekiaris et al., 1993). Moreover, a non-hybrid ∞/∞ analysis in the transformed composition space, which only consists of the single reactive residue curve shown in Figure 4.4, reveals that no multiplicities can exist in non-hybrid columns, either.

This result is straightforward from the fact that the non-hybrid reactive system is a binary ideal system in the transformed domain. In conclusion, no multiplicities exist for this system in a non-reactive or reactive non-hybrid column, i.e., MSS cannot be caused by a phenomenon leading to MSS of type IIa. MSS only exist in hybrid reactive columns and are therefore caused by the interaction of the non-reactive and the reactive VLE. Thus, the existence of MSS of type IIb is demonstrated.

Chapter 5 – Previous studies regarding TAME synthesis system

TAME (tert-amyl-methyl-ether) has been proposed as an alternative octane-enhancing component to MTBE because of its lower vapour pressure (which is a desirable property for fuel blends), and for the potentially lower manufacturing costs (Piccoli and Lovisi, 1995). Two works identified in literature about the TAME synthesis have been considered. One of them is done by Güttinger (PhD thesis, 1998) and assumes chemical equilibrium together with the presence of an inert component. The second study belongs to Thiel et al. (1997) and doesn't take into consideration the presence of the inert, the system is not in chemical equilibrium. Both studies are presented next in this chapter.

TAME is produced by liquid-phase synthesis from methanol (MeOH) and isoamylenes (IA) catalysed by a sulfonic acid ion exchange resin. Among the three isoamylenes only 2-methyl-1-butene (2M1B) and 2-methyl-2-butene (2M2B) are reactive in etherification; 3-methyl-1-butene (3M1B) is non-reactive. Besides the synthesis of TAME, simultaneously the isomerisation of the reactive isoamylenes takes place. Therefore, the reactive mixture taking part in the TAME synthesis consists of four components: MeOH, 2M1B, 2M2B and TAME. The reaction scheme can be described as follows (Oost *et al.*, 1995; Oost and Hoffmann, 1995a, b):



Even though MSS have been reported for some other reactive distillation systems, the application of the non-hybrid and hybrid predictions methods focuses on the industrially important production of fuel ethers. The prediction methods from Chapters 3 and 4 are applied to different designs of non-hybrid and hybrid columns, and the physical causes leading to MSS in this process are studied in detail. The existence of MSS is analyzed for the production processes of TAME (tert-amyl-methyl-ether) in a non-hybrid distillation column.

5.1 Analysis of the TAME Process (Güttinger (PhD thesis, 1998))

5.1.1. Thermodynamics and Process Description

Lieball (1998) studied the existence of MSS in non-hybrid columns for the TAME system. TAME (index 4) is formed by reaction of 2-methyl-1-butene (2M1B, index 1) and its isomer, 2-methyl-2-butene (2M2B, index 2), with methanol (index 3), in the presence of inert components. The TAME reactions have been shown to be reversible and fairly exothermic (March, 1985). Several side-reactions can occur, where the isomerization reaction between the two isoamylenes is the most important: $2\text{M1B} \leftrightarrow 2\text{M2B}$. Therefore, this reaction is taken explicitly into account,

resulting in a system with $c=5$ components, $r=2$ reactions and $2 - \pi + c - r = 3$ degrees of freedom.

The models and parameters used for describing the VLE are reported by Lieball (1998): Antoine's equation is used for the pure component vapour pressures and two different sets of binary Wilson parameters were studied for the Wilson activity coefficient model. The first set of Wilson parameters was retrieved from literature; the second set is based upon parameters estimated from UNIFAC (Aspen Plus, 1995). In addition, the reaction equilibrium correlation by Piccoli and Lovisi (1995) is applied (indices from above):

$$\ln(K_1) = \ln\left(\frac{a_4}{a_1 a_3}\right) = -8.64 + \frac{4330K}{T} \quad (5.2)$$

$$\ln(K_2) = \ln\left(\frac{a_2}{a_1}\right) = -0.54 + \frac{970K}{T} \quad (5.3)$$

Note that a third reaction between methanol and 2M2B is a linear combination of the two reactions listed above and thus, it must not be taken into account. Next, a feasible reactive transformation has to be found. Applying the rules by Ung and Doherty (1995e), TAME is selected as the reference component for reaction (5.2), and 2M1B for reaction (5.3). Then, the transformation equations take the form:

$$X_1 = \frac{x_1 + x_2 + x_4}{1 + x_4}$$

$$X_2 = \frac{x_3 + x_4}{1 + x_4} \quad (5.4)$$

$$X_3 = \frac{x_5}{1 + x_4}$$

$$P^D = P^N(1 + x_4^P) \quad (5.5)$$

Figure 5.1 depicts the calculated reactive residue curve map for the literature set of Wilson parameters and a pressure of 5 atm. All reactive residue curves originate from the non-reactive methanol-butane azeotrope and end at pure methanol. The residue curve map for the parameter set estimated from UNIFAC, as well as the two corresponding maps at a pressure of 3 atm do not qualitatively differ from Figure 5.1. Thus, all these reactive residue curve diagrams in the transformed composition space are topologically identical to the 001 class of a non-reactive ternary mixture (one minimum-boiling binary azeotrope between the “lightest-” and “heaviest-boiling” pure component of the mixture). Since the 001 class shows output multiplicities for any feed location in the ∞/∞ case, it can therefore be concluded by analogy that the non-hybrid MSS feed region of the TAME system consists of the full transformed compositions space. Thus, MSS exist for any physical feed composition in a non-hybrid reactive TAME column in the ∞/∞ case.

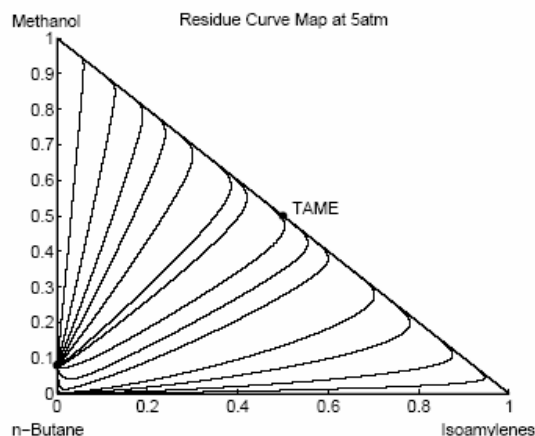


Figure 5.1. Reactive residue curve map of the TAME system at a pressure of 5 atm (Lieball, 1998). “Isoamylenes” denotes both 2M1B and 2M2B.

5.1.2 Non-Hybrid ∞/∞ Bifurcation Analysis

Figure 5.2a illustrates the transformed composition space of the TAME system (where “isoamylenes” is used to denote both 2M1B and 2M2B). Moreover, the diagram shows two specific lines: the “azeotropic” line connects the methanol-butane azeotrope with the point in chemical equilibrium with pure TAME ($X=[0.5 \ 0.5]$). The “equimolar” line consists of all feeds with a fraction of methanol identical to the sum of the fractions of the two isoamylenes. Note that the point $[0.5 \ 0.5]$ is not corresponding to pure TAME in a non-hybrid column, but to a mixture of all reactive components in chemical equilibrium with pure TAME.

The non-hybrid ∞/∞ bifurcation analysis is not explained in great detail here, since it performs completely analogous to the non-reactive ∞/∞ analysis of a 001-class ternary mixture (Bekiaris et al., 1993). Figure 5.2a depicts the resulting non-hybrid ∞/∞ product paths for an equimolar feed location. In Figure 5.2b, the corresponding ∞/∞ bifurcation diagram is illustrated. Clearly, the point $[0.5 \ 0.5]$ in chemical equilibrium with pure TAME, which by design is the desired product in a non-hybrid column, is obtained in the column's bottoms product at the second limit point. It can be shown that if a feed on the “azeotropic” line is used, the desired product would be obtained at the other limit point.

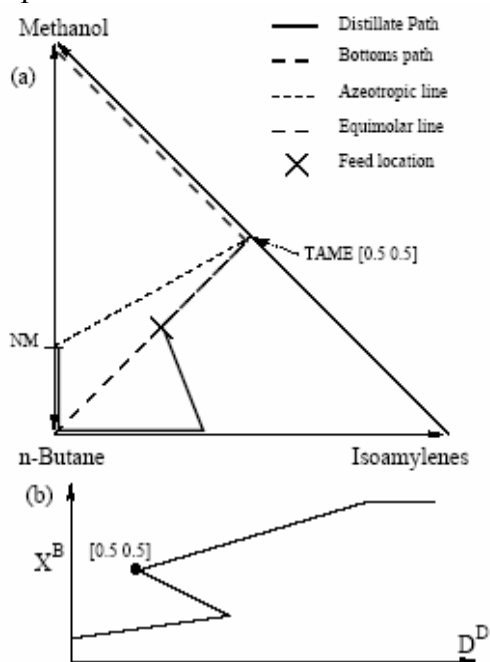


Figure 5.2. Illustration of the ∞/∞ product paths for an equimolar feed and the TAME system.

Using this knowledge from the ∞/∞ predictions, one can subdivide the transformed composition space into the four regions shown in Figure 5.3. For a feed in region A, the TAME point ([0.5 0.5]) is not part of any non-hybrid product path and can thus not be obtained in a non-hybrid column. For a feed in region B, the TAME point ([0.5 0.5]) would lie at one of the limit points or between the two points (as shown above). For a feed in regions C or D, [0.5 0.5] is obtained on the “upper branch” of the bifurcation diagram (Figure 5.3b). From a control point of view, it is desirable to select a design, i.e., a feed composition, where the “TAME point” is located outside the interval of the product flowrate where MSS exist. Therefore, the limiting line of feed compositions is to be found

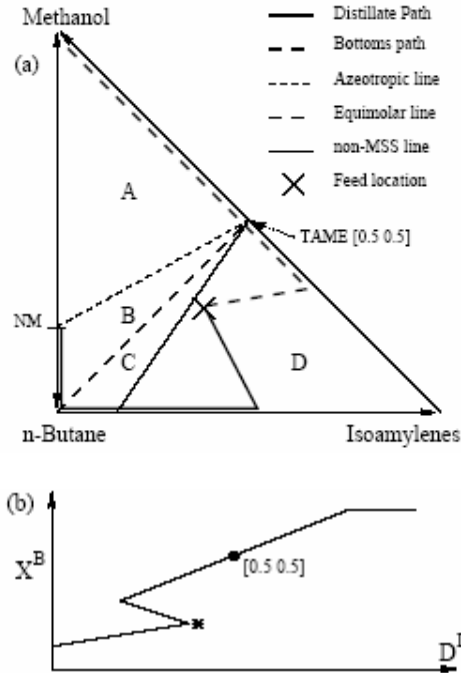


Figure 5.3. Illustration of the ∞/∞ product paths for a feed where TAME ([0.5 0.5]) lies outside the interval where MSS exist.

(denoted by “non-MSS line” in Figure 5.3), which separates the region of feeds C, where TAME is obtained inside the MSS interval, from the region D, where the steady state with a [0.5 0.5] product is unique.

5.1.3 ∞/∞ Favorable TAME Feed Locations

In this section, an inequality is derived for the transformed feed composition X^F such that in the ∞/∞ case of a TAME column, the bottoms product composition $X^B = [0.5 \ 0.5]$ is obtained outside the MSS interval (Figure 5.3). This goal can be expressed mathematically:

$$\left. \frac{D^D}{F^D} \right|_{TAME} > \left. \frac{D^D}{F^D} \right|_{L^F} \quad (5.6)$$

This means that the (relative) transformed distillate flowrate at the operating point where $X_1^B = X_2^B = 0.5$ (“TAME”) is greater than the (relative) transformed distillate flowrate at the limit point marked with “*” in Figure 5.3b.

At the limit point *, the distillate is located at the NM azeotrope, $X_1^D = 0$ and $X_2^D = X_2^{NM}$, where X^{NM} is the transformed composition of the NM azeotrope: [0.0 0.08]. The bottoms is located somewhere on the methanol-isobutene edge, $X_3^B = 0$, and thus $X_1^B + X_2^B = 1$. Combining this result with the component and the global mass balances in transformed units, one can

eliminate all remaining product compositions from the resulting system of linear equations and obtains:

$$\left. \frac{D^D}{F^D} \right|_{L_F} = \frac{1 - X_1^F - X_2^F}{1 - X_2^{NM}} \quad (5.7)$$

At the design point (“TAME”), B is at the location in reactive equilibrium with pure TAME, $X_1^B = X_2^B = 0.5$, and the distillate is located on the non-reactive butane-isoamylenes edge, $X_2^D = 0$. Again, the remaining product compositions can be eliminated from the equations:

$$\left. \frac{D^D}{F^D} \right|_{TAME} = 1 - 2X_2^F \quad (5.8)$$

By substitution of equations (5.7) and (5.8) into (5.6), the condition on the transformed feed location X^F is obtained after some re-ordering:

$$X_1^F > X_2^F - 2X_2^F X_2^{NM} + X_2^{NM} \quad (5.9)$$

TAME (in chemical equilibrium) can be obtained outside the MSS interval for all transformed feed locations fulfilling this inequality (5.9). By the derivation, these transformed feeds are located in region D from Figure 5.3a.

5.2. Residue curve maps for heterogeneously catalysed reactive distillation of fuel ether TAME

A principle sketch of the simple reactive batch distillation process is given in Figure 5.4. A heated still is filled with the molar liquid hold-up H , which consists of N components and has the composition $x = (x_1, \dots, x_N)^T$. In the liquid phase, where the heterogeneous ion exchange catalyst is present, the reversible etherification takes place, labelled by horizontal arrows in Figure 5.4.



It is also possible that several side reactions occur (e.g. isomer/sat/on of iso-alkenes), so in the following the model will be formulated with M reactions. Caused by the heating input Q , a distillation is carried out simultaneously which leads to a mass transfer from the liquid phase into the vapour phase labelled by vertical arrows in Figure 5.4 – and consequently, to a vapour molar flow rate \dot{V} with the composition $y = (y_1, \dots, y_N)^T$.

The hold-up H and the vapour flow rate \dot{V} are measured and the quotient H/\dot{V} is controlled via the heating input Q . In the still, there is an excess of catalytically active pellets, so the ratio between the wetted catalyst volume V_{cat} and the hold-up H is assumed to be constant.

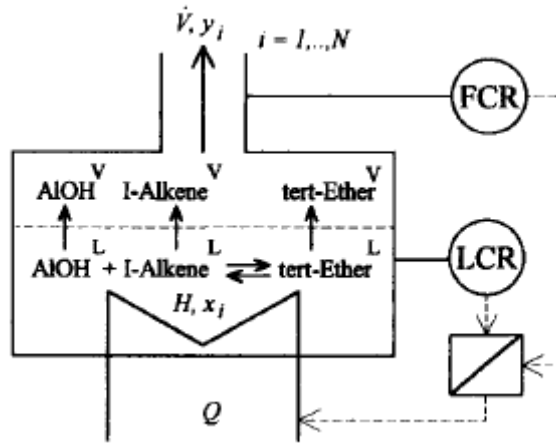


Figure 5.4. Sketch of a simple reactive batch distillation process

The liquid phase is in the boiling state so that the temperature in the still corresponds to the boiling temperature of the liquid composition x at the given operating pressure p

$$T = T(x, p) \quad (5.11)$$

According to this, vapour composition y and liquid composition x remain in phase equilibrium. A combination of the material balances leads to the following equation (Solokhin *et al.* 1990a, b; Venimadhavan *et al.*, 1994), which describes the change in time of the mole fraction x_i in the liquid phase of the still:

$$\frac{dx_i}{dt} = \frac{\dot{V}}{H} (x_i - y_i) + \sum_{j=1}^M \left[(v_{i,j} - x_i \cdot v_j) \cdot c_L \frac{V_{cat}^0}{H^0} \cdot r_j \right]$$

with

$$v_j = \sum_{i=1}^N v_{i,j} \quad \begin{array}{l} i = 1, \dots, N-1 \\ j = 1, \dots, M \end{array} \quad (5.12)$$

The first term on the right-hand side of equation (5.12) shows that a relation between hold-up H and vapour flow rate \dot{V} has to be found. This quotient depends on the control system of the process. In this paper, the following heating strategy will be used:

$$\frac{H}{\dot{V}} = \frac{H^0}{\dot{V}^0} = const \quad (5.13)$$

This policy is physically significant and leads to an autonomous model (Venimadhavan *et al.*, 1994). The intrinsic reaction rate r_j related to the number of acid groups of catalyst appearing in the second term on the right-hand side of eq. (5.12) has to be multiplied by the mean acid group concentration on the catalyst c_L and the quotient of wetted volume of catalyst V_{cat}^0 , to hold-up H^0 . In the following, two parameters are introduced to formulate equation (5.12) in a comprehensive way. These are the dimensionless time τ and the Damköhler number Da :

$$d\tau \equiv \frac{\dot{V}^0}{H^0} dt; \quad Da \equiv \frac{c_L \cdot k_f(T^*) \cdot V_{cat}^0}{\dot{V}^0} \quad (5.14a,b)$$

It is obvious that the transformation defined in equation (5.14a) only makes sense, if the heating strategy given in equation (5.13) is valid. In equation (5.14b), the rate constant of reaction k_f is related to the reference temperature $T^* = 333$ K. Consequently, equation (5.12) can be written in dimensionless form as follows:

$$\frac{dx_i}{d\tau} = (x_i - y_i) + \frac{Da}{k_f(T^*)} \sum_{j=1}^M [(v_{i,j} - x_i \cdot v_j) \cdot r_j]$$

$$i = 1, \dots, N-1$$

$$j = 1, \dots, M \quad (5.15)$$

As phase equilibrium is assumed, y_i can be evaluated from the relation at boiling point:

$$y_i = \frac{\gamma_i(x, T^b) \cdot p_i^s(T^b)}{p} \cdot x_i \quad i = 1, \dots, N \quad (5.16)$$

Consequently, the appropriate equation to compute the boiling temperature T^b reads in accordance with a combination of equation (5.16) and summation equation in the gas-phase:

$$0 = 1 - \sum_{i=1}^N \frac{\gamma_i(x, T^b) \cdot p_i^s(T^b)}{p} \cdot x_i \quad (5.17)$$

Since equation (5.17) cannot be explicitly solved for T^b , one has to use an appropriate iteration method. Hence, the turnover number r_j of reaction j is described by the following expression:

$$r_j = r_j(x, T^b) \quad , j = 1, \dots, M \quad (5.18)$$

Taking into account the dependence of T^b on composition vector x and operating pressure implicitly formulated in equation (5.17) – equation (5.15) can be written as:

$$\frac{dx_i}{d\tau} = [x_i - y_i(x, p)] + \frac{Da}{k_f(T^*)} \sum_{j=1}^M [(v_{i,j} - x_i \cdot v_j) \cdot r_j(x, p)]$$

$$i = 1, \dots, N-1$$

$$j = 1, \dots, M \quad (5.19)$$

To calculate the liquid mole fraction of the Nth component x_N , the condition of summation in the liquid phase is used:

$$1 = \sum_{i=1}^N x_i \quad (5.20)$$

The first term on the right-hand side of equation (5.19) describes the mass transfer across the vapour-liquid interphase, which means the influence of distillation. In the composition space, this term can be represented by the part of the separation vector SEP_i , to which component i contributes (Hauan and Lien, 1996).

$$\begin{aligned}
SEP_i(x, p) &\equiv x_i - y_i(x, p) \\
SEP_N(x, p) &= -\sum_{i=1}^{N-1} SEP_i(x, p) \quad i = 1, \dots, N-1
\end{aligned} \tag{5.21}$$

As shown above, SEP_i depends on the liquid-phase composition x and the operating pressure p . If $SEP_i = (SEP_1, \dots, SEP_N)^T$ equals the zero vector, no distillation occurs.

The second term on the right-hand side of equation (5.19) characterizes the mass conversion in the liquid phase due to the chemical reaction. According to Hauan and Lien (1996) this term denotes the part of the reaction vector REA , to which component i contribute:

$$\begin{aligned}
REA_i(x, p, Da) &\equiv \frac{Da}{k_f(T^*)} \sum_{j=1}^M [(v_{i,j} - x_i \cdot v_j) \cdot r_j(x, p)] \\
i &= 1, \dots, N-1 \\
j &= 1, \dots, M
\end{aligned} \tag{5.22}$$

$$\mathbf{REA}_N(x, p, Da) = -\sum_{i=1}^{N-1} \mathbf{REA}_i(x, p, Da)$$

REA_i shows a dependence on the liquid-phase composition x and the operating pressure p and additionally, a dependence on the Damköhler number Da . If $REA_i = (REA_1, \dots, REA_N)^T$ equals the zero vector, either chemical reaction is absent or the reaction is in chemical equilibrium. So equations (5.19)-(5.22) can be written vectorially as follows:

$$\left(\frac{dx_1}{d\tau}, \dots, \frac{dx_N}{d\tau} \right)^T = SEP + REA \tag{5.23}$$

From equation (5.23) it is easy to derive the conditions for the existence of a steady state. The appropriate composition x is called fixed point (FP). Hence steady state demands:

$$SEP^{FP} = - REA^{FP} \tag{5.24}$$

Finally it should be recapitulated that there are two independent parameters which determine SEP and REA . They are:

- Damköhler number Da ,
- operating pressure p .

As mentioned before, there are three reversible reactions taking place simultaneously in TAME-synthesis. To calculate residue curve maps for the synthesis of TAME, it is necessary to calculate the phase equilibrium between liquid and vapour phases, chemical equilibrium constants in the liquid phase and the kinetics of the chemical reactions.

According to equation (5.16) the liquid activity coefficients γ_i have to be evaluated. These can be computed by using the modified UNIFAC method (Weidlich and Gmehling, 1987; Gmehling *et al.*, 1993). The equations and parameters for calculation of γ_i for TAME-synthesis using this method and the vapour pressures p_i^s of all components can be taken from the quoted literature. Because of the fact that there are three reactions taking place simultaneously, three coupled chemical equilibria have to be considered. Rihko *et al.* (1994) proposed the following expressions which are based on their experiments (T in K):

- *TAME synthesis from 2M1B:*

$$K_{a,1} = 1.057 \times 10^{-4} \exp(4273.5/T) \quad (5.25a)$$

- *TAME synthesis from 2M2B:*

$$K_{a,2} = 1.629 \times 10^{-4} \exp(3374.4/T) \quad (5.25b)$$

- *isomerisation*

$$K_{a,3} = K_{a,1} / K_{a,2} \quad (5.25c)$$

It can be noticed that in the interesting region of temperature between 290 and 420 K the synthesis of TAME from 2M1B is thermodynamically favoured in relation to the synthesis of TAME from 2M2B. The chemical equilibrium of isomerisation depends only slightly on temperature and prefers the formation of 2M2B.

The micro-kinetics of the heterogeneously catalysed synthesis of TAME are formulated according to Oost and Hoffmann (1995b). Since the three reactions take place simultaneously and only two of them are linearly independent, the TAME-synthesis from 2M1B and from 2M2B are lumped together to a single reaction:



For this lumped reaction Oost and Hoffmann (1995b) give the following equation to describe the turnover number $r_{1,2}$:

$$r_{1,2} = r_1 + r_2 = k_{f,12} \cdot \left(\frac{a_{2M1B}}{a_{MeOH}} - \frac{1}{K_{a,1}} \frac{a_{TAME}}{a_{MeOH}^2} \right) \quad (5.27)$$

The reaction rate constant for the lumped TAME synthesis $k_{f,12}$ is given by the following Arrhenius equation:

$$\frac{k_{f,12}}{\text{mmol/eqs}} = (1 + K_{a,3}(T)) \cdot 2.576 \cdot \exp \left[-10.764 \times 10^3 \left(\frac{K}{T} - \frac{1}{333.15} \right) \right] \quad (5.28)$$

In addition, the kinetics of the isomerisation has to be considered. Oost (1995) reported the following equation to calculate the turnover number r_3 :

$$r_3 = r_{+3} + r_{-3} = k_{f,3} \cdot \left(a_{2M1B} - \frac{a_{2M2B}}{K_{a,3}} \right) \quad (5.29)$$

The reaction rate constant $k_{f,3}$ can be evaluated by using an appropriate Arrhenius expression:

$$\frac{k_{f,3}(T)}{\text{mmol/eqs}} = 1.078 \times 10^3 \cdot \exp \left[-10.861 \times 10^3 \left(\frac{K}{T} - \frac{1}{333.15} \right) \right] \quad (5.30)$$

The set of model equations for TAME is composed of three ordinary differential equations, material balances and two algebraic equations which are condition of summation in liquid and

vapour phase, to solve the liquid-phase composition x and the temperature T . In addition, a second chemical reaction has to be taken into consideration.

To simplify the graphical illustration in a triangle the mixture of isomers 2M1B and 2M2B are treated as one pseudo-component 'isoamylyene' (IA), so that

$$x_{IA} = x_{2M1B} + x_{2M2B} \quad (5.31)$$

Following the system of equations describing the model, the authors obtained the trajectories for the pure distillation of a nonreactive mixture IA/MeOH/TAME. Two binary azeotropic points were detected: between the olefin (IA) and the alcohol (MeOH), an unstable node, and between the ether (TAME) and the alcohol, a saddle point. These two points are linked by a distillation boundary, separatrix. Consequently there are two different stable nodes in the system: pure MeOH and pure TAME. If, in addition, the operating pressure p is varied, the following statement is valid: with increasing p both azeotropic points move towards pure MeOH.

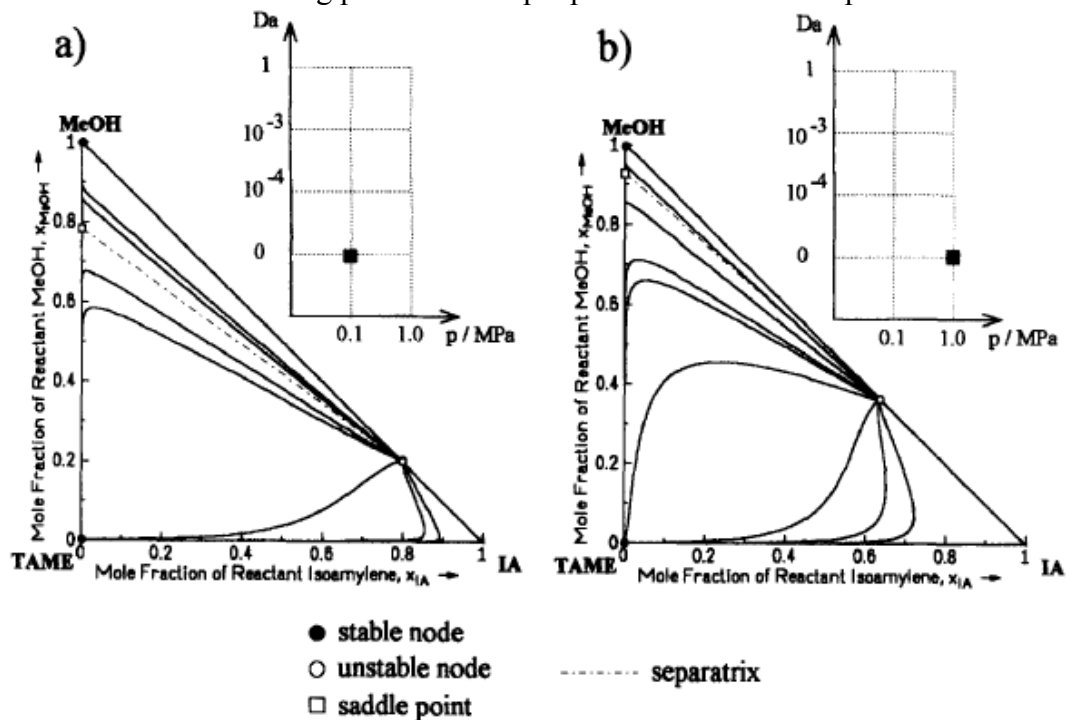


Figure 5.5. Residue curve maps for distillation without reaction ($Da = 0$) of the mixture IA/MeOH/TAME at operating pressure (a) $p = 0.1$ and (b) $p = 1.0$ MPa.

For the residue curve maps of reactive distillation for TAME-synthesis, the operating pressure p is discussed as second parameter besides the Damköhler number Da . The diagrams were calculated using different operating pressures: $p = 0.1$ MPa and $p = 1$ MPa. The Damköhler number Da is enhanced starting with the value 10^{-4} , via $Da = 10^{-3}$ to $Da = 1$.

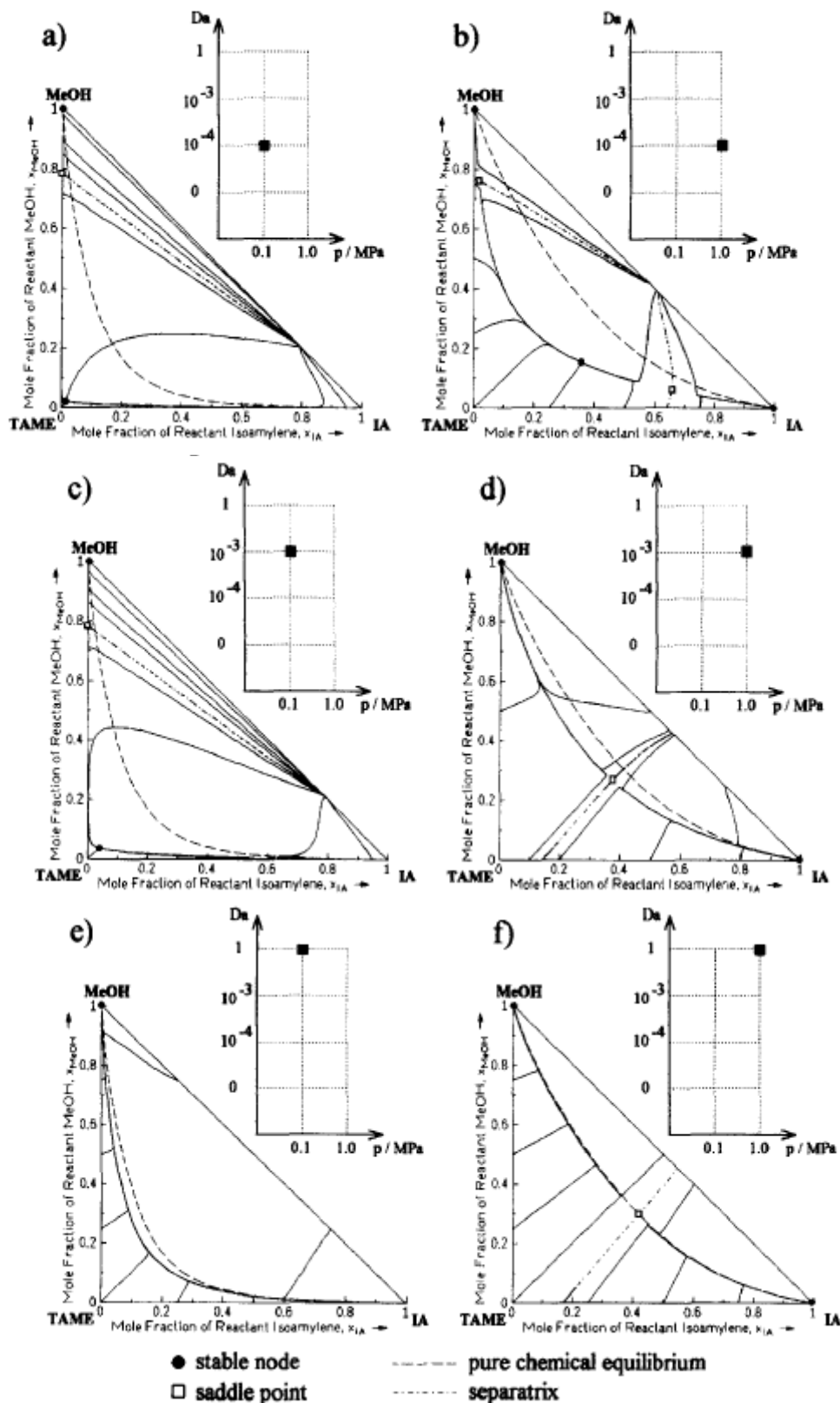


Figure 5.6. Residue curve maps for heterogeneously catalysed TAME-synthesis at operating pressure $p = 0.1$ and 1.0 MPa; Damköhler number: $Da = 10^{-4}$, 10^{-3} and 1 .

At a low Damköhler number $Da = 10^{-4}$, SEP is still dominating over REA, so that two stable nodes in MeOH and nearby TAME are developed. A slight enhancement of Da leads to $Da = 10^{-3}$. This case is qualitatively similar to the previous case except for the fact that the lower stable point has discharged from the TAME-vertex. If Da is increased to $Da = 1$, REA is strong

in comparison with SEP. Consequently, one stable node disappears and every trajectory runs into the collecting trajectory which is the only remaining separatrix in the composition space. This separatrix is in the vicinity of the chemical equilibrium line and ends in the MeOH vertex.

By raising the operating pressure p a new behaviour of the system can be studied. A new saddle point appears, with the consequence that at $Da = 10^{-4}$ and $p = 1.0$ MPa, three stable points exist. It is remarkable, as in addition to the stable node in MeOH vertex and in the region between chemical equilibrium and TAME vertex a third stable point is built in the isoamylene (IA) vertex. This circumstance is surprising as IA is the light-boiling pure component of the system. Thus, the statement that it is possible to enrich the highest volatile component above a certain pressure and a certain magnitude of REA is correct.

It was shown above that two different kinds of saddle points can appear, caused by the combination of distillation and chemical reaction. The crucial parameters for occurrence and position of these saddles in residue curve maps are the Damköhler number Da and the operating pressure p . At an operating pressure $p = 0.1$ MPa the line of chemical equilibrium lies in the vicinity of the product TAME and the temperature profile is continuously rising from pure IA (right margin of figure) to pure MeOH (left margin of figure). Raising the pressure leads to an enhancement of the temperature in the still, because of the exothermic characteristic of the TAME-synthesis; the line of chemical equilibrium is shifted towards the reactants MeOH and IA. The closer the line of chemical equilibrium gets to the line of the binary mixture MeOH/IA, the more the binary azeotropic point between MeOH and IA has an influence on the shape of the line of the boiling temperature. This leads, for adequately high pressure, to the formation of a minimum boiling temperature between MeOH and IA.

An adequately high pressure can lead to the formation of a saddle point in the region of high mole fraction of reactant isoamylene. It can be explained by the existence of a temperature minimum along the line of chemical equilibrium, which has been moved into the vicinity of the binary methanol-isoamylene azeotrope.

Chapter 6 – Application of the infinite/infinite analysis to the TAME synthesis

6.1. Analysis of the chemical non-equilibrium system – non-hybrid case

An efficient use of the energy is as important as the care taken for energy production. Distillation handles about 3% of the total U.S. energy consumption (Stephenson and Anderson, 1980), more than 90% of all product recovery and purification separations in U.S. (Humphrey, 1995) and more than 95% of chemical industries consumption worldwide (Ognisty, 1995). Data from U.S. DOE (United States Department of Energy) (US DOE, 1995) indicate that distillation columns in U.S. consume $2.87 \cdot 10^{18}$ J (2.87 million TJ) by year which is equivalent to a continuous power consumption of 91 GW. To have an idea of how large is this number; the 441 nuclear power plants in operation all over the world have a total net installed capacity of 367 GW (IAEA PRIS, 2005). The distillation processes are very energy-consuming systems and any small improvement on distillation can provide huge savings of energy. The energy consumption of a distillation process can be used in preliminary calculations as a key indicator of environmental impact and economical costs.

The process intensification by combining several operations in the same unit is an option that can be sometimes very advantageous (Plesu et al, 2008). Tools and methodologies to evaluate the process integration and intensification opportunities are useful to optimize the energy used in the separation processes. The reactive distillation combines the reaction and separation inside the distillation column. Reactive distillation can naturally use the heat of reaction as a heating or cooling source.

A useful tool used at the early stages of design to perform input-output analysis relating to distillation process systems is the infinite/infinite analysis which is based on residue curve maps. Infinite reflux and infinite number of stages are the simplifying hypotheses which have inspired the name of the ∞/∞ analysis. This analysis was firstly proposed by Petlyuk and Avetyan (1971), but with a low impact on the scientific community outside USSR. The potential of this analysis was rediscovered by Bekiaris et al. (1993) which led it to a great grade of maturity (Bekiaris and Morari, 1996a), it was extended to heterogeneous systems (Bekiaris et al., 1996b), hybrid distillation columns with reactive and non reactive sections (Güttinger and Morari, 1999) and its potential in process synthesis to find and rank feasible separation schemes according to the energetic consumption (Ulrich, 2002) has been studied. It is able to take into account the energy savings in the first steps of designing a distillation process and it can be used to evaluate new opportunities for the existing distillation systems. Barbosa and Doherty (1987a,b) and Doherty (1990) developed reactive residue curves in transformed coordinates. Ung and Doherty (1995) proposed a lever rule using this reduced coordinate space. In this reduced coordinated space based on reaction invariant compositions, it is not possible to fix the advance of the reaction to other values provided by the reaction equilibrium and mass balance. Hauan, Omtveit and Lien (1996), Hauan, Werterberg and Lien (1999a) introduced the reaction difference point. They showed that reaction moves in the composition space along straight lines, all of which pass through this same difference point behaving similarly to a difference point for an extractive distillation column (Hoffman, 1964). Lee et. al. (2000) introduced the concept of pseudo-feed and how it may be used to formulate a lever rule for the mass balance. The use of the pseudo-feed concept joint with the infinite/infinite analysis extends the capabilities to this analysis to solve reactive distillation systems taking into account the reaction kinetics. Venimadhaven et al. (1994) studied the effects of kinetics on reactive distillation residue curve maps. They tracked the singular points as a function of the Damköhler number (Da) which is the ratio of a characteristic liquid residence time to a characteristic retention time. At large Da, the reaction

achieves equilibrium on every reactive stage, and at lower Da , the column is kinetically controlled.

The applicability of the infinite/infinite analysis as a tool for an early oriented energy consumption minimization is extended in this paper to kinetically controlled reactions in reactive distillation columns including also hybrid configurations. For the hybrid configuration is used the approximate method (only one pinch on column profile) proposed by Güttinger (1999). The TAME synthesis is used as illustrative example for its importance on providing environmental friendly gasoline additives. The analysis is applied graphically on the reactive residue curve maps determined by Thiel et al. (1997).

The infinite/infinite analysis is called in this way because, as mentioned in previous chapters, it assumes that the number of stages is infinite and the reflux rate is also infinite. In a non reactive distillation column or in a reactive distillation column assuming equilibrium in all the stages, there are only two degrees of freedom in the model; in order to fulfill the degrees of freedom, the pressure and the distillate or bottom flow rate can be used. When the chemical equilibrium is not reached, then there are two variables more to define: the Damköhler number and the overall reaction turnover. As the number of stages is considered infinite, although the Damköhler number will be small, the column can reach any reaction turnover that satisfies the conditions of the analysis. A column feasible with an infinite number of stages does not mean that the same results can be reached with a reasonable number of stages but we get the limit conditions. The infinite/infinite analysis must be applied with caution to multiple feed columns as a maximum reflux could exist. The infinite/infinite analysis allows checking the feasibility and interrelation of the system streams without any column design considerations, detects the presence of multiplicity regions and a first comparative evaluation of energy requirements is obtained.

The vapour flow rate generated at the reboiler is proportional to the energy provided to the distillation column. Assuming the McCabe-Thiele hypothesis (1925), this vapour flow rate is constant along the column and the heat provided at the reboiler is the same that is eliminated at the condenser but at a lower temperature. Applying a mass balance around the condenser and the definition of reflux ratio, the next expression is obtained:

$$Q_{reb} \approx V = D \cdot (r + 1)$$

For distillation columns, an heuristic for a first approach can be to minimize the distillate flow rates instead of the minimizing the feed flow rate to each unit. Then the energy requirements can be considered proportional to the distillate flow rate (D) which can be calculated easily from the infinite/infinite analysis because its optimal value is independent of the number of stages and reflux. These assumptions were used successfully by Ulrich et al (2002).

The conditions that must be fulfilled to get a feasible separation are the next:

- The distillate and the bottom must be connected by a column profile described by residue curves.
- The column profile contains at least one singular point and not all the profile is on the unfavorable formation of products for kinetically controlled reactions.
- Fulfillment of the mass balance.

At infinite reflux, the column profile of any packed column must be coincident with a section of a residue curve. At infinite reflux and infinite number of stages, a singular point where the liquid and vapor compositions are the same (pure component or azeotrope) must be in the column profile. The existence or position of the reactive azeotropes and the role of the pure components

and azeotropes depends on the Damköhler number. For non reactive systems, the distillate, feed and bottoms compositions must be aligned fulfilling the lever rule when are represented graphically. For kinetically controlled reactions, the distillate, pseudo-feed and bottoms must be aligned and the pseudofeed must be aligned with the feed and reaction difference point. The pseudo-feed indicates the reaction turnover, in other words, the advance of the reaction inside the reactive distillation column.

But the application of the infinite/infinite analysis is not straightforward for the chemical non-equilibrium systems because the advance of the reaction is an unknown parameter. For an equilibrium reaction it can be demonstrated that the lever rule is satisfied for the transformed reactive compositions. The feed assuming equilibrium reaction becomes fixed, but when there is a chemical non-equilibrium, the infinite/infinite hypothesis lets one degree of freedom without being fixed and the feed point can be in any position over a line defined by the stoichiometry of the reaction (figure 6.1)

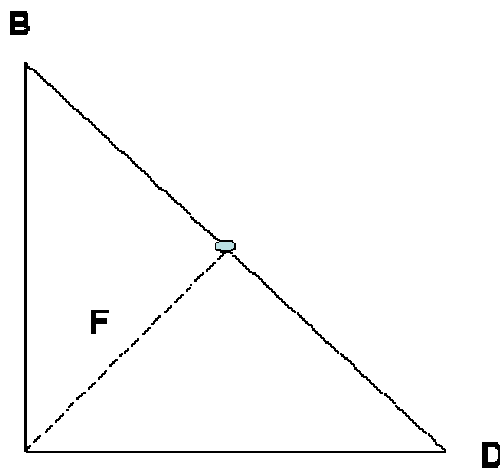


Figure 6.1. Possible feed locations

In order to apply the infinite/infinite analysis, a pseudo-feed composition is assumed to express the advance of the reaction along the column. The overall column mass balances for a non reactive system where the lever rule is applied are:

$$\begin{aligned}
 F &= D + B \\
 Fx_i^F &= Dx_i^D + Bx_i^B
 \end{aligned}
 \tag{6.1}$$

Next, it is considered the following reversible reaction for an ideal mixture, where reactants $A1$ and $A2$ convert into product $B1$. It is assumed that $A1$ is light, $A2$ intermediate and $B1$ heavy in terms of their volatilities, $A1$ and $A2$ forming a stoichiometric mixture.



In the case of TAME synthesis, $A1$ = Isoamylenes, $A2$ = Methanol, $B1$ = TAME.

This reaction takes place inside the reactive distillation column. The reaction is catalytic and therefore, the extent to which it occurs on any tray can be defined. A feed stream containing species $A1$ and $A2$ enters the column. The total and component material balances around the column are presented in Eqs. (6.2).

$$F = D + B - \sum_i \nu_i \cdot \xi$$

$$Fx_i^F = Dx_i^D + Bx_i^B - \nu \cdot \xi$$
(6.2)

In Eq. (6.2), $\sum_i \nu_i$ is the sum of the stoichiometric coefficients of the reactants and products, where the coefficients of the reactants are taken as negative and those of the products as positive since the reaction consumes the reactants and generates the products. Hence, we have $\sum_i \nu_i$ as minus one (= -1 + -1 + 1) for the above reaction. ξ is the total molar turnover of the reaction (as a flowrate in mol/time), and ν is the stoichiometric coefficient vector, $[-1, -1, 1]^T$, for the specified reaction.

From Eq. (6.2), if the term $Dx_i^D + Bx_i^B$ is combined as $(D + B)x_{F^*}$, by performing the substitution in Eq. (6.2), the following Eq. (6.3) is obtained. x_{F^*} is the pseudo-feed composition, $(Dx_i^D + Bx_i^B)/(D + B)$, and δ_R is the reaction difference point, that is $\nu/\sum_i \nu_i$ (Hauan et al., 1999a). In Eq. (6.3), x_{F^*} is the vector combining the distillate and bottom composition vectors and can be called a pseudo-feed composition vector since it is the linear combination of the distillate and bottoms product streams.

$$\frac{\sum_i \nu_i \cdot \xi}{(D + B)} = \frac{(x_i^F - x_i^{F^*})}{(x_i^F - \delta_R)}$$
(6.3)

Conceptually, the reaction in the column converts the feed stream F into the pseudo-feed stream F^* . Then, we obtain the distillate product D and the bottom product B from the pseudo-feed F^* . The location of the real feed composition x_F (figure 6.2), according to relative amounts of $(D+B)$ and $\left| \sum_i \nu_i \xi \right|$ using the lever rule is on the straight line between the pseudo-feed (x_{F^*}) and reaction difference point ($\delta_R = [1, 1, -1]^T$), because the total sum of stoichiometric coefficients $\sum_i \nu_i$ is negative. Another important implication of Eq. (2.4) is that the composition change from feed to pseudo-feed is linear even for a cascade system with reaction and separation in a composition space just as for a system with only reaction (Hauan et al., 1999a). Hence, the extent of the linear shift from the real feed to the pseudo-feed is that of net overall reaction in the column.

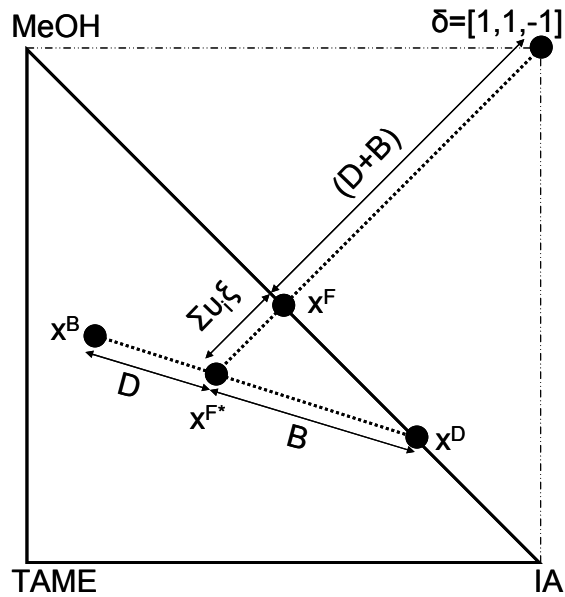


Figure 6.2. The illustration of the reactive lever rule in composition space.

The lever rule can be applied for the resulting pseudo feed composition, distillate and bottoms compositions. For the mass balances with the reaction term, the lever rule is not fulfilled but the reaction term can be moved to the left side of the equations resulting:

$$F + \sum_i \nu_i \cdot \xi = D + B \quad (6.4)$$

$$F x_i^F + \nu_i \cdot \xi = D x_i^D + B x_i^B$$

Making a change of variable, the feed flowrate F and the feed composition x_i^F can be transformed into the pseudo-feed indicated with F^* and $x_i^{F^*}$ respectively, according to the following equations:

$$F^* = F + \sum_i \nu_i \cdot \xi \quad (6.5)$$

$$F^* x_i^{F^*} = F x_i^F + \nu_i \cdot \xi$$

In this case, the system of equations for the column mass balances becomes:

$$F^* = D + B \quad (6.6)$$

$$F^* x_i^{F^*} = D x_i^D + B x_i^B$$

After the calculations, the real compositions and flowrate of the feed can be obtained by applying equation (6.5).

Using equations (6.6), the lever rule is fulfilled, the expressions of it being as follows:

$$\frac{B}{D} = \frac{(x_i^D - x_i^{F^*})}{(x_i^{F^*} - x_i^B)} \quad \frac{B}{F^*} = \frac{(x_i^D - x_i^{F^*})}{(x_i^D - x_i^B)} \quad \frac{D}{F^*} = \frac{(x_i^{F^*} - x_i^B)}{(x_i^D - x_i^B)} \quad (6.7)$$

Hence, we will apply graphically the lever rules from the equations 6.3 and 6.7 to solve each of the mass balances:

$$\frac{B}{D} = \frac{(x_i^D - x_i^{F*})}{(x_i^{F*} - x_i^B)} \quad \frac{\sum_i v_i \cdot \xi}{(D + B)} = \frac{(x_i^F - x_i^{F*})}{(x_i^F - \delta_R)}$$

All the residue curve maps obtained by Thiel et al. (1997) are taken for further study, considering that the pseudo-feed composition is equal to the corresponding chemical equilibrium composition. A stoichiometric feed of both reactants without containing any product will react inside the column until a desired conversion; if the infinite/infinite analysis is applied directly to this feed composition, it is equivalent to consider that there is no advance of the reaction and in this case, the reactants are simply separated by a binary distillation (figure 6.2). Then, the pseudo-feed must not be understood as the feed composition to the column, it must be considered as a measure of the advance of the reaction in the column.

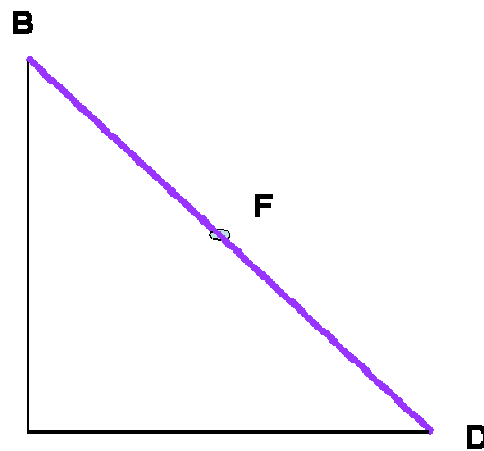


Figure 6.3. Mass balance for simple binary distillation

The analysis is applied to non reactive distillation columns and to reactive distillation columns. For the non reactive columns, it is supposed a configuration containing a pre-reactor which reaches the chemical equilibrium composition that is fed to the distillation column. The crude feed is fixed at the stoichiometric composition of reactants: 1:1. The pseudo feed to the reactive distillation column is fixed to the same reaction turnover that is obtained by the traditional scheme of reactor and column in order to compare them easily. The influence of the pressure is evaluated using 1 and 10 bar and several values of the Damköhler number are evaluated in the reactive distillation column: 0,0001; 0,001 and 1. The influence of changing the reaction turnover is evaluated by using a pressure of 1 bar and using the turnover reaction obtained by the traditional system of reactor and column at 10 bar. The choice of the variables allows comparing their influence.

The continuation paths satisfying the required conditions of the infinite/infinite analysis are determined and the bifurcations diagrams are calculated to provide information on the influence of the pressure and the Damköhler number on the presence of multiple steady states and the purities attained on the streams. The bifurcation diagrams illustrate the influence of the output flowrates on the distillate and bottoms composition. At the value $B/F=0$, all the feed is recovered by the distillate and the distillate has the same composition as the pseudo-feed. At the value $B/F = 1$, all the feed is recovered in the bottom of the column which has the same composition as the pseudo-feed. The feasibility and the influence of the bottoms flow rate on the distillate and bottoms purities for each one of the evaluated situations is detailed in the following paragraphs.

The first system evaluated is a traditional system of a reactor followed by a distillation column at 1 bar (figure 6.4). The reactor is fed with a stoichiometric mixture of the reactants methanol (MeOH) and isoamylenes (IA) indicated in the continuation diagram as x_F . According to the stoichiometry of the reaction, the differential point δ is obtained. The composition at the exit of the reactor must be on the straight line defined by δ and x_F ; the composition at the exit of the reactor is indicated as the pseudo feed to the reactive distillation columns with an asterisk (x_{F^*}). There are several scenarios where the compositions of the reactor exit can be located. The residue curve map is divided by a boundary line in two distillation regions. The azeotropic composition of methanol and isoamylenes is the unstable node from where all the residue curves depart. Some of the residue curves converge to the stable node of the methanol in the upper distillation region and some other residue curves converge to the TAME vertex in the lower distillation region. If the advance of the reaction produces a composition of x_{F^*} in the upper region, then it is not possible to collect pure TAME at the column bottoms: there is not any residue curve from the upper region that reaches pure TAME. On the other hand, if the extent of the reaction is big enough inside the reactor and the composition at the exit of the reactor is on the lower distillation region, then there is an optimal value of bottoms flow rate that provides pure TAME at the column bottoms. According to the lever rule, at higher reactor conversion then higher pure TAME flow rate can be collected at the bottoms. The maximum conversion inside a reactor is limited by the chemical equilibrium; in this case its value using as a calculation basis one mole of crude feed is of 0,39. Figure 6.4 shows this optimal case when the composition at the exit of the reactor is at chemical equilibrium. It is observed that at the highest bottoms flow rate that produces pure TAME, there is some TAME that it is lost by the distillate due to the presence of the boundary line. But as the distillate composition is depending on the pressure and the reaction kinetics, in order to be able to make comparisons of the effect of each variable we will keep the stoichiometric feed to the reactor. The conclusions derived from the other figures (figures 6.4 – 6.14) are presented in the next paragraphs.

When the column profile is of type II, the situation corresponds to low values of B/F, in this case the bottom composition is constant at the pure TAME for the non reactive systems. The column profile type II for reactive distillation systems produces a bottom composition corresponding to the ternary azeotrope (IA-MeOH-TAME); the ternary azeotrope becomes poorer in TAME when the Da number increases. When the Da number equals to 1, then the ternary azeotrope disappears and pure methanol is obtained in the bottom of the column. Hence, as the Da number increases, the TAME purity in the bottom decreases and its maximum value is obtained at higher values of bottom flowrate B/F. Therefore, the highest bottom flowrate collecting pure TAME is obtained by the traditional reactor and column system. In the type II profiles, the TAME composition in the distillate decreases until a value around 0.1, while the isoamylenes and methanol composition increases for most of the cases. Da=1 and P=1 bar is one of the exceptions, in this case the TAME is collected by the distillate while the methanol is obtained at the bottom of the column; the TAME composition in the distillate stream increases until a maximum value around 0.7; at the same time the isoamylenes composition also exhibits an increasing tendency. A similar behaviour can be noticed in the case of Da=0.001 and P=10 bar, but here the main component in the distillate is the isoamylenes and not TAME, which only increases until around 0.3. For a Da=0.0001 and P=10 bar, it is observed that the composition of isoamylenes in the distillate remains constant in this segment of bifurcation diagram.

When the column profile is of type III, the TAME composition begins to decrease due to the presence of the methanol collected in the bottoms instead of being in the distillate. In the case of Da=1 and P=1 bar, the TAME changes from being recovered mainly in the distillate to being recovered at a similar purity in the bottoms. The methanol composition decreases in distillate and bottom while the isoamylenes composition increases. An important aspect is that a multiplicity zone around B/F=0.5 is clearly defined for the case of Da=0.0001 and P=10 bar. The multiple

steady state has three branches: two stable and one unstable. The difference in methanol in the distillate between the upper branch and lower branch is around 0.1. The convergence of a commercial simulator in a multiplicity zone is very complicated and the column presents the risk to change its operation from one branch to the other. Usually the multiplicities zones must be avoided if there are not great advantages to operate on the domain defined by them. In the case of $P=1$ bar, there are multiplicities noticed when the column profile changes from type II to type III, for $Da=0.001$ and 0.0001 ($B/F = 0.61$ and 0.64 respectively). These multiplicities are quite small but they are just near the values that maximize the TAME production and separation. In this case, it can be recommended to work on the multiplicities zone. Due to the multiplicity, the isoamylenes are absent in the bottom stream or they are present in a low concentration.

When the column profile is of type I, the distillate is at the azeotropic composition of isoamylenes and methanol. This azeotrope is sensitive to the operating pressure and the methanol purity on the distillate changes from 0.20 at 1 bar to 0.36 at 10 bar. The concentration of methanol remains constant at the bottoms while the isoamylenes increase their concentration provoking a further decrease of TAME concentration in the bottom. In the case of $P=1$ bar and $Da=1$, pure isoamylenes are recovered on the distillate; its composition increases in the bottom while the methanol and TAME compositions decrease.

From the results obtained, it can be observed the influence of the pressure on the TAME synthesis. For the non integrated reactor and column systems, the optimum B/F at 10 bar is 0.26 while at 1 bar is 0.60, while the TAME lost in the distillate compositions at 10 bar is 0.03 and at 1 bar is 0.1. The optimum B/F is considered to be the value which allows a maximum purity of TAME with smaller losses of TAME in the other stream. Qualitatively, the traditional system is not influenced by the pressure. On the other hand, for the reactive distillation system, the pressure has a great influence on the results. At $Da=0.0001$, the $P=1$ exhibits a small multiplicity while the multiplicity at $P=10$ atm is very pronounced. At $Da=0.001$, the bifurcation analysis is qualitatively similar to the obtained at $Da=0.0001$ at $P=1$ bar; on the other hand, at $P=10$ bar and $Da=0.001$, the results of the analysis are qualitatively more similar to the ones obtained at $P=1$ bar and $Da=1$. For $Da=1$ at $P=10$ bar, the bifurcation analysis can not be performed because the pseudo-feed is on the boundary line.

One of the main conclusions that can be obtained from the infinite/infinite analysis is that when the Da increases then the purity of the main product TAME decreases on the bottom stream; at high values of $Da=1$ the TAME can be recovered in the distillate instead of the bottom. Then, from the obtained results, it does not seem too much advantageous to use an entire reactive distillation in contrast with using the traditional system of a reactor followed by a distillation column. From this point of view, a hybrid reactive distillation column could be a more advantageous solution.

Up to this point, it has been considered that the pseudo-feed composition was in the chemical equilibrium of the corresponding pressure. The pseudo-feed composition is not defined in one fixed point, but it is situated on a locus defined over a line of compositions according to the crude feed and stoichiometry of the reaction. Therefore, in order to be able to compare the influence of this pseudo-feed composition, it has been fixed at the value corresponding to the higher chemical equilibrium pressure. This allows us to study the influence of the same pseudo-feed at different pressure and the influence of the same pressure with a different pseudo-feed.

When the comparison is made at the same pressure ($P=1$ bar) with a lower conversion in the column, the bifurcation diagrams are qualitatively quite similar, but there are some remarkable differences as the type III region is situated in a larger zone of the bifurcation diagram and the multiplicities becomes smaller. The most different diagram is at $Da=1$: the type III profiles region becomes narrower. The decrease of conversion on $Da=1$ at the bottom leads to the result

that the composition of TAME is lower and in a sharpest shape at the maximum. The effect in the distillate is that the isoamylenes become the predominant component in the distillate compositions instead of the TAME; the TAME composition presents a sharper maximum when the profile changes from type II to type III, the methanol composition is very low not only for profile type I but also for type III. In the bottoms, the methanol presents a sharp maximum at the change from profile III to I.

When the study is made at two different pressures ($P=1$ bar and $P=10$ bar) at the same conversion in the column, the bifurcation diagrams show some remarkable differences. These differences are not remarkable for non reactive systems, but for the reactive distillation systems the differences are significant. For a $Da=0.0001$ and $P=10$ bar, the presence of multiple steady states was on a quite big region; for $Da=0.0001$ and $P=1$ bar, the presence of multiplicities was smaller but clearly observed; for $P=1$ bar and the same pseudo-feed composition used for $P=10$ bar then the multiple steady states disappears completely. On the other hand, for $Da=0.001$ at $P=10$ bar there were not multiplicities detected and for $P=1$ bar with the same pseudo-feed there is a small bifurcation zone detected when the profile changes from type II to III. It is also remarkable that for $Da=1$ there was no solution for $P=10$ bar, but it is feasible for $P=1$ bar. The shape of the bifurcation diagrams remains qualitatively quite similar when the pseudo-feed changes, but the effect of the pressure has a high impact over the system due to the influence on the azeotropic compositions, providing qualitatively different results.

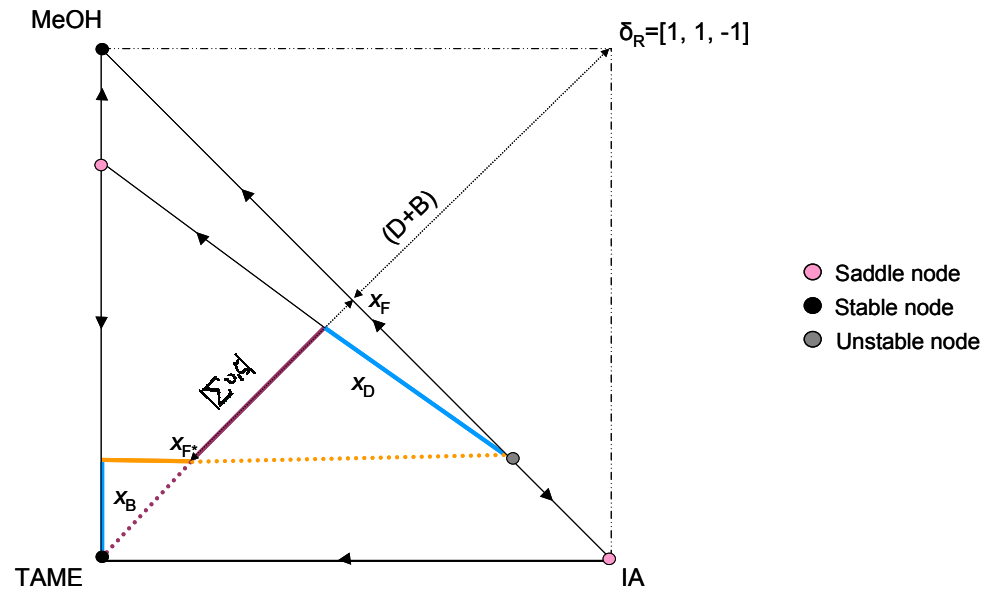
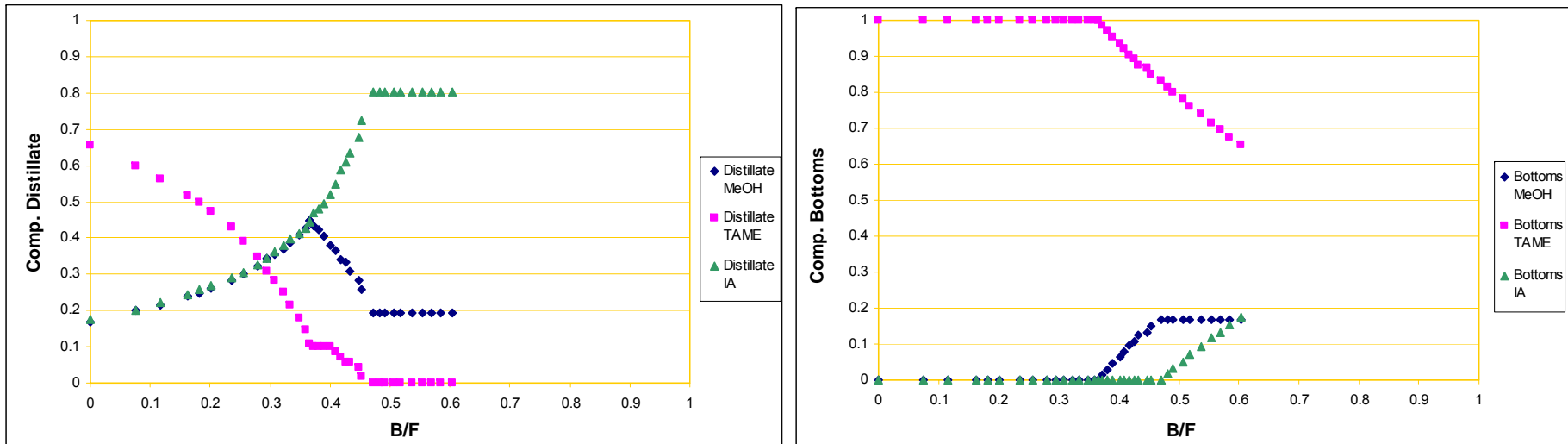


Figure 6.4. Bifurcation diagram of distillate compositions for the TAME synthesis at $Da=0$, $P=1$ bar and real-feed composition at the corresponding chemical equilibrium at 1 bar.

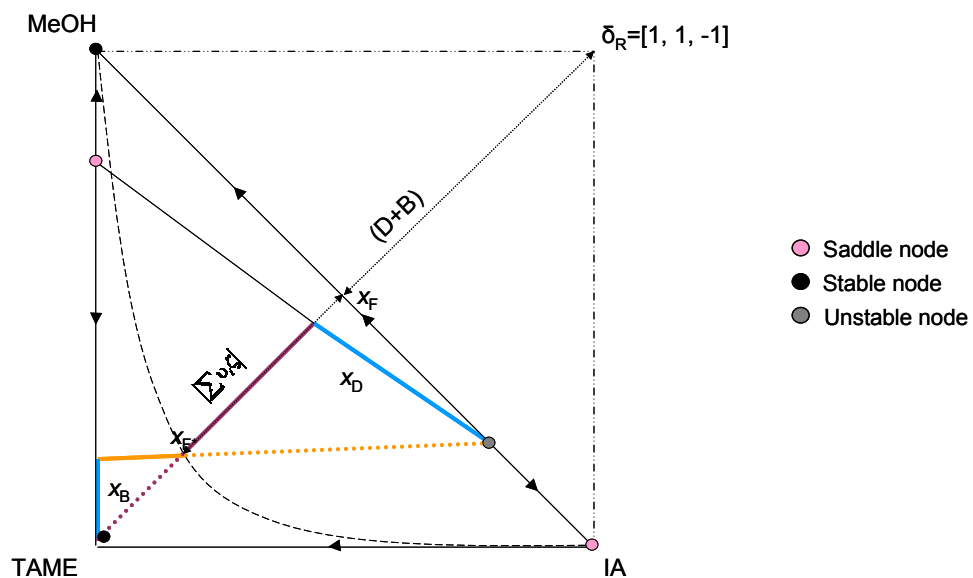
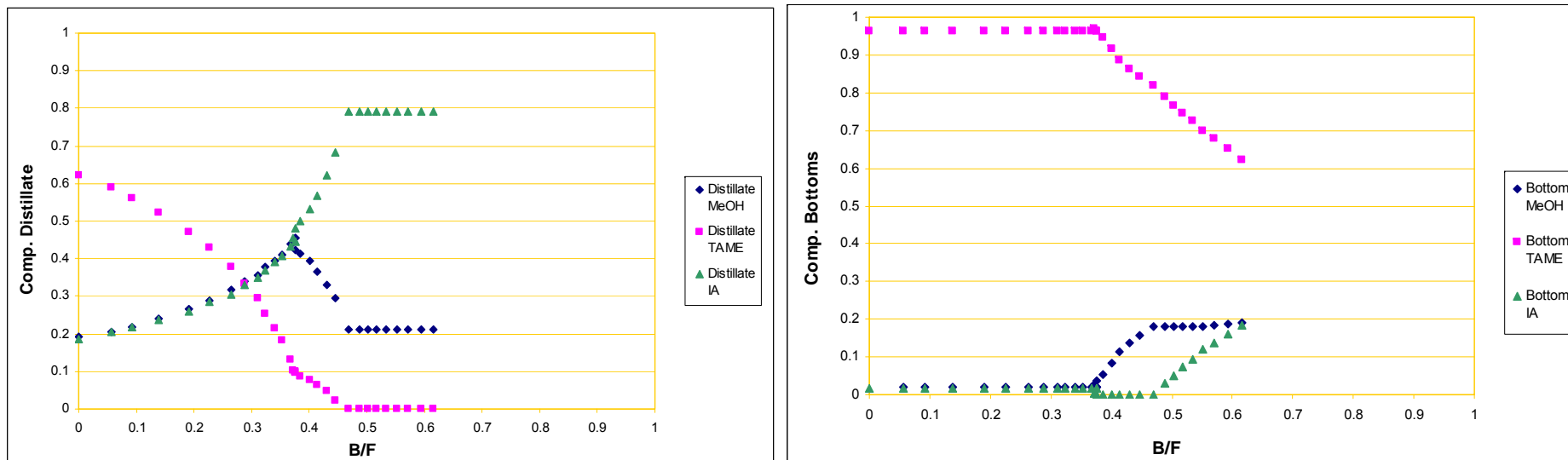


Figure 6.5. Bifurcation diagram of distillate compositions for the TAME synthesis at $Da=0.0001$, $P=1$ bar and real-feed composition at the corresponding chemical equilibrium at 1 bar.

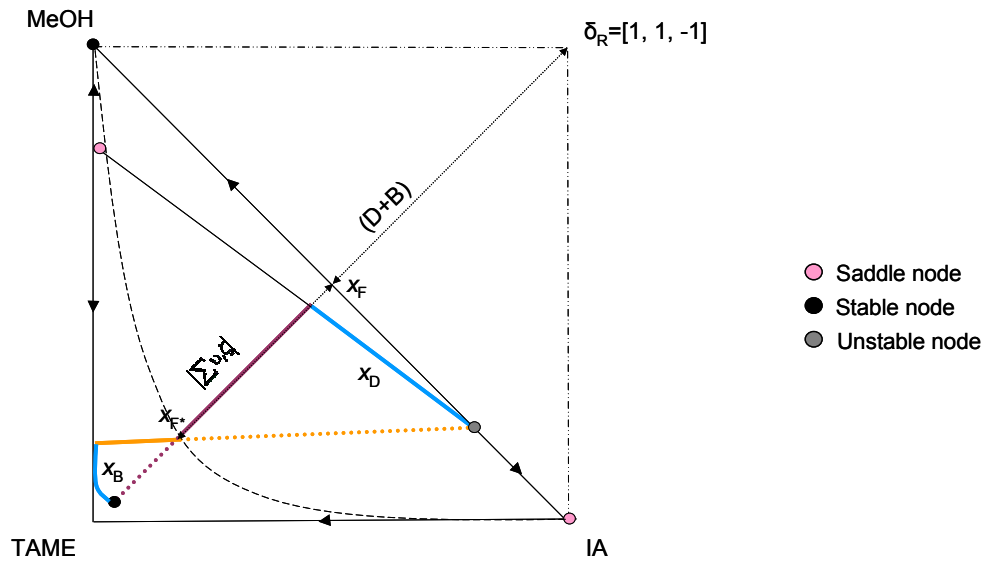
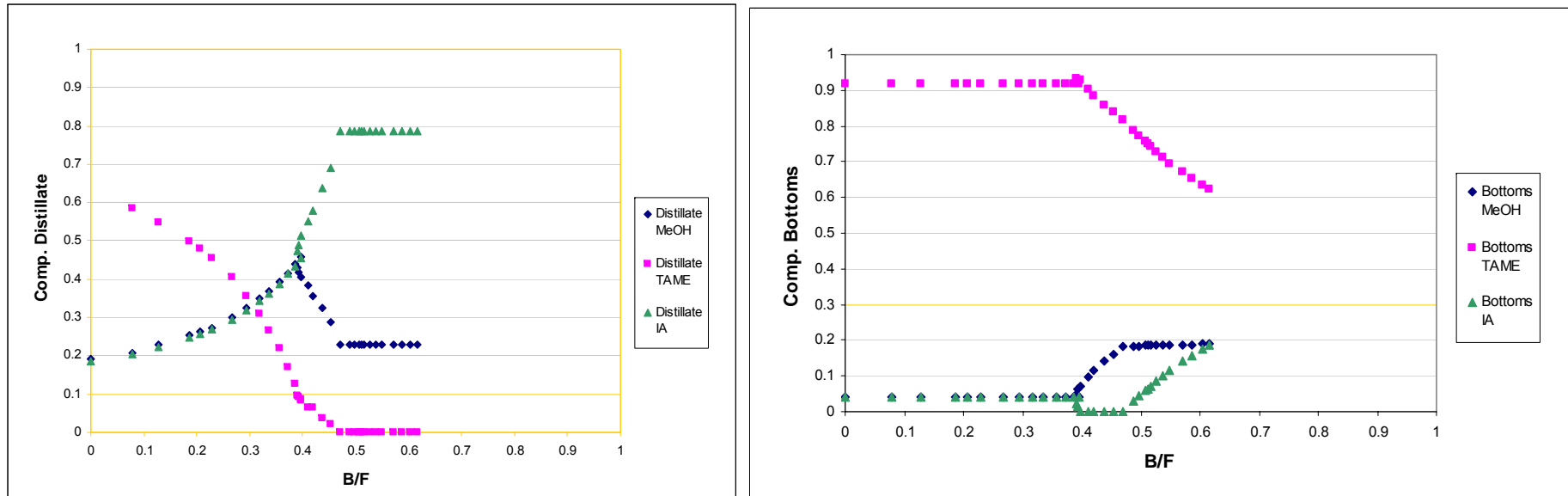


Figure 6.6. Bifurcation diagram of distillate compositions for the TAME synthesis at $Da=0.001$, $P=1$ bar and real-feed composition at the corresponding chemical equilibrium at 1 bar.

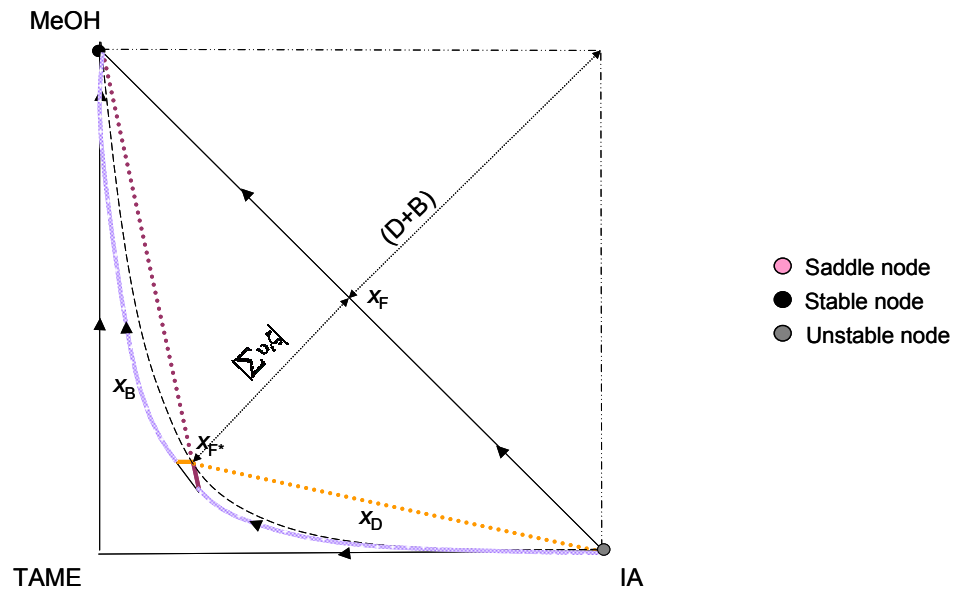
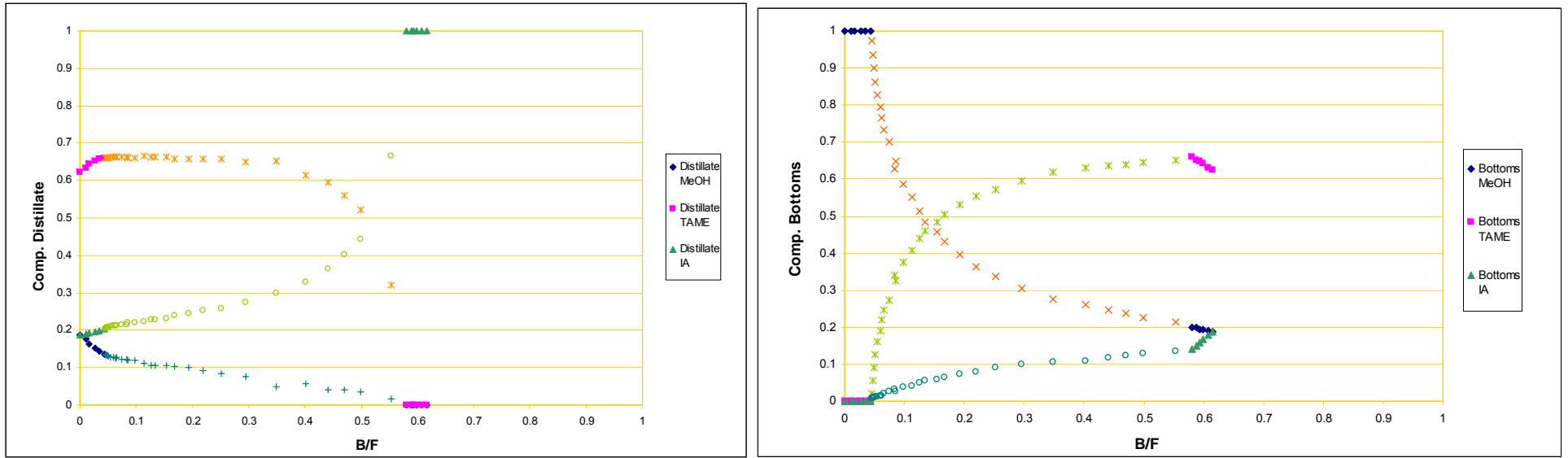


Figure 6.7. Bifurcation diagram of distillate compositions for the TAME synthesis at $Da=1$, $P=1$ bar and real-feed composition at the corresponding chemical equilibrium at 1 bar.

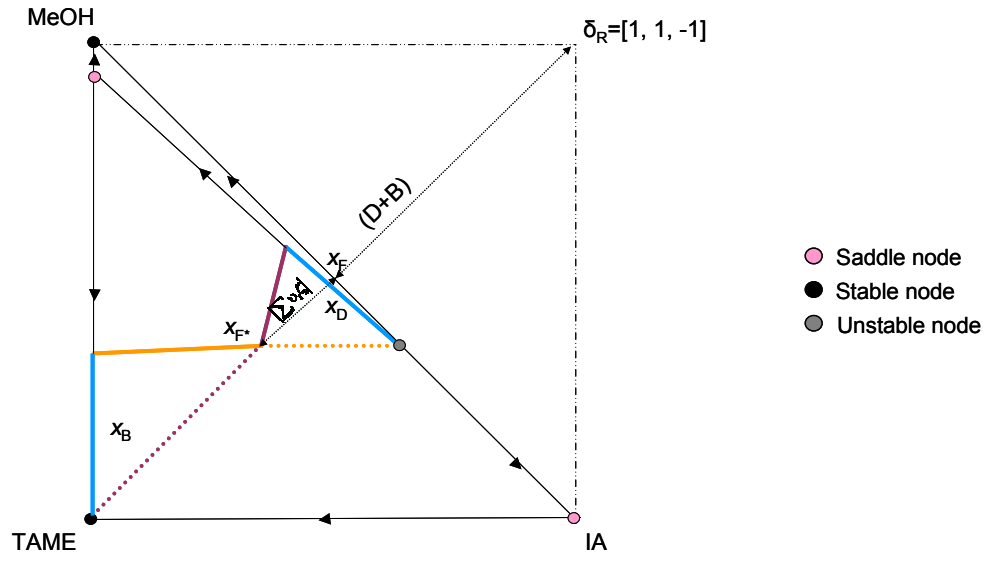
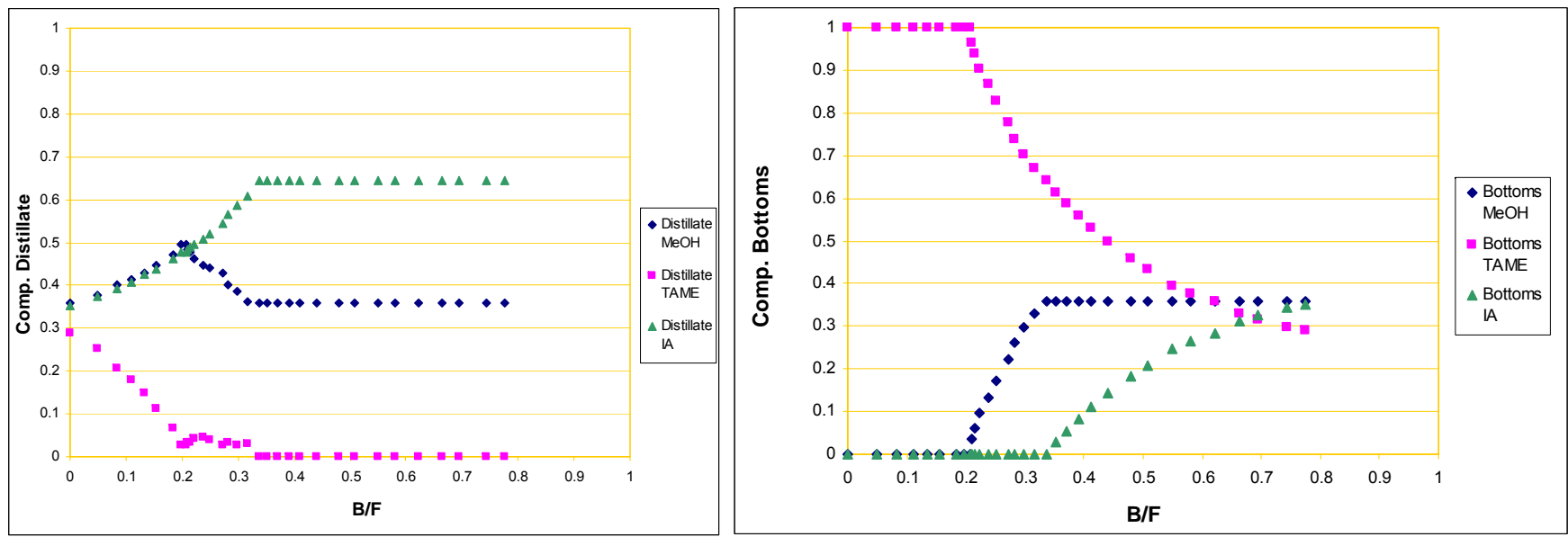


Figure 6.8. Bifurcation diagram of distillate compositions for the TAME synthesis at $Da=0$, $P=10$ bar and real-feed composition at the corresponding chemical equilibrium at 10 bar.

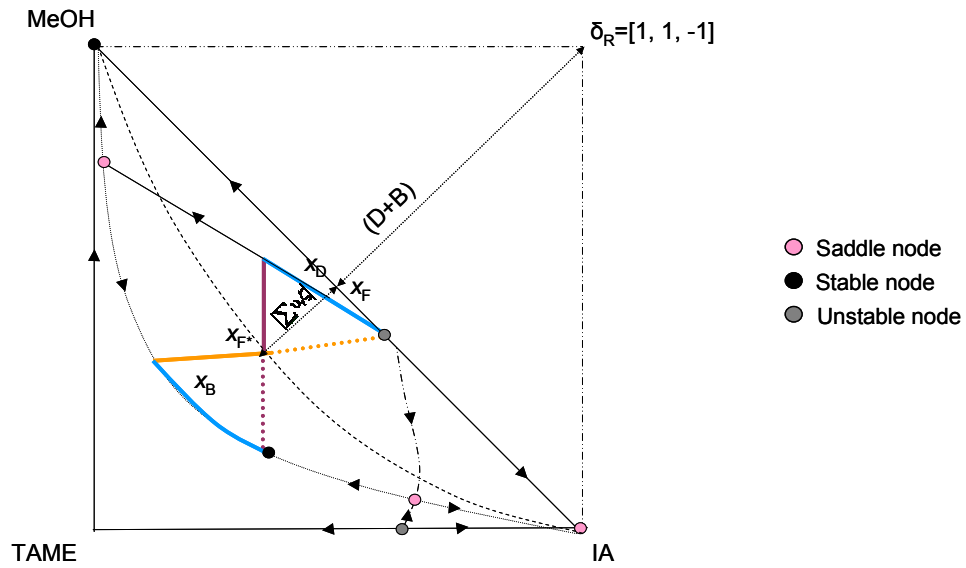
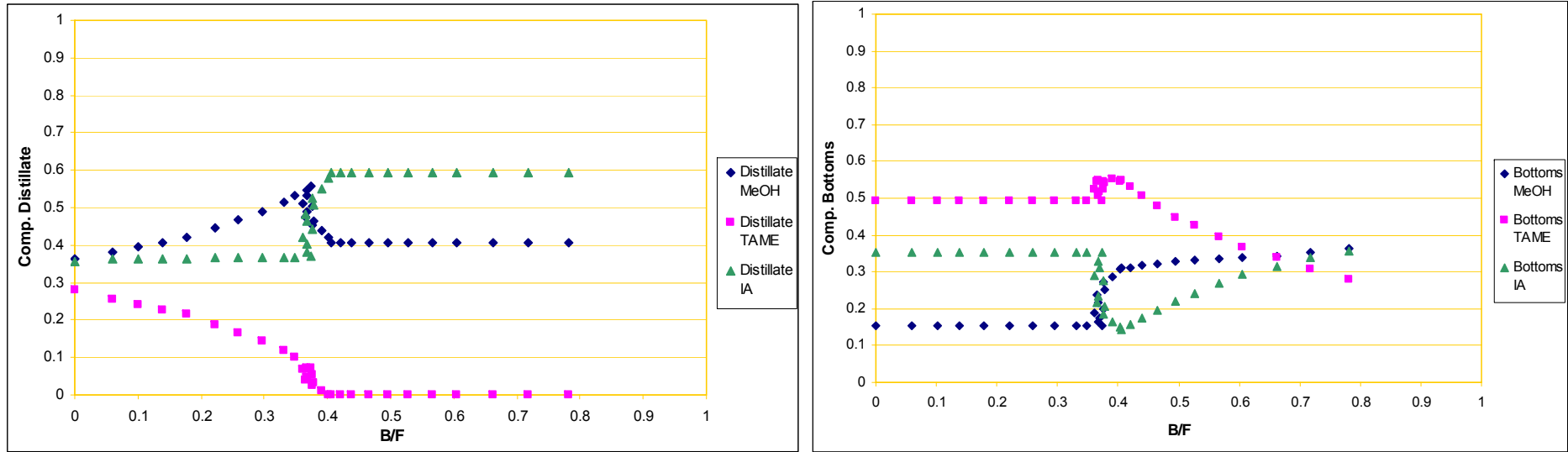


Figure 6.9. Bifurcation diagram of distillate compositions for the TAME synthesis at $Da=0.0001$, $P=10$ bar, real-feed composition at the corresponding chemical equilibrium at 10 bar.

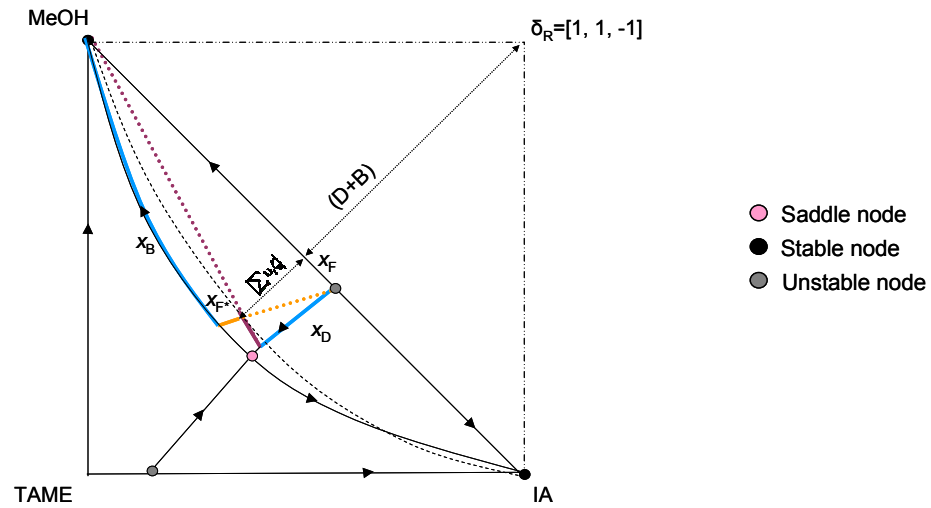
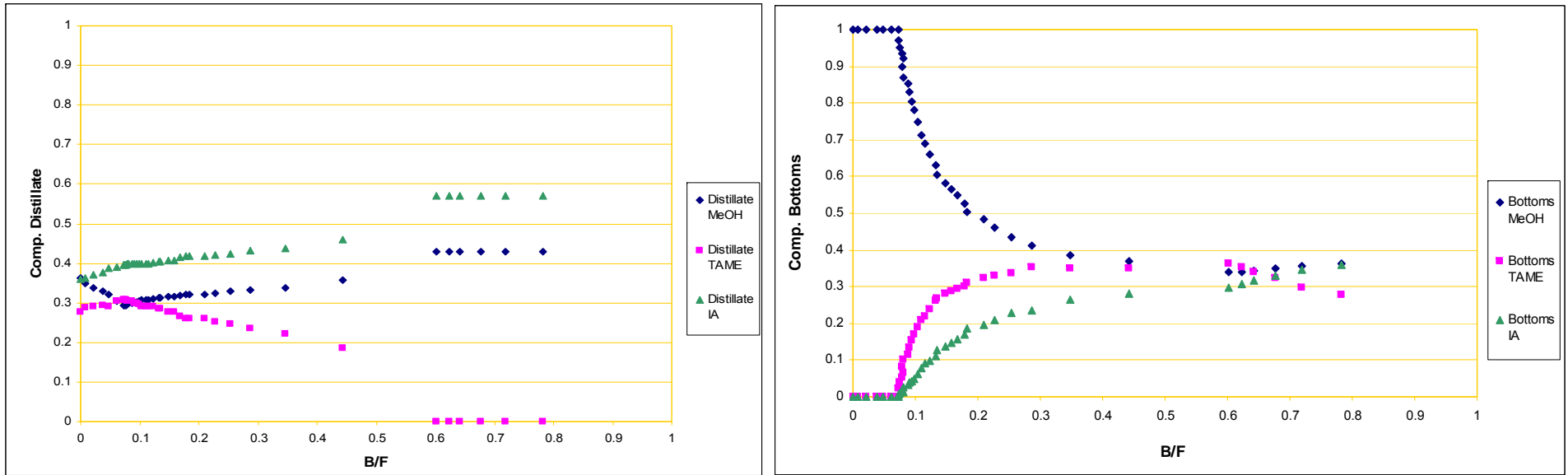


Figure 6.10. Bifurcation diagram of distillate compositions for the TAME synthesis at $Da=0.001, P=10$ bar and real-feed composition at the corresponding chemical equilibrium at 10 bar.

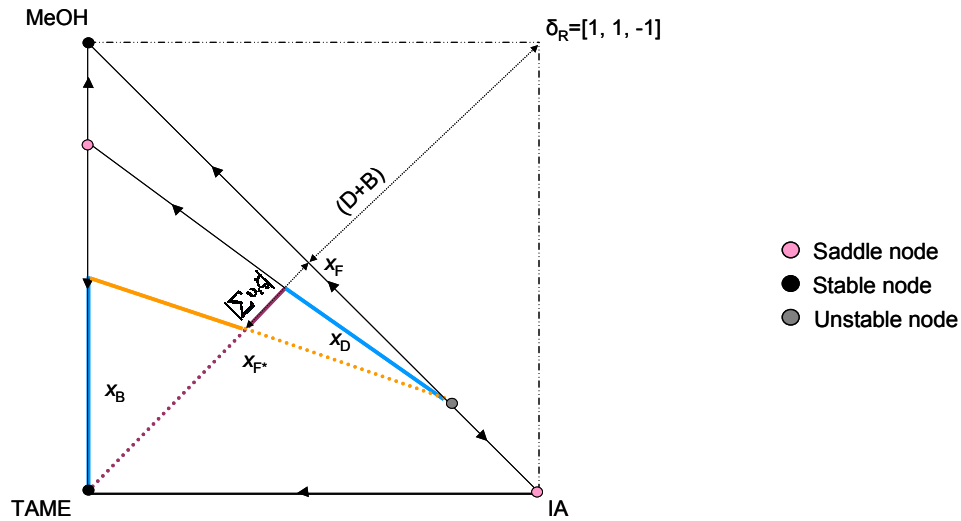
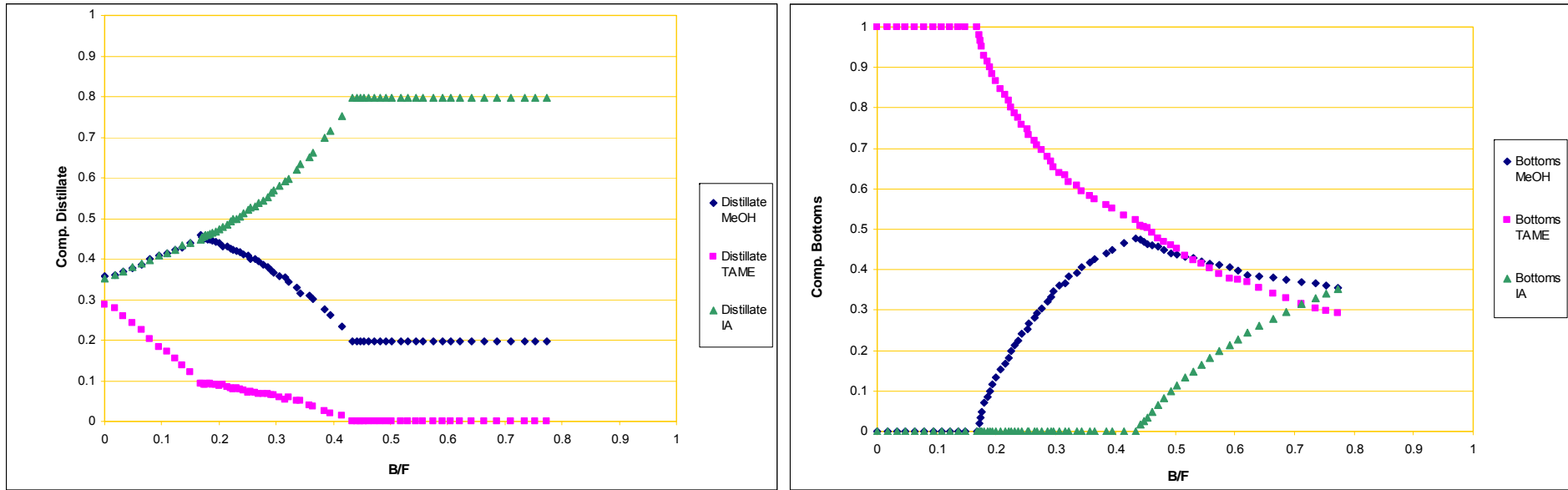


Figure 6.11. Bifurcation diagram of distillate compositions for the TAME synthesis at $Da=0$, $P=1$ bar and real-feed composition at the corresponding chemical equilibrium at 10 bar.

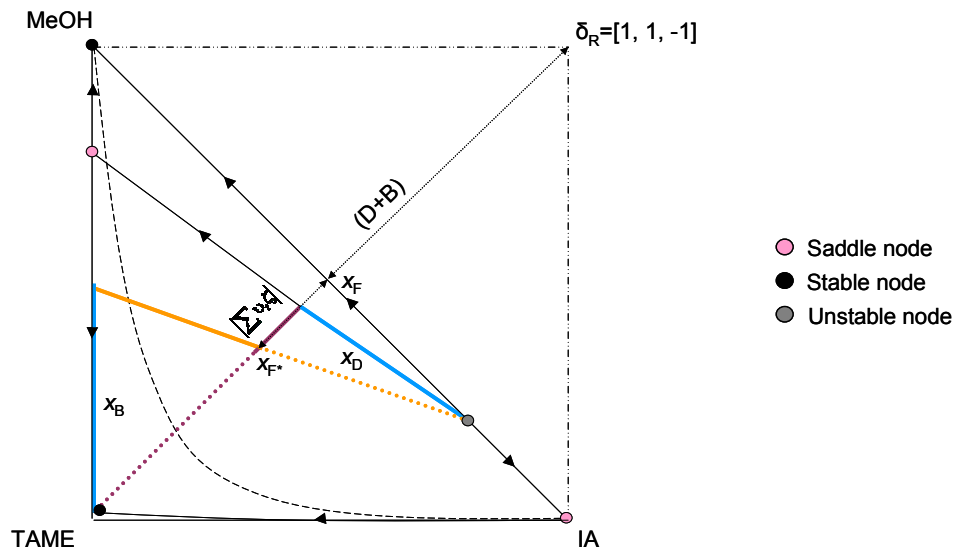
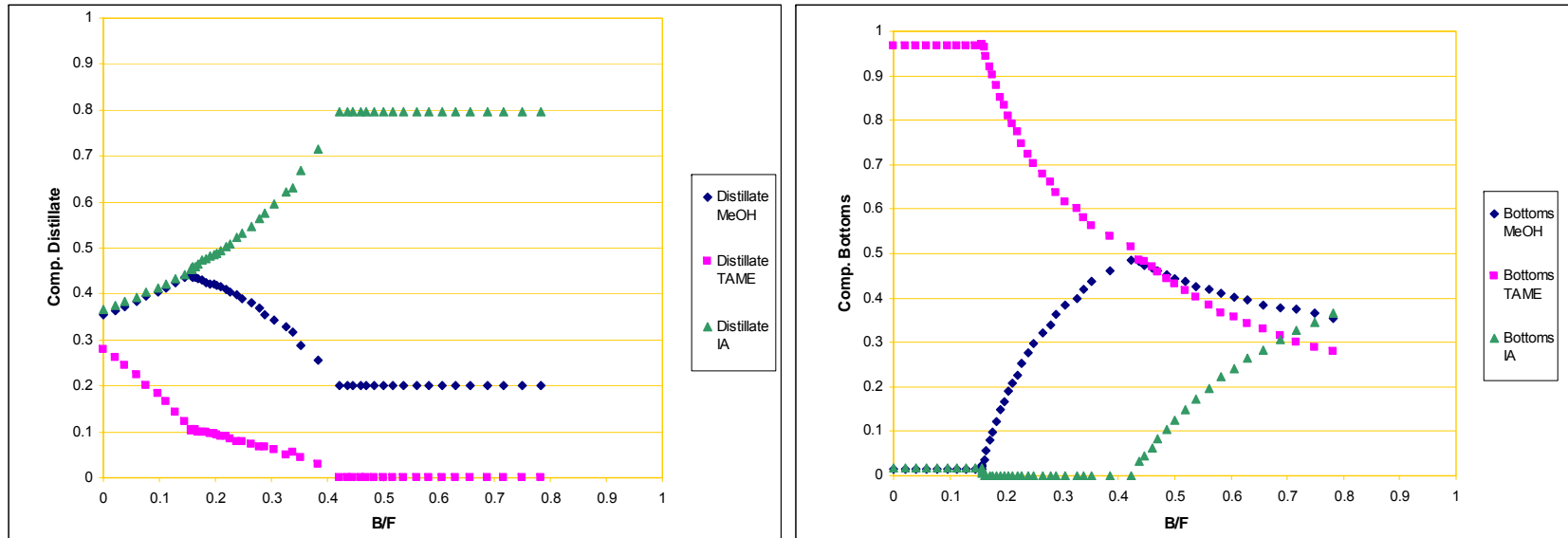


Figure 6.12. Bifurcation diagram of distillate compositions for the TAME synthesis at $Da=0.0001, P=1$ bar and real-feed composition at the corresponding chemical equilibrium at 10 bar.

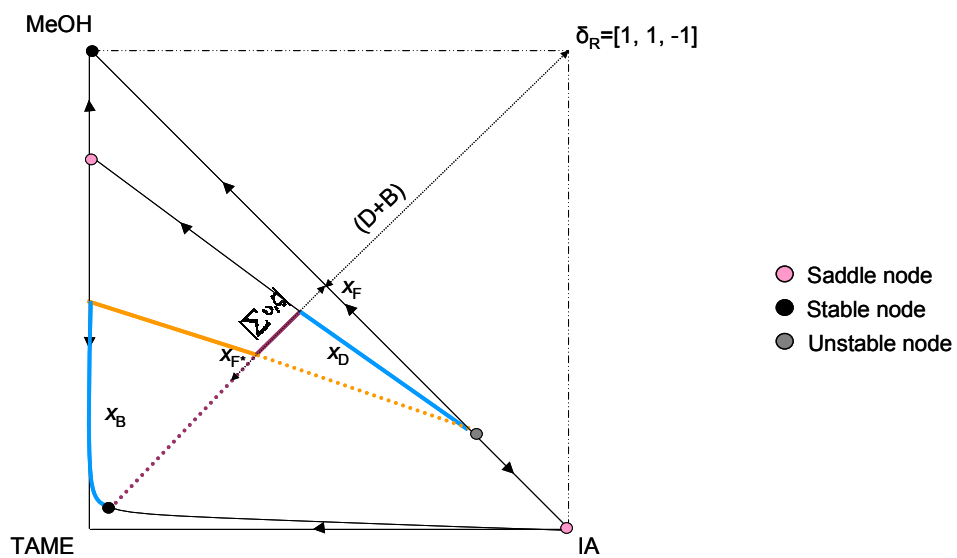
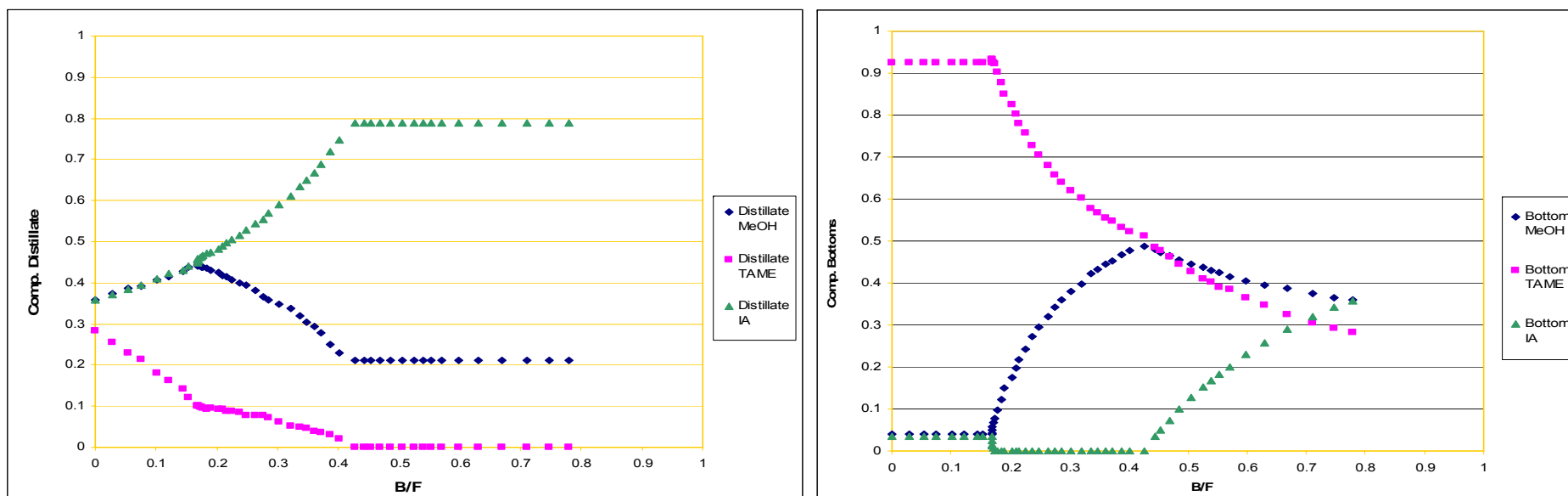


Figure 6.13. Bifurcation diagram of distillate compositions for the TAME synthesis at $Da=0.001$, $P=1$ bar and real-feed composition at the corresponding chemical equilibrium at 10 bar.

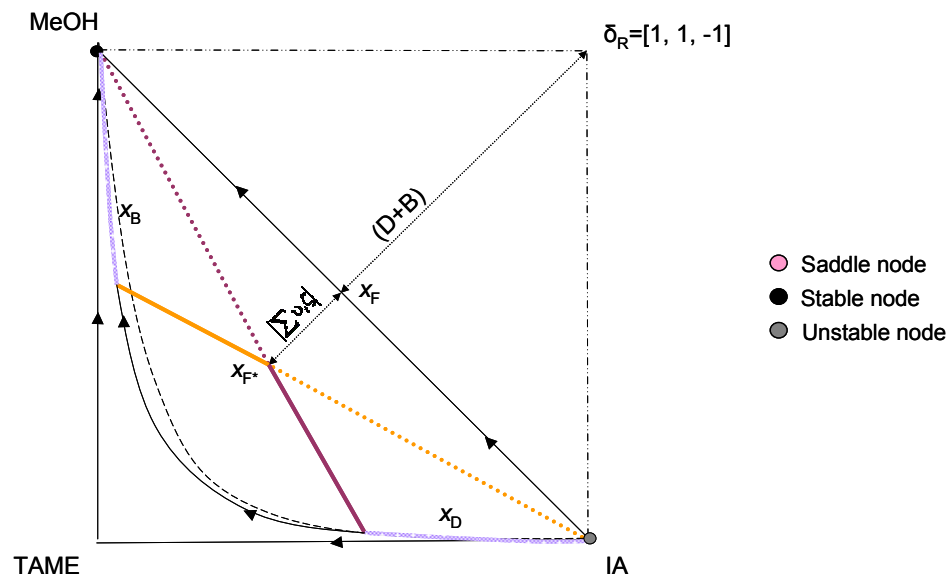
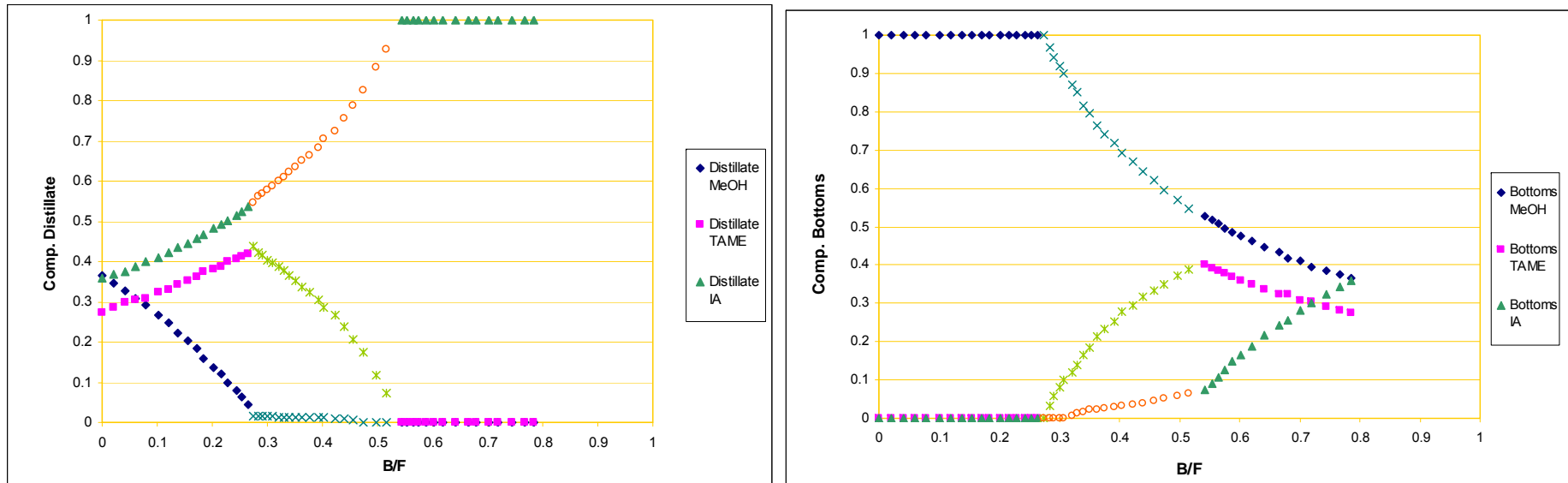


Figure 6.14. Bifurcation diagram of distillate compositions for the TAME synthesis at $Da=1$, $P=1$ bar and real-feed composition at the corresponding chemical equilibrium at 10 bar.

6.2. Analysis of the chemical non-equilibrium system in a hybrid distillation column

In the last section it was seen that due to the reaction on the entire column, TAME decomposes on methanol and isoamylene and can not be obtained pure TAME at the bottoms. The use of a hybrid column with a reaction section at the upper part and a non reactive section at the lower part, could give the benefits of both kinds of operations (reaction and separation). It was seen in the last section that with a non reactive column is possible to reach pure TAME at the bottoms and with a reactive column, the azeotrope in the distillate can disappear.

The same resolution procedure applied to the last section can be used for hybrid distillation columns. In this case, there is not an unique residue curve from the distillate to the bottoms, the column profile would be defined by two residue curves: at the lower part of the column a non reactive curve and at the upper part of the column a reactive curve. Both residue curves must intersect in order to have a feasible column profile. According to Güttinger (1999) we will apply the approximate method that requires only one pinch point for the entire column. For the hybrid systems evaluated, there are not multiplicities.

Figure 6.15 shows the analysis of a hybrid column with a Damköhler number of 0,0001 and 10 bar. In the hybrid column it is possible to reach pure TAME at the bottoms but the reaction only changes the position of the boundary line increasing the quantity of TAME in the distillate. Due to the complexity of this hybrid graphics that superposes the non reactive in green color with the reactive in red color, it will be explained in more detail the fulfilment of the conditions of feasibility.

At the beginning when $B/F=0$ all the pseudofeed is collected at the bottoms, the bottoms composition coincides with the pseudo-feed and the distillate corresponds to the azeotrope methanol isoamylene. An increase of the bottoms flow rate leads to the compositions described by the orange line. In this case, the profiles contain the pinch point of the azeotrope methanol-isoamylene which is the unstable node of three distillation regions on the reactive residue curve map. All the profiles situated in the left side of the discontinuous line indicating the chemical equilibrium converges to this azeotrope. It is a condition of feasibility that a part of the column profile must be on the zone where the reaction that forms the product takes place. All the non reactive residue curves diverges from the azeotrope methanol-isoamylene which is in the reaction zone where the formation of product takes place. This fact assures that any non reactive residue curve reaches the zone where the reactive curves converge to their unstable node. When the bottoms composition does not contain isoamylenes and the bottoms flow rate is increased, then the bottoms compositions follows the edge of the triangle towards pure TAME meanwhile the distillate follows the reactive boundary line. Both lines are indicated on the continuation diagram by blue lines. The column profile follows the triangle edge methanol-TAME until the saddle point of the non reactive map for this mixture, then follows a very short distance the non reactive boundary line indicated in green until the reactive boundary line in red is met, which is then used to reach the reactive saddle point. We are following a path against the direction of the residues curves, towards the unstable node. The presence of the saddles on the profile and the existence of residue curves from the bottoms to the distillate assure the feasibility. Finally, the distillate composition moves towards the pseudo feed meanwhile the bottoms composition is pure TAME. This last movement is indicated in violet; as the distillates are on the distillation region of the stable node (TAME) for the non reactive map, the existence of residue curves from the distillate to the bottoms is assured. It is important to notice that a pseudo feed at the left side of the reactive equilibrium curve could not be reached because all the column profile would be in regions where the formation of product TAME is not favourable.

In figure 6.16 there are some points that are a clear example of the fact where all the requirements are fulfilled but all the profile is on the unfavourable zone of formation of TAME. The part of continuation path in colour violet and the last small section of the blue one run over the reactive boundary until the non reactive boundary and to the non reactive azeotrope. The

profiles contain a pinch, the lever rule is satisfied and there is a feasible profile from the distillate to the bottoms but any part of the profile is not favourable to form TAME. In this situation, it can be used a pseudo feed enriched with isoamylene as was explained at the last section for the non reactive column. In this way, it would be possible to collect pure TAME at the bottoms and the azeotrope methanol with isoamylene on the distillate. Figure 6.17 for a Damköhler of 1 shows that although the Damköhler increases similar results are obtained. Figure 6.18 shows that the pressure has an important role in the process and with a Damköhler equal to 1 and 1 bar is not feasible to obtain the pure TAME because the unstable node for the reactive residue curve map is pure isoamylene.

According to the results obtained, using a stoichiometric crude feed to the system, the worst results are obtained by the use of an entire reactive distillation column because TAME decomposes before being collected at the bottoms and it is not possible to collect pure TAME. The hybrid column with a non reactive section at the bottoms overcomes this limitation and reports some advantages as the use of the heat of reaction in the distillation column and simplifies the system as the reactor is not required anymore. The presence of some small proportion of TAME product at the distillate is not a problem as it can be recycled to the system jointly with the non reacted components. The presence of TAME in the distillate can be avoided by increasing the content of isoamylene in the feed of the column in order that the distillate reaches the azeotropic mixture isoamylene-methanol instead of the boundary line. Then pure TAME is collected at the bottoms and the azeotrope of methanol and isoamylene at the distillate. The distillate composition is mixed with the crude stoichiometric feed that provides the feed of the reactor. The lever rule is also fulfilled for mixing streams. From the representation of the bifurcation diagram are not observed multiplicities. The calculations of the bifurcation and continuation diagrams presented in the previous pages are referencing the distillate flow rate to a crude feed without the recirculation of the distillate. When a recirculation of the distillate with TAME is taken into account for the traditional system of at 1 bar at the optimal point, the value reported of D/F is of 0.146, a value smaller than the one obtained by using an excess of isoamylene in the distillate that leads a value of 0,306. When the recirculation of the distillate with TAME is considered for the system at 10 bar, the value of D/F becomes 1,385 in front of a value 1,286 obtained by the excess of isoamylene on the column feed. The traditional system of reactor and distillation column at 1 bar (figure 6.20) provides a lower recirculation distillate flow rate than the system at 10 bar (figure 6.21) because the advance of the reaction to produce TAME in the reactor is higher. The hybrid reactive distillation column is able to overcome the equilibrium limitation of the reaction and a total conversion is attainable (figure 6.22). Figure 6.23 shows the relation between the distillate flow rate and the advance of the reaction according to the feed to the reactor or the overall feed to the reactive distillation column. For the traditional system of reactor and column at 1 bar, 10 bar and the reactive hybrid column, the main difference is noticed in regard of the advance of the reaction that can be achieved. Taking into account that B/F is constant and equal to 0,5 for all the situations with recycle stream, for low reaction conversions the distillate flow rate is huge in relation with the bottoms flow rate of product. At low advance of the reaction, any small increase on the advance of the reaction leads to an important decrease of the recycled flow rate and the energy requirements. At high advance of the reaction, the benefits of a small increase on the advance of the reaction leads to poor improvements. The advance of the reaction in the traditional system depends on the temperature of the reactor, at higher pressure considered leads to higher boiling point and higher temperatures. The decrease of the temperature in order to push the equilibrium constant to form a higher quantity of TAME can lead to lower reaction kinetics. At the hybrid reactive distillation, the chemical equilibrium is not a restriction and seems the best option from the operational and energetical point of view.

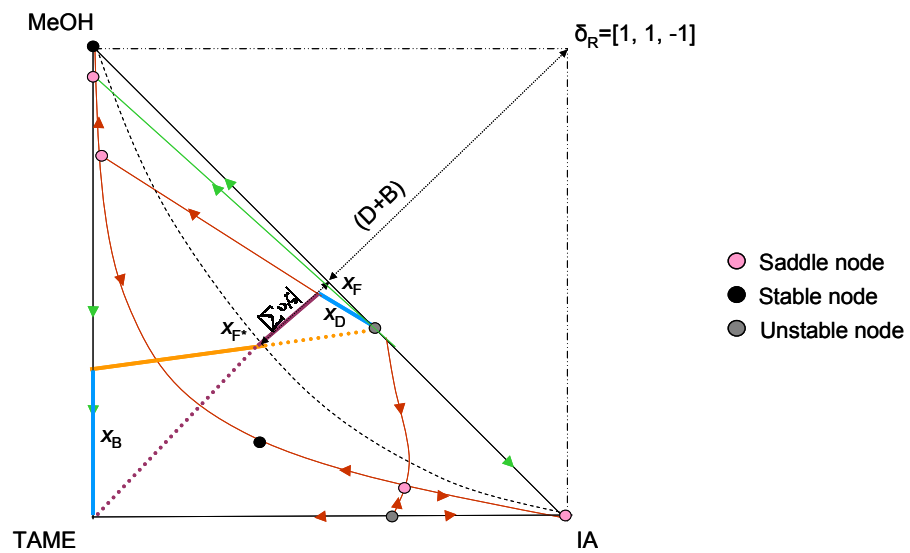
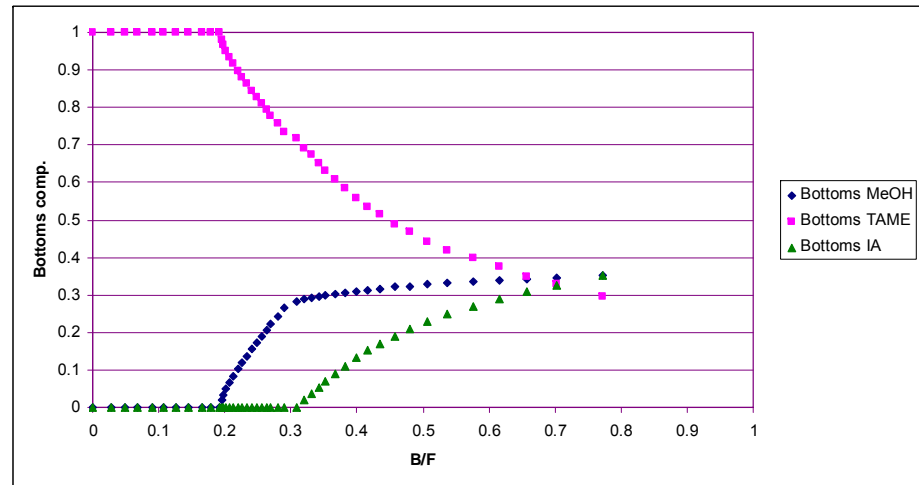
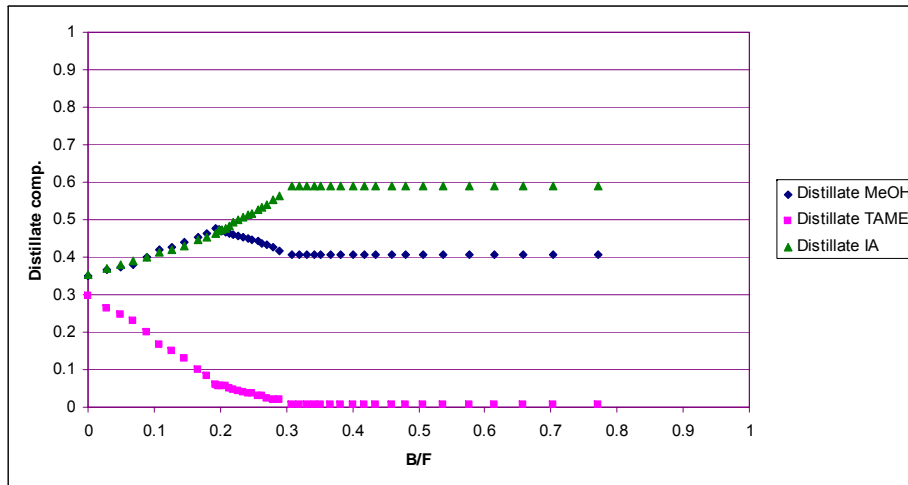


Figure 6.15. Bifurcation diagram of distillate compositions for the TAME synthesis in hybrid distillation column, at $Da=0.0001$, $P=10$ bar and real-feed composition at the corresponding chemical equilibrium at 10 bar.

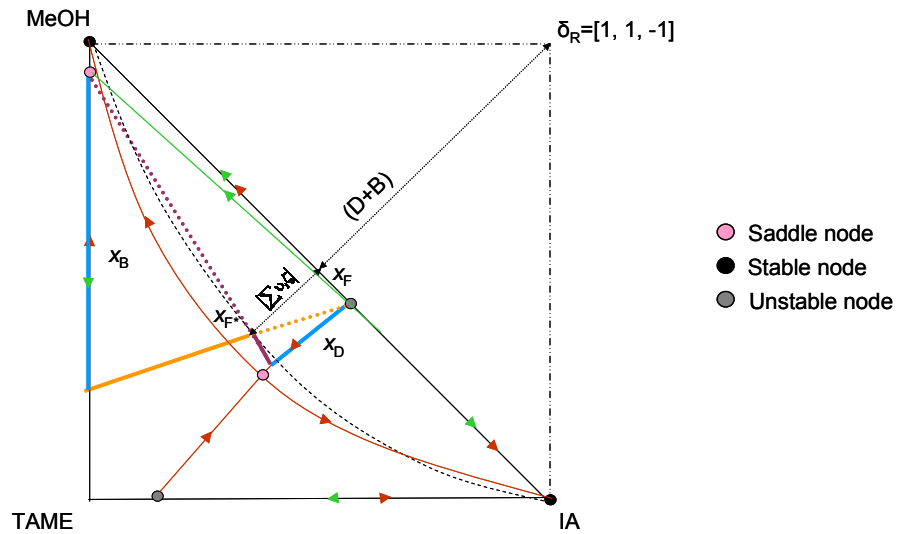
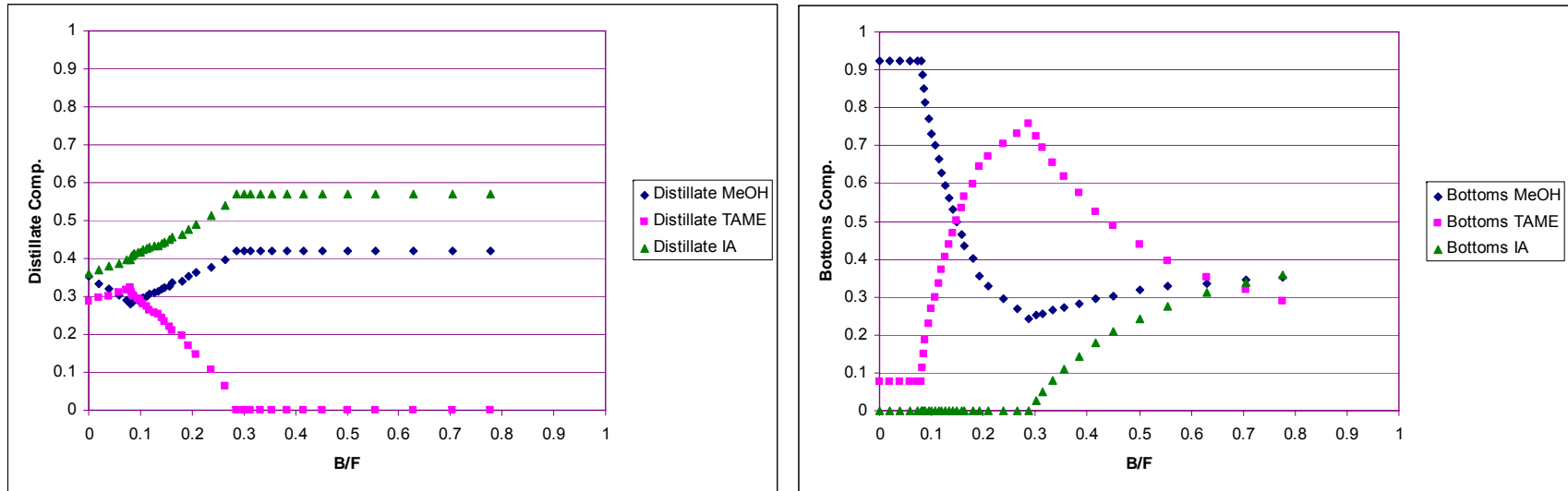


Figure 6.16. Bifurcation diagram of distillate compositions for the TAME synthesis in hybrid distillation column, at $Da=0.001$, $P=10$ bar and real-feed composition at the corresponding chemical equilibrium at 10 bar.

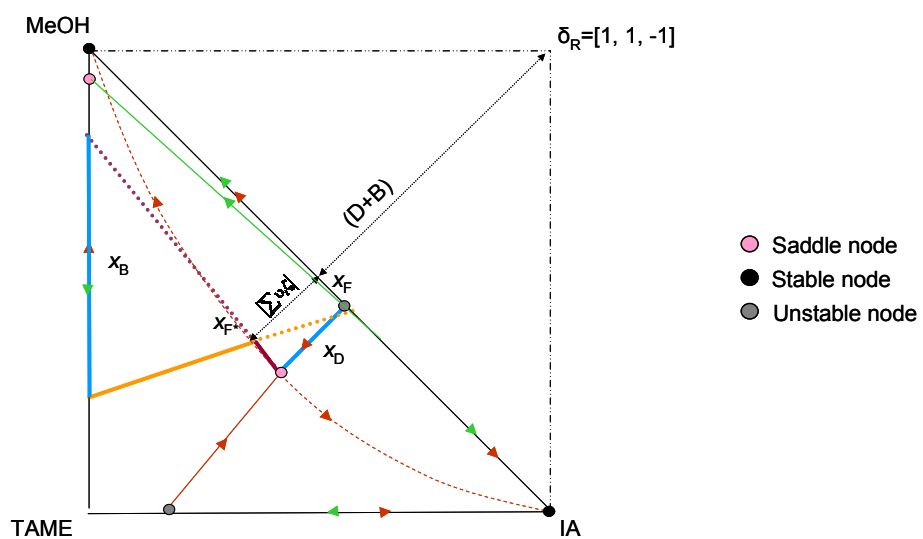
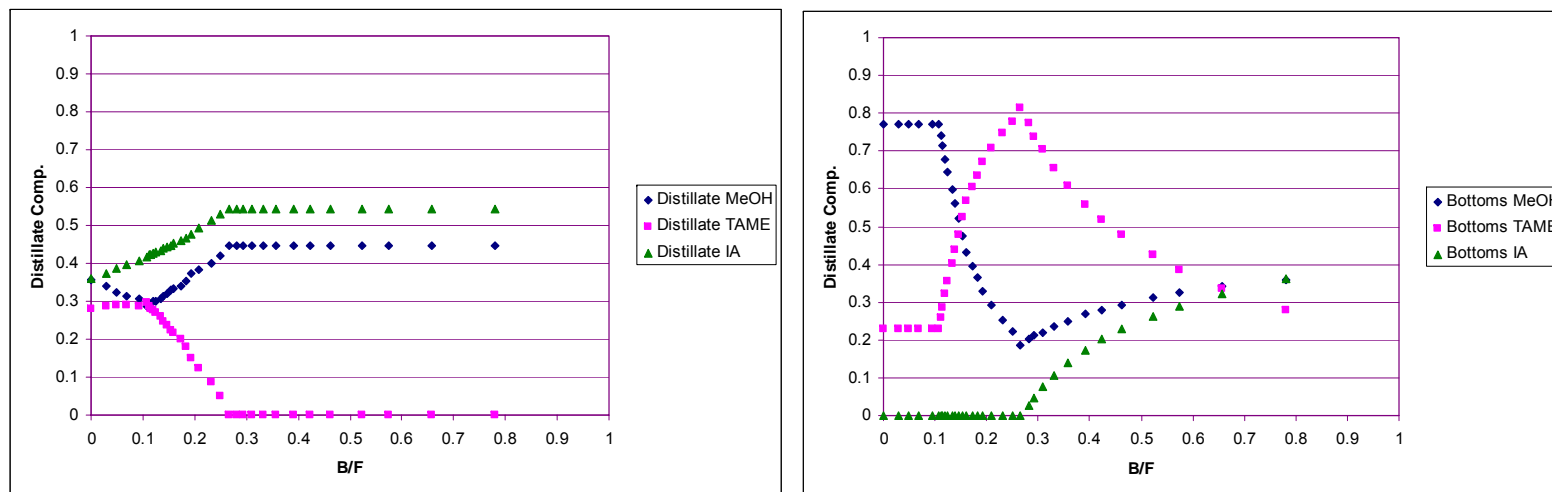


Figure 6.17. Bifurcation diagram of distillate compositions for the TAME synthesis in hybrid distillation column, at $Da=1$, $P=10$ bar and real-feed composition at the corresponding chemical equilibrium at 10 bar.

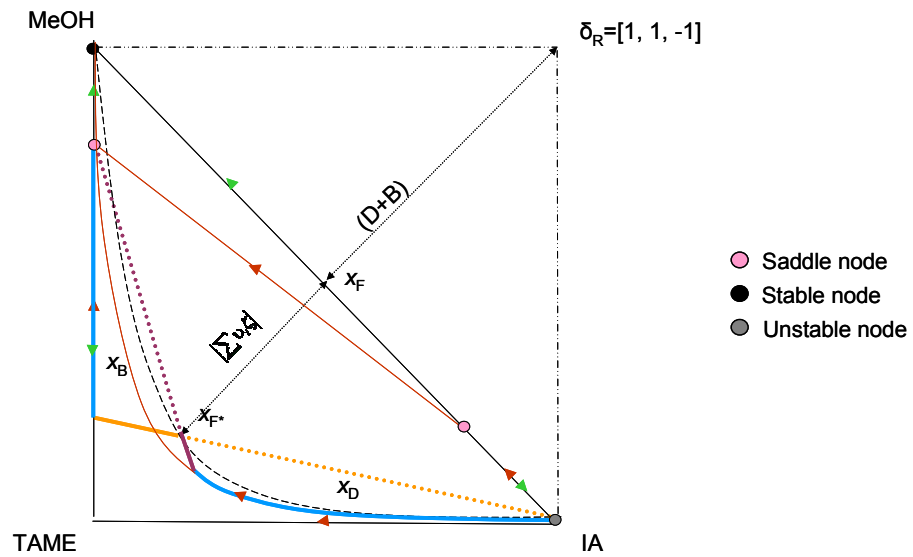
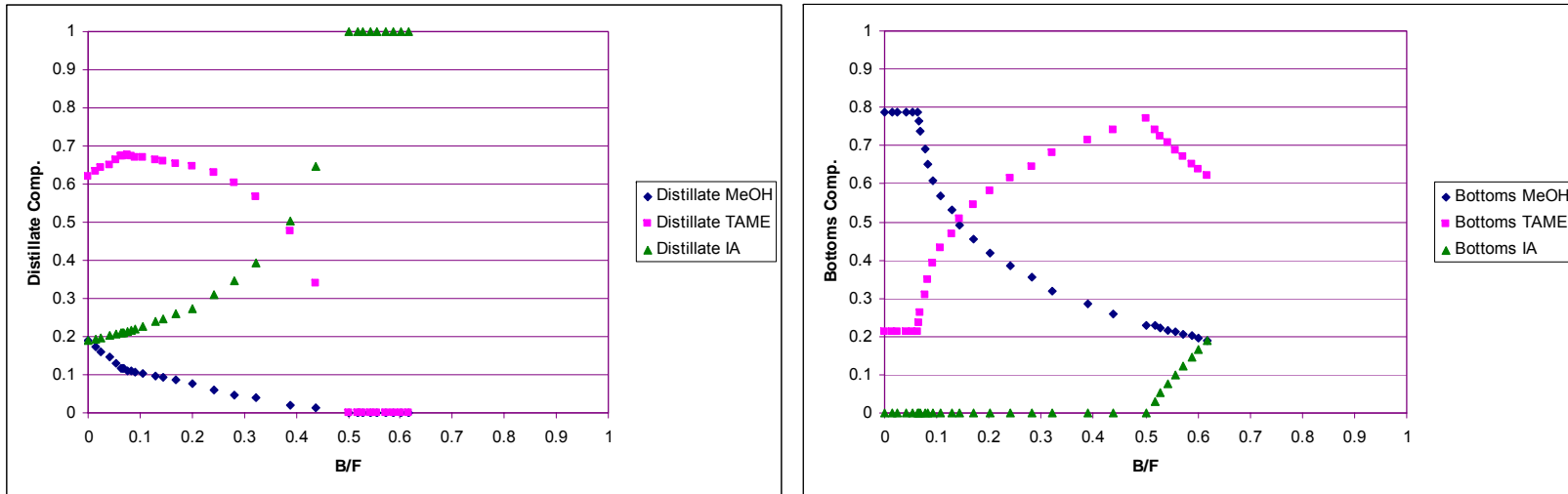


Figure 6.18. Bifurcation diagram of distillate compositions for the TAME synthesis in hybrid distillation column, at $Da=1$, $P=1$ bar and real-feed composition at the corresponding chemical equilibrium at 1 bar.

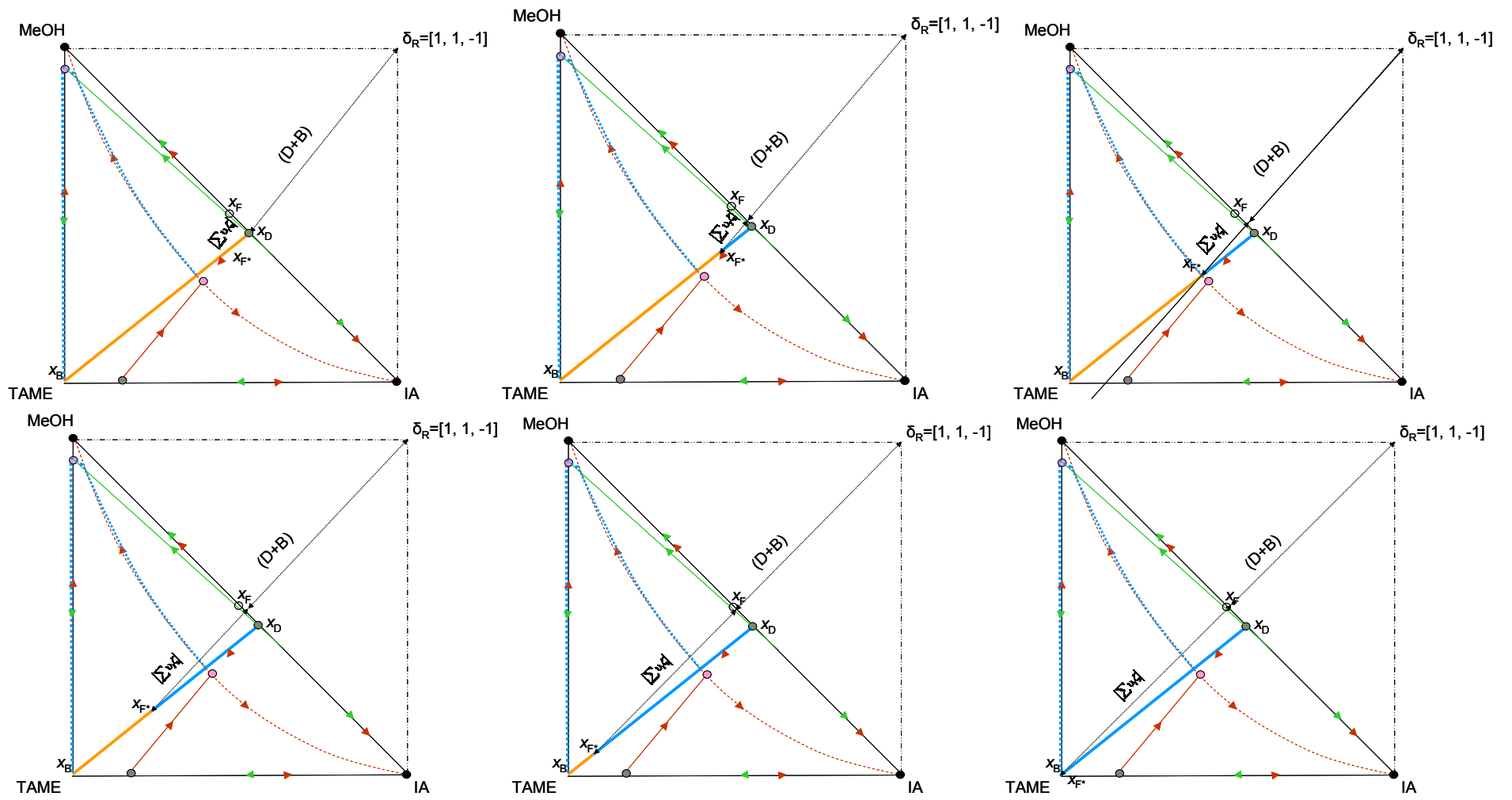


Figure 6.19. Hybrid reactive distillation column overcoming chemical equilibrium

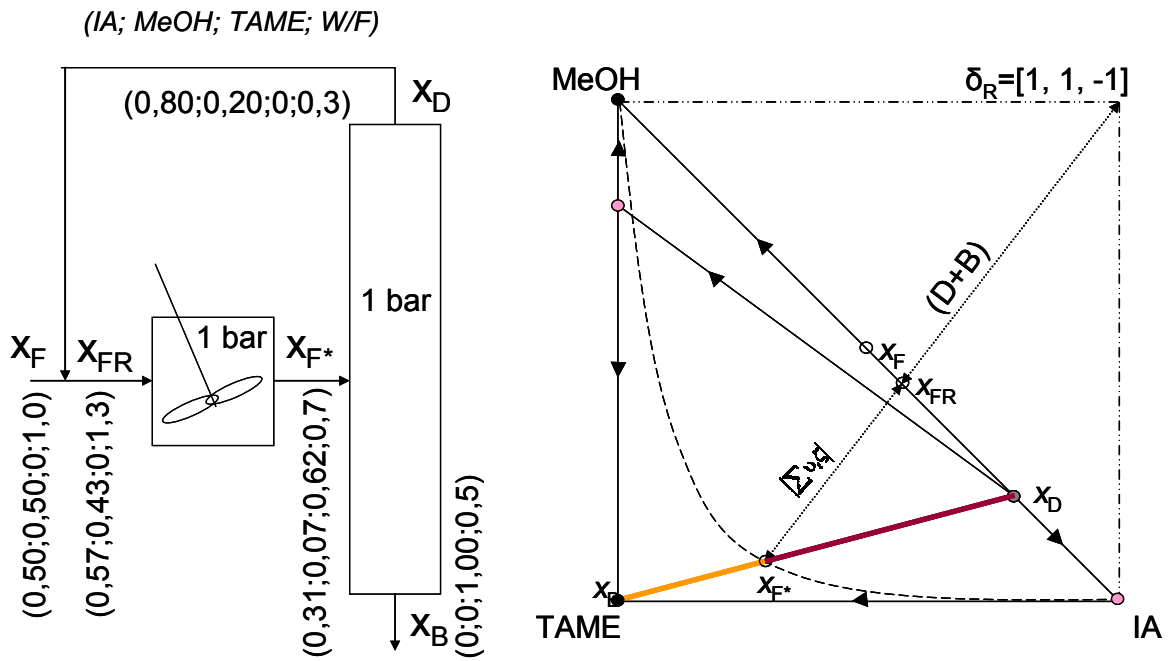


Figure 6.20. Traditional system of reactor and distillation column at 1 bar using an excess of isoamylene on the reactor feed.

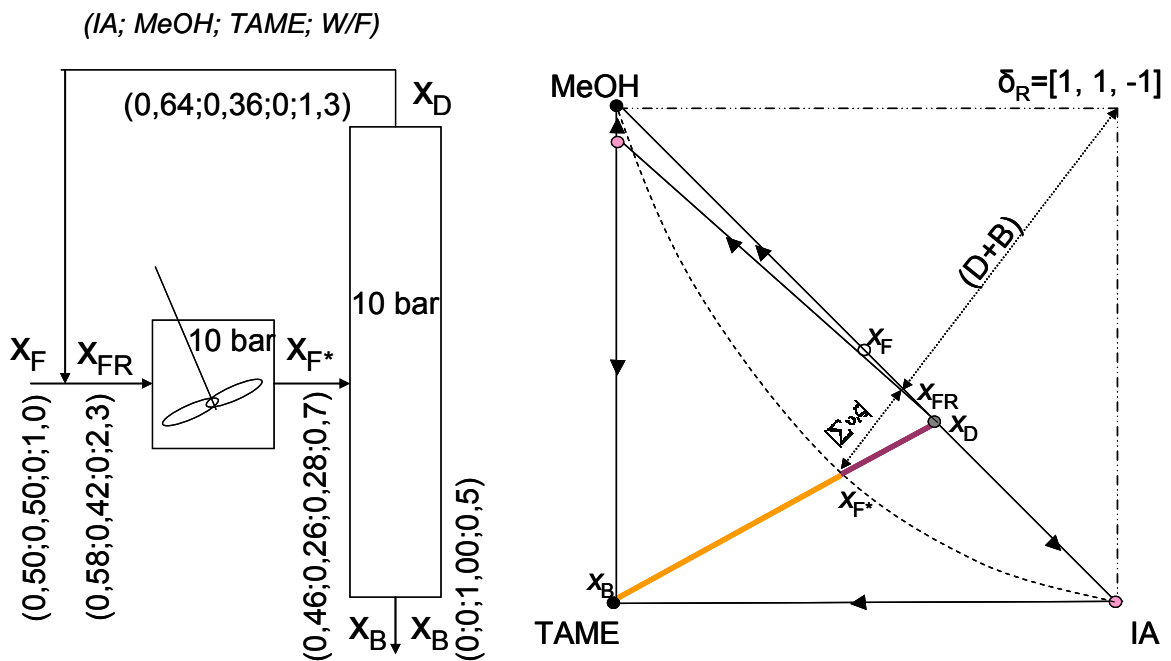


Figure 6.21. Traditional system of reactor and distillation column at 10 bar using an excess of isoamylene in the reactor feed.

(IA; MeOH; TAME; W/F)

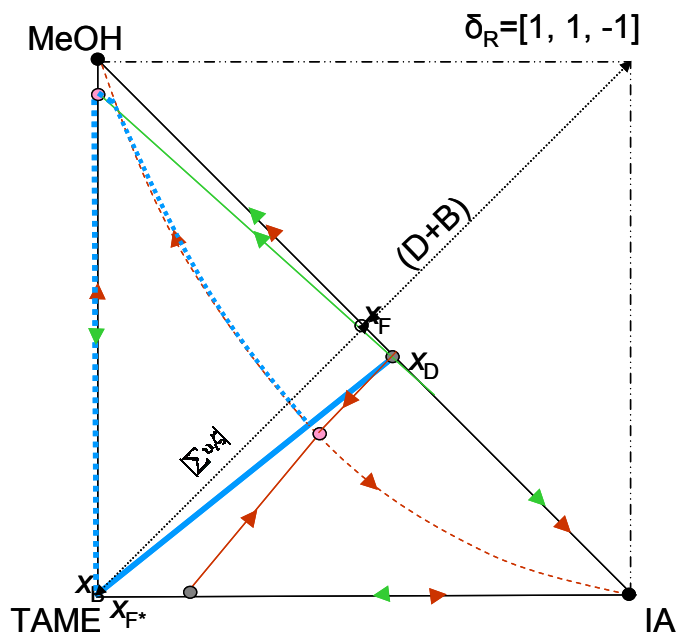
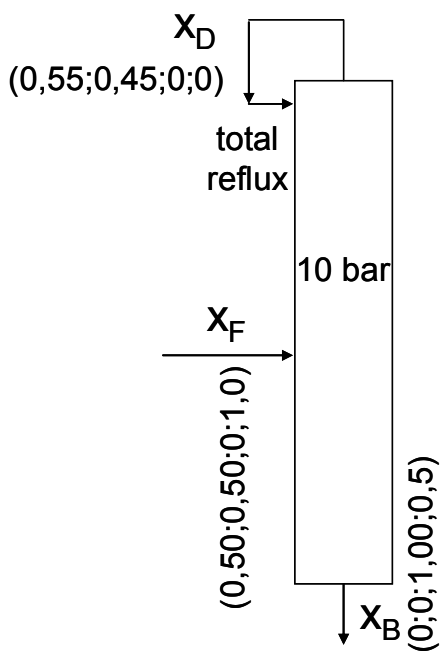


Figure 6.22. Hybrid reactive distillation column at 10 bar using an excess of isoamylene in the column feed.

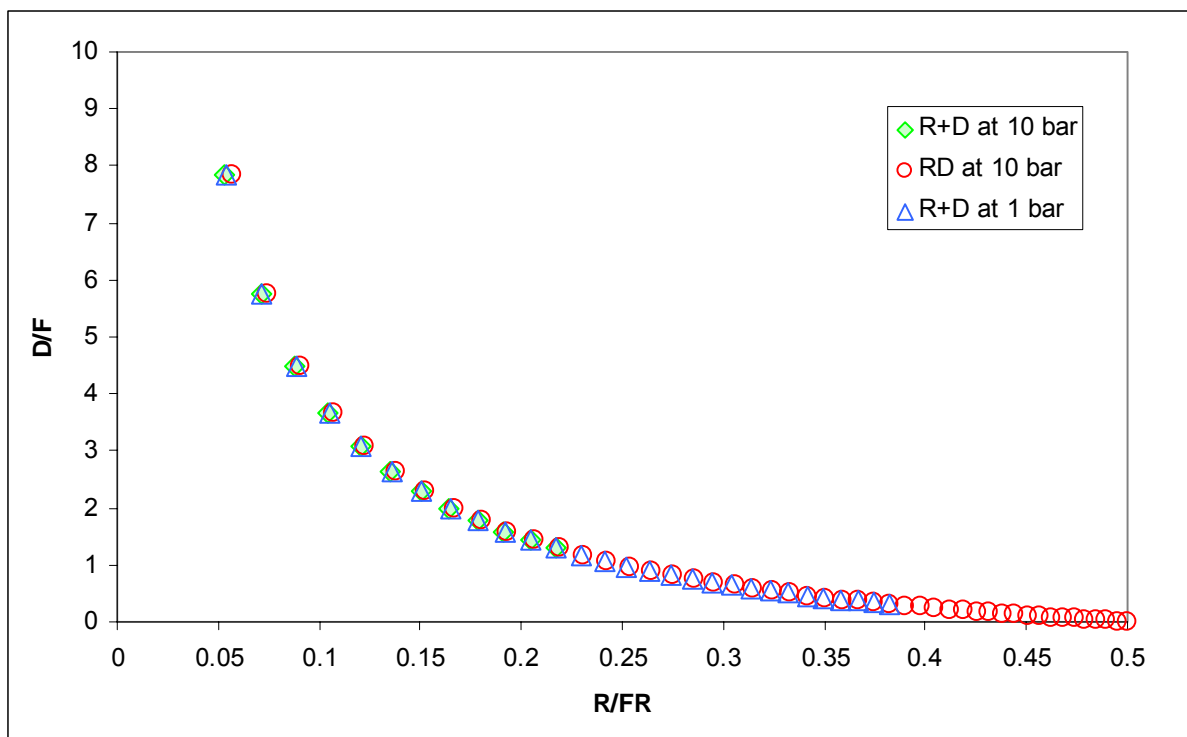


Figure 6.23. Influence of the advance of the reaction on the performance of various process configurations

Conclusions

This study extends the infinite/infinite analysis to chemical non-equilibrium systems by the use of a pseudo-feed which is related to the overall advance of the reaction on the column.

A type of multiplicity is detected by the infinite/infinite analysis; this multiplicity depends on the Da number, at Da=0 and Da=1 there are not multiplicities while some multiplicities are observed when the Da number varies between 0 and 1.

The reactive distillation columns for TAME synthesis show some multiple steady states in some of the bifurcation diagrams. These multiple steady states can be avoided by changing the Da number, the column pressure or the pseudo-feed composition.

At Da=1 and P= 10 bar, the TAME is the predominant component in the distillate of most of the bifurcation diagrams. When it is used stoichiometric feed, some quantity of TAME is collected by the distillate due to the presence of a boundary line in the residue curve map.

The traditional system of a reactor followed by a distillation column has been compared to the use of an entire reactive distillation system. The traditional system configuration is more advantageous than the reactive distillation system because pure TAME can not be obtained in the column bottoms due to its decomposition in methanol and isoamylenes.

When the boundary line is close to the residue curve map edge as in 10 bar, it is preferable to introduce stoichiometric feed at the reactor and recirculate the non reacted components with some of the TAME product than use an excess of isoamylyene to avoid this presence. When the boundary line is more distant to the edge as happens at 1 bar, it is preferable to use the excess of isoamylyene to avoid the presence of TAME in the distillate.

In the traditional system of reactor and column, to maximize the advance of the reaction and minimize the recycle flow rates of the distillate of the column, the temperature of the reactor must be refrigerated at low temperature.

The hybrid reactive distillation columns overcomes the limitation of the chemical equilibrium and pure TAME can be collected using a non reactive section at the bottoms. The heat of the reaction is used directly by the reactive distillation column.

From the results, it seems as a promising alternative the use of a hybrid reactive distillation column with a total reflux to avoid the recycle of reactants and reach a total conversion.

The next step is to proceed with rigorous simulations to validate the results.

References

- Balashov, M., Grishunin, A. and Serafimov, L. (1970). Physical and Chemical Foundations of Rectification, Moscow Lomonosov Institute of Fine Chemical Technology, Moscow, Russia, chapter on the Investigation of the Regions of Continuous and Batch Distillation, 205-215. In Russian.
- Barbosa, D. and Doherty, M. (1988a). Design and Minimum-Reflux Calculations for Single-Feed Multicomponent Reactive Distillation Columns, *Chem. Eng. Sci.* **43(7)**, 1523-1537.
- Barbosa, D. and Doherty, M. (1988b). The Influence of Equilibrium Chemical Reactions on Vapor-Liquid Phase Diagrams, *Chem. Eng. Sci.* **43(3)**, 529-540.
- Barbosa, D. and Doherty, M. (1988c). The Simple Distillation of Homogeneous Reactive Mixtures, *Chem. Eng. Sci.* **43(3)**, 541-550.
- Barbosa, D., & Doherty, M. F. (1987a). Theory of phase diagrams and azeotropic conditions for two-phase reactive system. *Proceedings of the Royal Society of London A*, **413**, 443-458.
- Barbosa, D., & Doherty, M. F. (1987b). A new set of composition variables for the representation of reactive phase diagram. *Proceedings of the Royal Society of London A*, **413**, 459-464.
- Bartlett, D. and Wahnschafit, O. (1997). Dynamic Simulation and Control Strategy Optimization for the Production of MTBE in Reactive Distillation, AIChE Annual Meeting, Chicago IL. Session 34, paper i.
- Bekiaris, N., Güttinger, T. and Morari, M. (1998). Multiple Steady States in Distillation: VLLE Inaccuracies, Multiplicities and ∞/∞ Predictions, Technical report, Automatic Control Laboratory, ETH Zentrum, CH-8092 Zürich, Switzerland. <http://www.aut.ethz.ch>.
- Bekiaris, N., Meski, G., Morari, M. (1996b). Multiple Steady States in Heterogeneous Azeotropic Distillation. *Ind. Eng. Chem. Res.*, **35(1)**, 207-227.
- Bekiaris, N., Meski, G., Radu, C. and Morari, M. (1993). Multiple Steady States in Homogeneous Azeotropic Distillation, *Ind. Eng. Chem. Res.* **32(9)**, 2023-2038.
- Bekiaris, N., Meski, G., Radu, C., Morari, M. (1993). Multiple Steady States in Homogeneous Azeotropic Distillation. *Ind. Eng. Chem. Res.*, **32(9)**, 2023-2038.
- Bekiaris, N., Morari, M. (1996a). Multiple Steady States in Distillation: infinite/infinite Predictions, Extension, and Implications for Design, Synthesis, and Simulation. *Ind. Eng. Chem. Res.*, **35**, 4264-4280.
- Bessling, B., Schembecker, G. and Simmrock, K. (1997). Design of Processes with Reactive Distillation Line Diagrams, *Ind. Eng. Chem. Res.* **36(8)**, 3032-3042.
- Bossen, S., Jørgensen, S. and Gani, R. (1993). Simulation, Design, and Analysis of Azeotropic Distillation Operations, *Ind. Eng. Chem. Res.* **32**, 620-633.

- Bravo, J., Pyhalahti, A. and Järvelin, H. (1993). Investigations in a Catalytic Distillation Plant: Vapour/Liquid Equilibrium, Kinetics, and Mass-Transfer Issues, *Ind. Eng. Chem. Res.* **32(10)**, 2220-2225.
- Cairns, B. and Furzer, I. (1990). Multicomponent Three-Phase Azeotropic Distillation: 3. Modern Thermodynamic Models and Multiple Solutions, *Ind. Eng. Chem. Res.* **29(7)**, 1383-1395.
- Ciric, A. and Miao, P. (1994). Steady State Multiplicities in an Ethylene Glycol Reactive Distillation Column, *Ind. Eng. Chem. Res.* **33(11)**, 2738-2748.
- DeGarmo, J., Parulekar, V. N. and Pinjala, V. (1992). Consider Reactive Distillation, *Chem. Eng. Prog.* **88(3)**, 43-50.
- Doherty, M. and Buzad, G. (1992). Reactive Distillation by Design, *Trans. Inst. Chem. Engrs.* **70(9)**, 448-458.
- Doherty, M. and Caldarola, G. (1985). Design and Synthesis of Homogeneous Azeotropic Distillations 3: The Sequencing of Columns for Azeotropic and Extractive Distillations, *Ind. Eng. Chem. Fundam.* **24(4)**, 474-485.
- Doherty, M. and Perkins, J. (1978a). On the Dynamics of Distillation Processes I: The Simple Distillation of Multicomponent Non-Reacting, Homogeneous Liquid Mixtures, *Chem. Eng. Sci.* **33**, 281-301.
- Doherty, M. and Perkins, J. (1978b). On the Dynamics of Distillation Processes II: The Simple Distillation of Model Solutions, *Chem. Eng. Sci.* **33**, 569-578.
- Doherty, M. and Perkins, J. (1979). On the Dynamics of Distillation Processes III: The Topological Structure of Ternary Residue Curve Maps, *Chem. Eng. Sci.* **34**, 1401-1414.
- Doherty, M. and Perkins, J. (1982). On the Dynamics of Distillation Processes IV: Uniqueness and Stability of the Steady State in Homogeneous Continuous Distillations, *Chem. Eng. Sci.* **37**, 381-392.
- Doherty, M. F. (1990). A topological theory of phase diagrams for multiphase reacting mixtures. *Proceedings of the Royal Society of London A*, **430**, 669-678.
- Dorn, C., Güttinger, T., Wells, J., Morari, M., Kienle, A., Klein, E. and Gilles, E. (1998). Stabilization of an Azeotropic Distillation Column, *Ind. Eng. Chem. Res.* **37(2)**, 506-515.
- Espinosa, J., Aguirre, P. and Pérez, G. (1995a). Product Composition Regions of Single-Feed Reactive Distillation Columns: Mixtures Containing Inerts, *Ind. Eng. Chem. Res.* **34(3)**, 853-861.
- Espinosa, J., Aguirre, P. and Pérez, G. (1995b). Some Aspects in the Design of Multicomponent Reactive Distillation Columns Including Nonreactive Species, *Chem. Eng. Sci.* **50(3)**, 469-484.
- Espinosa, J., Aguirre, P. and Pérez, G. (1996). Some Aspects in the Design of Multicomponent Reactive Distillation Columns with a Reacting Core: Mixtures Containing Inerts, *Ind. Eng. Chem. Res.* **35(12)**, 4537-4549.

- Fien, G. and Liu, Y. (1994). Heuristic Synthesis and Shortcut Design of Separation Processes Using Residue Curve Maps: A Review, *Ind. Eng. Chem. Res.* **33**, 2505-2522.
- Gani, R. and Jørgensen, S. (1994). Multiplicity in Numerical Solutions of Nonlinear Models: Separation Processes, *Comput. Chem. Eng.* **18**, Supplement S55.
- Gehrke, V. and Marquardt, W. (1997). A Singularity Theory Approach to the Study of Reactive Distillation, *Comput. Chem. Eng.* **21**, Supplement S1001-S1006.
- Gmehling, J., Li, J. and Schiller, M. (1993) A modified UNIFAC Model. 2. Present parameter matrix and results for different thermodynamic properties. *Ind.Engng.Chem. Res.* **32**, 178-193.
- Grosser, J., Doherty, M. F. and Malone, M. F. (1987). Modeling of Reactive Distillation Systems, *Ind. Chem. Eng. Res.* **26(5)**, 983-989.
- Gurikov, Y. (1958). Some Questions Concerning the Structure of Two-Phase Liquid-Vapor Equilibrium Diagrams of Ternary Homogeneous Solutions, *Zh. Fiz. Khim.* **32**, 1980-1996.
- Güttinger, T. and Morari, M. (1997). Predicting Multiple Steady States in Distillation: Singularity Analysis and Reactive Systems, *Comput. Chem. Eng.* **21**, Supplement S995-S1000.
- Güttinger, T. and Morari, M. (1998a). Predicting Multiple Steady States in Equilibrium Reactive Distillation: 1. Analysis of Non-Hybrid Systems, Technical Report AUT98-06, Automatic Control Laboratory, ETH Zentrum, CH-8092 Zürich, Switzerland. <http://www.aut.ethz.ch>.
- Güttinger, T. and Morari, M. (1998b). Predicting Multiple Steady States in Equilibrium Reactive Distillation: 2. Analysis of Hybrid Systems, Technical Report AUT98-07, Automatic Control Laboratory, ETH Zentrum, CH-8092 Zürich, Switzerland. <http://www.aut.ethz.ch>.
- Güttinger, T., Dorn, C. and Morari, M. (1997). Experimental Study of Multiple Steady States in Homogeneous Azeotropic Distillation, *Ind. Eng. Chem. Res.* **36(3)**, 794-802.
- Güttinger, T. (1998). *Multiple Steady States in Azeotropic and Reactive Distillation*, PhD Thesis, ETH No. 12720, ETH Zürich, Switzerland. available via <http://www.control.ethz.ch/~disti>.
- Güttinger, T.E., Morari, M. (1999a). Predicting Multiple Steady States in Equilibrium Reactive Distillation. 1. Analysis of Nonhybrid Systems. *Ind. Eng. Chem. Res.*, **38(4)**, 1633-1648.
- Güttinger, T.E., Morari M., (1999b). Predicting Multiple Steady States in Equilibrium Reactive Distillation. 2. Analysis of Hybrid Systems, *Ind. Eng. Chem. Res.*, **38(4)**, 1649-1665
- Hägglblom, K. (1996). Mathematical Proof of Output Multiplicity in Binary Homogeneous Distillation, Paper 115d, presented at the AIChE Annual Meeting 1996.
- Hauan, S. and Lien, K. M. (1996) Geometric visualization of reactive fixed points *Comput. Chem. Engng* **20** (Suppl.) S133-S138.
- Hauan, S., Hertzberg, T. and Lien, K. (1995). Why Methyl tert-Butyl Ether Production by Reactive Distillation May Yield Multiple Solutions, *Ind. Eng. Chem. Res.* **34(3)**, 987-991.
- Hauan, S., Omtveit, T., & Lien, K. M. (Nov. 1996). Anaysis of reactive separation systems. Paper 5f, *A.I.Ch.E. Annual Meeting*, Chicago.

- Hauan, S., Schrans, S. and Lien, K. (1997). Dynamic Evidence of the Multiplicity Mechanism in Methyl tert-Butyl Ether Reactive Distillation, *Ind. Eng. Chem. Res.* **36(9)**, 3995-3998.
- Hauan, S., Westerberg, A. W., & Lien, K. M. (1999a). Phenomena based analysis of fixed points in reactive separation systems. *Chemical Engineering Science*, **55(6)**, 1053-1075.
- Hoffman, E. J. (1964). *Azeotropic and extractive distillation*. New York: Wiley(Interscience) March (1991). *Petrochemical Handbook '91, Hydrocarbon processing*, **70**, 162.
- Humphrey, J. (1995). Separation Processes: Playing a Critical Role, *Chem. Eng. Progr.* **91(10)**, 31-41.
- IAEA PRIS Database (January 2005): <http://www.iaea.org>.
- Isla, M. and Irazoqui, H. (1996). Modeling, Analysis, and Simulation of a Methyl tert-Butyl Ether Reactive Distillation Column, *Ind. Eng. Chem. Res.* **35(8)**, 2696-2708.
- Jacobs, R. and Krishna, R. (1993). Multiple Solutions in Reactive Distillation for Methyl tert-Butyl Ether Synthesis, *Ind. Eng. Chem. Res.* **32(8)**, 1706-1709.
- Jacobsen, E. and Skogestad, S. (1991). Multiple Steady States in Ideal Two-Product Distillation, *AIChE Journal* **37(4)**, 499-511.
- Jacobsen, E., Laroche, L., Morari, M., Skogestad, S. and Andersen, H. (1991). Robust Control of Homogeneous Azeotropic Distillation Columns, *AIChE Journal* **37(12)**, 1810-1824.
- Kaibel, G. and Blass, E. (1989). Möglichkeiten zur Prozessintegration bei destillativen Trennverfahren, *Chem. Ing. Tech.* **61(2)**, 104-112.
- Karpilowski, O., Pisarenko, Y. and Serafimov, L. (1997). Multiple Solutions in Single-Product Reactive Distillation, in R. Darton (ed.), *Distillation and Absorption '97*, Vol. two of IChemE Symposium Series No. **142**, IChemE, Rugby, UK, 685-694.
- Kienle, A. (1995). Modeling, Dynamics and Control of Distillation Columns, HCM Workshop in Stuttgart, July 27-28 1995. Personal Communication.
- Kienle, A., Groebel, M. and Gilles, E. (1995). Multiple Steady States in Binary Distillation | Theoretical and Experimental Results, *Chem. Eng. Sci.* **50(17)**, 2691-2703.
- Kingsley, J. and Lucia, A. (1988). Simulation and Optimization of Three-Phase Distillation Processes, *Ind. Eng. Chem. Res.* **27(10)**, 1900-1910.
- Kister, H. (1997). Are Column Malfunctions Becoming Extinct | or Will They Persist in the 21st Century?, in R. Darton (ed.), *Distillation and Absorption '97*, Vol. one of IChemE Symposium Series No. **142**, IChemE, Rugby, UK, 59-112.
- Koggersbøl, A., Andersen, T., Bagterp, J. and Jfirgensen, S. (1996). An Output Multiplicity in Binary Distillation, Experimental Verification, *Comput. Chem. Eng.* **20**, Supplement S835-S840.
- Kovach III, J. and Seider, W. (1987a). Heterogeneous Azeotropic Distillation-Homotopy-Continuation Methods, *Comput. Chem. Eng.* **11(6)**, 593-605.

- Kovach III, J. and Seider, W. (1987b). Heterogeneous Azeotropic Distillation: Experimental and Simulation Results, *AIChE Journal* **33(8)**, 1300-1314.
- Kunesh, J., Kister, H., Lockett, M. and Fair, J. (1995). Distillation: Still Towering Over Other Options, *Chem Eng. Progr.* **91(10)**, 43-54.
- Laroche, L., Bekiaris, N., Andersen, H. and Morari, M. (1991). Homogeneous Azeotropic Distillation: Comparing Entrainers, *Can. J. of Chem. Eng.* **69(12)**, 1302-1319.
- Laroche, L., Bekiaris, N., Andersen, H. and Morari, M. (1992a). Homogeneous Azeotropic Distillation: Separability and Flowsheet Synthesis, *Ind. Eng. Chem. Res.* **31(9)**, 2190-2209.
- Laroche, L., Bekiaris, N., Andersen, H. and Morari, M. (1992b). The Curious Behavior of Homogeneous Azeotropic Distillation | Implications for Entrainer Selection, *AIChE Journal* **38(9)**, 1309-1328.
- Lee, J.W., Hauan, S., Lien, K.M., Westerberg, A.M. (2000). Difference points in extractive and reactive cascades. II. Generating design alternatives by the lever rule for reactive systems, *Chemical Engineering Science* **55**, 3161-3174
- Lieball, K. (1998). Topological Analysis of Reactive Distillation Systems, Diploma thesis, Swiss Federal Institute of Technology, ETH Zürich, Institute of Process Engineering, ETH Zentrum, CH-8092 Zürich.
- Magnussen, T., Michelsen, M. L. and Fredenslund, A. (1979). Azeotropic Distillation using UNIFAC, Third International Symposium on Distillation, I.Chem.E. Symposium Series No. **56**, The Institution of Chemical Engineers, 1-19.
- March, J. (1985). *Advanced Organic Chemistry*, 3rd edn, John Wiley & Sons, New York.
- Matsuyama, H. and Nishimura, H. (1977). Topological and Thermodynamic Classification of Ternary Vapor-Liquid Equilibria, *J. Chem. Eng. Jpn.* **10(3)**, 181-187.
- McCabe, W.L.; Thiele, E.W. (1925) Graphical design of fractionating columns. *Industrial and engineering chemistry*, **17**, 605-611.
- Mohl, K., Kienle, A., Gilles, E., Rapmund, P., Sundmacher, K. and Hoffmann, U. (1997). Nonlinear Dynamics of Reactive Distillation Processes for the Production of Fuel Ethers, *Comput. Chem. Eng.* **21**, Supplement S989-S994.
- Morud, J. (1996). Studies on the Dynamics and Operation of Integrated Plants, *PhD thesis*, University of Trondheim, Trondheim, Norway.
- Müller, D. and Marquardt, W. (1997). Experimental Verification of Multiple Steady States in Heterogeneous Azeotropic Distillation, *Ind. Eng. Chem. Res.* **36(12)**, 5410-5418.
- Nijhuis, S., Kerkhof, F. and Mak, A. (1993). Multiple Steady States during Reactive Distillation of Methyl tert-Butyl Ether, *Ind. Eng. Chem. Res.* **32(11)**, 2767-2774.

- Okasinski, M. and Doherty, M. (1997a). Effects of Unfavorable Thermodynamics on Reactive Distillation Column Design, in R. Darton (ed.), *Distillation and Absorption '97*, Vol. two of IChemE Symposium Series No. **142**, IChemE, Rugby, UK, 695-704.
- Okasinski, M. and Doherty, M. (1997b). Thermodynamic Behaviour of Reactive Azeotropes, *AIChE Journal* **43(9)**, 2227-2238.
- Ognisty, T. P. (1995). Analyze distillation columns with thermodynamics. *Chem. Eng. Prog.*, **91(2)**, 40-46.
- Ostwald, W. (1900). *Lehrbuch der Allgemeinen Chemie*, Engelmann, Leipzig.
- Petlyuk, F. and Avet'yan, V. (1971). Investigation of the Rectification of Three- Component Mixtures with Infinite Reflux, *Theor. Found. Chem. Eng.* **5(4)**, 499-507.
- Pham, H. and Doherty, M. (1990). Design and Synthesis of Heterogeneous Azeotropic Distillations II: Residue Curve Maps, *Chem. Eng. Sci.* **45(7)**, 1837-1843.
- Piccoli, R. and Lovisi, H. (1995). Kinetic and Thermodynamic Study of the Liquid-Phase Etherification of Isoamylenes with Methanol, *Ind. Eng. Chem. Res.* **34**, 510-515.
- Pilavachi, P., Schenk, M., Pfierez-Cisneros, E. and Gani, R. (1997). Modeling and Simulation of Reactive Distillation Operations, *Ind. Eng. Chem. Res.* **36(8)**, 3188-3197.
- Pisarenko, Y., Epifanova, O. and Serafimov, L. (1987). Steady States for a Reaction-Distillation Column with One Product Stream, *Theor. Found. Chem. Eng.* **21(4)**, 281-286.
- Pleșu, A.E., Bonet, J., Ciornei, C.I., Pleșu, V., "Energy-Saving Issues in Reactive Distillation Schemes", Early Market Introduction of New Energy Technologies in Liaison with Science and Industry (EMINENT) Workshop, University of Pannonia, Veszprém, Hungary
- Pöllmann, P. and Blass, E. (1994). Best Products of Homogeneous Azeotropic Distillations, *Gas Separation & Purification* **8(4)**, 194-229.
- Prokopakis, G., Seider, W. and Ross, B. (1981). Azeotropic Distillation Towers with Two Liquid Phases, in R. Mah and W. Seider (eds), *Foundations of Computer-Aided Chemical Process Design*, *AIChE*, 239-272.
- Rihko, L. K., Linnekoski, J. A. and Krause, A. O. (1994) Reaction equilibria in the synthesis of TAME and TAEE in the liquid phase. *J. Chem.Engng. Data* **39**, 700-704.
- Rosenbrock, H. (1962). A Lyapunov Function with Applications to some Nonlinear Physical Systems, *Automatica* **1**, 31-53.
- Rovaglio, M. and Doherty, M. (1990). Dynamics of Heterogeneous Azeotropic Distillation Columns, *AIChE Journal* **36**, 39-52.
- Rovaglio, M., Faravelli, T. and Doherty, M. (1991). Operability and Control of Azeotropic Heterogeneous Distillation Sequences, *Proceedings of the 4th International Symposium on Process Systems Engineering*, Vol. II, Montebello, Quebec, Canada, 17.1-17.15.

- Rovaglio, M., Faravelli, T., Biardi, G., Gafiuri, P. and Soccol, S. (1993). The Key Role of Entrainer Inventory for Operation and Control of Heterogeneous Azeotropic Distillation Towers, *Comput. Chem. Eng.* **15(5/6)**, 535-547.
- Schmitz, R. (1975). Multiplicity, Stability and Sensitivity of Stats in Chemically Reacting Systems: A Review, *Adv. Chem. Ser.* **148**, 156-211.
- Schrans, S., de Wolf, S. and Baur, R. (1996). Dynamic Simulation of Reactive Distillation: An MTBE Case Study, *Comput. Chem. Eng.* **20**, Supplement S1619-S1624.
- Schreinemakers, F. (1901). Stöchiometrische Verwandtschaftl., *Z. Phys. Chem.* **36**, 257.
- Serafimov, L., Pisarenko, Y. and Timofeev, V. (1993). Reaction-Mass Transfer Processes: Problems and Prospects, *Theor. Found. Chem. Eng.* **27(1)**, 1-10.
- Serafimov, L., Timofeev, V. and Balashov, M. (1973). Rectification of Multicomponent Mixtures II: Local and General Characteristics of the Trajectories of Rectification Processes at Infinite Reflux Ratio, *Acta Chim. (Budapest)* **75(2)**, 193-211.
- Shewchuk, C. (1974). Computation of Multiple Distillation Towers, PhD thesis, University of Cambridge, Chemical Engineering Department, Pembroke Street, Cambridge CB2 3RA, Great Britain.
- Smith, J., Ness, H. V. and Abbott, M. (1996). Introduction to Chemical Engineering Thermodynamics, Chemical Engineering Series, fifth edn, McGraw-Hill companies, New York.
- Sneesby, M., Tadé, M. and Smith, T. (1997). Implications of Steady-State Multiplicity for Operation and Control of Etherification Columns, in R. Darton (ed.), *Distillation and Absorption '97*, Vol. one of IChemE Symposium Series No. **142**, IChemE, Rugby, UK, 205-216.
- Solokhin, A. V., Blagov, S. A., Serafimov, L. A. and Timofeev, V. S. (1990a) Open evaporation processes accompanied by chemical reaction in the liquid phase. *Theor. Found. Chem. Engng* **24**, 103-109.
- Solokhin, A. V., Blagov, S. A., Serafimov, L. A. and Timofeev, V. S. (1990b) Dynamical system for open evaporation process in presence of $A \sim B$ chemical reaction. *Theor. Found. Chem. Engng* **24**, 377-382.
- Sridhar, L. (1997). Multistage standard specification, *AIChE Journal* **43(5)**, 1369-1371.
- Stephenson, R. M., Anderson, T. F. (1980) Energy conservation in distillation. *Chem. Eng. Prog.*, **76(8)**, 68-71.
- Stichlmair, J. and Herguijuela, J.-R. (1992). Separation Regions and Processes of Zeotropic and Azeotropic Distillation, *AIChE Journal* **38(10)**, 1523-1535.
- Stichlmair, J., Fair, J. and Bravo, J. (1989). Separation of Azeotropic Mixtures via Enhanced Distillation, *Chem. Eng. Prog.* **85**, 63-69.
- Sundmacher, K. and Hoffmann, U. (1995). Oscillatory Vapor-Liquid Transport Phenomena in a Packed Reactive Distillation Column for Fuel Ether Production, *Chem. Eng. J.* **57**, 219-228.

- Sundmacher, K., Riihko, L. and Hofmann, U. (1994). Classification of Reactive Distillation Processes by Dimensionless Numbers, *Chem. Eng. Comm.* **127**, 151-167.
- Thiel C., Sundmacher K., Hoffmann U. (1997). Residue curve maps for heterogeneously catalysed reactive distillation of fuel ethers MTBE and TAME, *Chem. Engineering Science*, **52**, 993-1005.
- Ulrich, J. (2002). Operation and control of azeotropic distillation column sequences. PhD Thesis. ETH No. 14890, Zurich, Switzerland.
- Ung, S. and Doherty, M. (1995a). Calculation of Residue Curve Maps for Mixtures with Multiple Equilibrium Chemical Reactions, *Ind. Eng. Chem. Res.* **34(10)**, 3195-3202.
- Ung, S. and Doherty, M. (1995b). Necessary and Sufficient Conditions for Reactive Azeotropes in Multireaction Mixtures, *AIChE Journal* **41(11)**, 2383-2392.
- Ung, S. and Doherty, M. (1995c). Synthesis of Reactive Distillation Systems with Multiple Equilibrium Reactions, *Ind. Eng. Chem. Res.* **34(8)**, 2555-2565.
- Ung, S. and Doherty, M. (1995d). Vapor-Liquid Phase Equilibrium in Systems with Multiple Chemical Reactions, *Chem. Eng. Sci.* **50(1)**, 23-48.
- US DOE (1995). (United States Department of Energy): <http://www.doe.gov>
- Vadapalli, A. and Seader, J. (1997). Computing Multiple Solutions with Aspen Plus and Speedup, AspenWORLD '97, Aspen Technology Inc., Cambridge, U.S.A.
- Venimadhavan, G.; Buzad, G.; Doherty, M. F. (1994). Effects of Kinetics on Residue Curve Maps for Reactive Distillation. *AIChE J.*, **40**, 1814.
- Venkataraman, S. and Lucia, A. (1988). Solving Distillation Problems by Newton-like Methods, *Comput. Chem. Eng.* **12(1)**, 55-69.
- Venkataraman, S., Chan, W. K. and Boston, J. F. (1990). Reactive Distillation using Aspen Plus, *Chem. Eng. Prog.* **86(8)**, 45-53.
- Wang, C., Wong, D., Chien, I.-L., Shih, R., Wang, S. and Tsai, C. (1997). Experimental Investigation of Multiple Steady States and Parametric Sensitivity in Azeotropic Distillation, *Comput. Chem. Eng.* **21, Supplement** S535-S540.
- Weidlich, U. and Gmehling, J. (1987). A modified UNIFAC Model. 1. Prediction of VLE, h^E and γ^∞ , *Ind. Engn. Chem. Res.* **26**, 1372-1381.
- Westerberg, A. and Wahnschafit, O. (1996). The Synthesis of Distillation-Based Separation Systems, Vol. 23 of *Advances in Chemical Engineering*, Academic Press, San Diego, CA, USA, 63-167.
- Widagdo, S. and Seider, W. (1996). Azeotropic Distillation, *AIChE Journal* **42(1)**, 96-130.
- Widagdo, S., Seider, W. and Sebastian, D. (1989). Bifurcation Analysis in Heterogeneous Azeotropic Distillation, *AIChE Journal* **35(9)**, 1457-1464.

Zharov, V. (1968). Phase Representations and Rectification of Multicomponent Solutions, *J. Appl. Chem. USSR* **41**, 2530.

Zharov, V. and Serafimov, L. (1975). *Physicochemical Fundamentals of Simple Distillation and Rectification*, *Khimiya, Leningrad*, 160-168. In Russian.